Université de Montréal

Mechanotransduction Impairment in Adolescent Idiopathic Scoliosis

By Niaz Oliazadeh

Department of Biochemistry and Molecular Medicine
Faculty of Medicine

Dissertation presented to
the Faculty of Graduate Studies to obtain
the degree of Doctor of Philosophy (Ph.D.)
in Biochemistry and Molecular Medicine

April 2019

Résumé

La scoliose idiopathique de l'adolescent (SIA) est une courbure rachidienne tridimensionnelle de plus de 10° qui affecte 4% de la population pédiatrique. L'hétérogénéité de ce désordre musculo-squelettique complexe explique notre incompréhension des causes de la SIA. Néanmoins, plusieurs facteurs biologiques ont été associées à son étiologie. Les réponses osseuses aux stimulations mécaniques normalement appliquées sont nécessaire au fonctionnement optimal du système squelettique. Cependant, la mécanotransduction des tissus musculo-squelettiques dans la SIA est méconnu.

L'objectif principal de cette thèse était d'étudier l'apport de la mécanotransduction dans l'étiologie de la SIA au niveau cellulaire et moléculaire. Nous avons étudié les ostéoblastes des patients atteints de SIA et des sujets témoins. L'induction mécanique a été réalisée à l'aide d'une application d'écoulement de fluide oscillatoire. L'immunofluorescence (IF) et la microscopie confocale ont été utilisées pour évaluer les cils, l'actine et les tests fonctionnels. Les modifications moléculaires ont été étudiés par qPCR ou ELISA. Un séquençage d'exome entier sur une cohorte de 73 SIA et 70 sujets témoins appariés a été fait, pour vérifier l'hypothèse que l'accumulation de variants rares dans des gènes impliqués dans la mécanotranduction cellulaire contribueraient à l'étiologie de la SIA.

Nous avons découvert une élongation anormale des cils des ostéoblastes SIA, qui étaient significativement plus longs que ceux des sujets témoins dans des conditions de ciliogenèse. Les cellules SIA soumises à une application d'écoulement de fluide, n'ont pas été capable d'ajuster la longueur de leurs cils proportionnellement à la force appliquée. La réponse de l'ajustement de la longueur des cils était significativement différente de celle des ostéoblastes témoins, par des stimulations à court et à long terme.. L'expression des facteurs ostéogéniques était significativement réduite dans les ostéoblastes SIA, suggérant une diminution de la mécanosensibilité. De plus, l'analyse transcriptomique en réponse aux forces appliquées a révélé une altération de l'expression des gènes impliqués dans la voie canonique de Wnt. L'augmentation de la sécrétion du facteur VEGF-A en réponse aux forces appliquées dans les ostéoblastes témoins n'a pas été détectée dans les ostéoblastes SIA. Notre analyse SKAT-O des données du séquençage d'exomes entiers a confirmé

l’accumulation de variants rares dans la SIA au niveau de gènes associés à la mécanotransduction cellulaire. Les conséquences de ces anomalies de mécanotransduction ont été étudié par des études cellulaires fonctionnelles, démontrant que les ostéoblastes SIA n’ont pas réussi à se positionner ni à s’allonger proportionnellement au flux bidirectionnel appliqué. Le réarrangement des filaments d'actine induit par l’application d’un flux a été compromis dans la SIA. . Enfin, il a été démontré que le flux de fluide avait un effet inhibiteur sur leur migration.

Nos données suggèrent une mécanotransduction altérée dans les ostéoblastes SIA affectant les cils, les voies moléculaires de signalisation, le cytosquelette et le comportement de la cellule en réponse à l'écoulement appliqué. La réponse cellulaire à ces stimulations joue un rôle dans la structure, la force, la forme et le fonctionnement du système squelettique. Etudier le profil de réponse altérée des cellules osseuses scoliotiques peut mener à la conception des approches thérapeutiques plus efficaces

Mots-clés : scoliose, ostéoblastes, mécanotransduction, cils, Wnt, VEGF

Abstract

Adolescent idiopathic scoliosis (AIS) is a three-dimensional spinal curvature that affects up to 4% of children. As a complex disorder, the cause of AIS is still poorly understood. However, multiple categories of biological factors have been found to be associated with its etiology. The role of biomechanics has been acknowledged by clinicians both in the description of deformity and in relation to bracing treatments. Bone responses to routinely applied forces are an important part in a tightly regulated network that is necessary for the optimal function of the skeletal system. However, little is known about the mechanotransduction of musculoskeletal tissues in AIS.

The main goal of this dissertation was to investigate the contribution of mechanotransduction in the etiology of AIS from a cellular-molecular aspect. We studied primary osteoblasts obtained intraoperatively from AIS patients and compared them to samples from trauma cases as controls. Fluid flow application was used for mechanical induction. Immunofluorescence staining, and confocal microscopy was used to assess cilia, actin and cellular tests. Molecular changes were followed using RT-PCR or ELISA. We also performed whole exome sequencing (WES) to test the hypothesis that rare variants accumulation in genes involved in cellular mechanotransduction could contribute to AIS etiology.

We found an abnormal cilia elongation among AIS osteoblasts, which grew significantly longer than controls. AIS cells after fluid flow application failed to adjust their cilia length in proportion to the applied force. Under both short- and long-term flow applications, their cilia length adjustment was significantly different from controls. Notably, the elevation in the expression of osteogenic factors, that was normally observed with control osteoblasts, was significantly reduced in AIS osteoblasts, suggesting a decrease in their mechanosensitivity. Moreover, transcriptomic analysis following the applied forces revealed an altered expression of genes involved in the Wnt canonical pathway. Strain induced increase in secreted VEGF-A in control osteoblasts was not detected in AIS flow-conditioned media. At the genomic level, our SKAT-O analysis of the WES data also supported the involvement of heterogenous defects in genes pertaining to the cellular mechanotransduction machinery. We tested the consequence of these

mechanotransduction abnormalities in a series of functional cellular studies. As expected and unlike controls, AIS osteoblasts failed to position or elongate themselves in proportion to the bidirectional applied flow. The strain-induced rearrangement of actin filaments was compromised in AIS osteoblasts. Finally, fluid flow showed to have an inhibitory effect on their migration contrasting with control cells that migrated significantly faster under flow.

In summary, our data strongly suggest an impaired mechanotransduction in AIS osteoblasts that affect cilia, downstream signaling molecular pathways, cytoskeleton and finally the behaviour of the whole cell in response to flow. Fluid flow is one of the main mechanical forces applied physiologically to the bone cells. Cellular responses to these stimulations play a critical role in the structure, strength, shape and optimal performance of the skeletal system. Mapping the impaired profile response of scoliotic bone cells can help in designing more efficient therapeutic approaches or explaining the mechanisms behind less than optimal bracing outcomes.

Key words: Adolescent idiopathic scoliosis, Osteoblasts, Mechanotransduction, Cilia, Wnt, VEGF

Table of Content

List of Tables

List of Figures

List of Supplementary Tables

List of Supplementary Figures

Abbreviation list

AC:	Adenylate cyclase
AIS:	Adolescence idiopathic scoliosis
ALP:	Alkaline phosphatase
Alpha-MEM:	Minimum Essential Medium Eagle – Alpha Modification
ANOVA:	Analysis of variance
ATP:	Adenosine triphosphate
BMD:	Bone mineral density
BMP2:	Bone morphogenetic protein 2
BSA:	Bovine serum albumin
Ca:	Calcium
CADD:	Combined Annotation Dependent Depletion
CaM:	Calmodulin
cAMP:	Cyclic adenosin monophosphate
CLASP1:	Cytoplasmic linker associated protein 1
COX:	Cyclooxygenase
CTFC:	Corrected total cell fluorescence
CTNNB1:	Catenin Beta 1
DNA:	Deoxyribonucleic acid
ECM:	Extracellular matrix
ELISA:	enzyme-linked immunosorbent assay
ERK:	Extracellular signal regulated kinases
ERs:	Estrogen receptors
FAK:	Focal adhesion kinase
FBS:	Fetal bovine serum
FGF23:	Fibroblast growth factor23
GH:	Growth hormone
GPCRs:	G protein-coupled receptors
GSK3beta:	Glycogen Synthase Kinase 3 beta
GWAS:	Genome-wide association study
IFT:	Intraflagellar transport
IP3:	Inositol triphosphate 3
ITGB1:	Integrin beta 1
KIF:	Kinesin superfamily proteins
LBX1:	Ladybird Homeobox 1
LiCl:	Lithium chloride
LRP:	Lipoprotein receptor-related protein
MAF:	Minor allele frequency
MAPK:	Mitogen activated protein kinase

MATN1:	Matrilin 1, cartilage Matrix Protein
mRNA:	Messenger RNA
MSCs:	Mesenchymal stem cells
NIH:	National institute of health
OPG:	Osteoprotegrin
OPN:	Osteopontin
PBS:	Phosphate-buffered saline
PCP:	Planar cell polarity
PCR:	Polymerase chain reaction
PFA:	Paraformaldehyde
PGE2:	Prostaglandin E2
PKA:	Protein kinase A
POC5:	Protein of centriole 5
PSSE:	Physiotherapeutic Scoliosis Specific Exercises
PTGS2:	Prostaglandin-Endoperoxide Synthase 2
PTK7:	Protein Tyrosine Kinase 7
RANK:	Receptor Activator of NF-KapaB
RANKL:	Receptor Activator of NF-KapaB ligand
RNA:	Ribonucleic acid
RT-qPCR:	Reverse transcriptase quantitative PCR
RUNX2:	Runt-related transcription factor 2
SKAT-O:	Optimal SKAT
SKAT:	Sequence kernel association test
SNPs	Single nucleotide polymorphisms
SNVs:	Single nucleotide variants
TGF1:	Transforming growth factor type
TRAP:	Tartrate-resistant acid phosphatase
VEGF:	Vascular endothelial growth factor

To my mother: Azam

To my love: Alireza

To my son & my sun: Rodwin Leo

Acknowledgments

I would like to express my deepest gratitude to my PhD supervisor Prof. Alain Moreau for accepting me as one of his doctoral students, and for his continues support throughout this journey. Alain generously shared his knowledge and time. He trusted me and gifted me with the freedom I needed to grow and develop my own scientific and academic expertise. This journey would not have been possible without him and his mentorship.

I am grateful to my doctoral committee members, Prof. Zoha Kibar and Prof. Muriel Aubry, for the scientific discussions and sincere supports that they provided when I needed the most. I also want to thank Prof. Carolina Alfieri, for her heartwarming presence and for hours of valuable discussions that I was privileged to enjoy with her learning about life and science.

Working with Alain's group, I had the opportunity to meet and learn from a group of exceptional colleagues. Valuable friendships formed through these years which made everything much more fun. I learned critical thinking and scientific analysis from heated, enjoyable discussions with Prof. Kristen F. Gorman, who was a post doctorate fellow back then and is a dear friend now. I also learned a great deal of laboratory discipline and project management from Anita Franco. Her outstanding memory and organization made everything so much easier. I would also like to thank Dr. J. F. Lavoie, Dr. Cedric Julien, and other members of the lab, Lakshmi Suvarnan, Dr. Nancy Karam, Dr. Mohamed Elbakry and Dr. Dina Nada for their friendship and company.

I specially want to thank my mother for her continuous and unconditional support whenever I needed. Her brave scarifies helped me move forward. I experienced the joy and hardship of motherhood during last years of my PhD and if it was not for her warm presence and amazing support, I would not have made it. Also, many thanks to my father, who has always been proud of my achievements, small or big, since I was a child, encouraging me every step of the way.

Last but not least, my beloved family. My little son, Rodwin Leo, your big brown eyes overload me with joy and life, fueling me to push forward everyday. Alireza, thanks

for your love, support, encouragement, great patience and brutally frank criticisms throughout this journey.

I also would like to acknowledge the agencies who funded this research: Fondation CHU Sainte- Justine, Network of Applied Medical Genetics (RMGA), La Fondation Yves Cotrel de l'Institut de France, Paris, France, Paradigm Spine LLC/Fourth Dimension Spine LLC (NYC, USA), and Génome Québec (Montreal, Canada)

Thank you all!

Chapter I

Literature review

1.1 Adolescence idiopathic scoliosis (AIS)

1.1.1 Introduction and definition

The term “scoliosis” originates from Greek, meaning “crooked”, and was first used by Hippocrates (A.D. 460–370), to explain all kinds of malalignments in the human spine. Ambroise Paré (1510–1590), provided the first accurate description of Adolescent Idiopathic scoliosis (AIS) and tried to treat his patients with the historical well-known iron brace [1].

Today scoliosis is defined as a three-dimensional spinal deformity. The diagnosis is based on measuring the angle of the major spinal curve using the Cobb method. This method involves measuring the angle between the top surface of the most tilted upper vertebra and bottom surface of the most tilted lower vertebra in the spinal curve (Fig. 1-1). This angle is commonly referred to as the “Cobb angle”. A spinal curve with a Cobb angle greater than 10^{o} is diagnosed with Scoliosis [2].

1.1.2 Epidemiology

Adolescent type of idiopathic scoliosis develops between 11 to 18 years of age and accounts for about 90% of idiopathic scoliosis. The remaining 10% include the Infantile and Juvenile types of idiopathic scoliosis, with age of onset being between 0-3 and 4-10 respectively. The prevalence of AIS varies for different ethnic and geographic groups. With a global prevalence of up to 5.2%, AIS is a common disease [3]. It represents a serious and

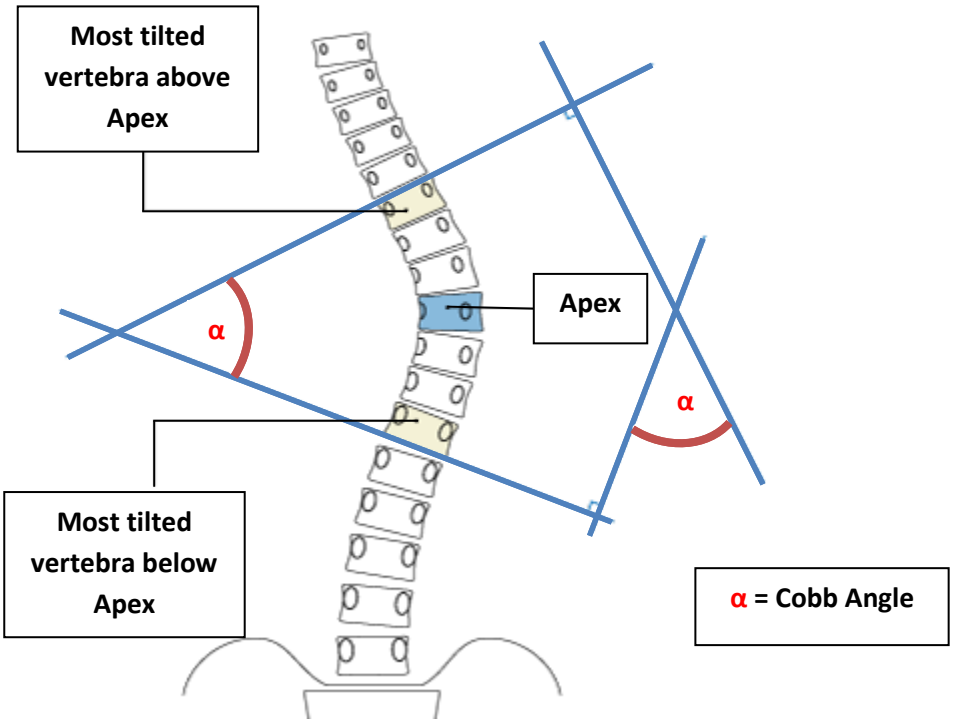

Figure 1-1 Cobb angle measurement.

Redrawn based on information on the "Spine Health" website https://www.spine-health.com/conditions/scoliosis/cobb-angle-used-measure-scoliosis-curves

chronic health condition impacting individuals throughout their lives. Most patients are diagnosed with scoliosis between the ages of 10 and 15, and one out of every four cases would have a progressive curve requiring active treatment [4]. AIS prevalence is also sex and age dependent, with an increased ratio in girls. In fact, Luk KD. *et al.* [5] studied a large cohort of scoliotic children, from age 10 until skeletal maturity at 19, and found that AIS was more common in girls than boys for all curve severities. Asher *et al.* [6] have also shown that AIS patinates who are still undergoing spinal growth have a higher risk of curve progression by the end of skeletal maturity.

1.1.3 Disease management

Due to the lack of specific biomarkers, AIS patients are usually referred to clinicians following screening exams. As a consequence of its persistently idiopathic nature, the standard care for AIS has not significantly changed in decades. Currently, diagnosed patients are generally observed for spinal deformity progression. Bracing is the chosen treatment in case of progression and spinal fusion surgery is used as a last resort. Because of patients' discomfort and risk, the application of current treatments is delayed until a significant deformity or progression is detected. This results in suboptimal treatment, significant psychological negative effects, and significant economic burden for the families and healthcare systems.

Physiotherapy has been recommended as a first step in treatment of AIS while the patient is observed for curve progression. Whether physiotherapy is effective for AIS management is still debated among clinicians [7], [8]. While this conservative approach is routinely used in several European countries, North American physicians do not generally advocate its use. It is argued that generic physiotherapy exercises are less effective than Physiotherapeutic Scoliosis Specific Exercises (PSSE) protocols that are designed specifically and adapted individually to curve site, magnitude and clinical characteristics of each patient [9].

Curve progression is more probable in patients with immature skeletons. Cases with Cobb angles less that 20° are simply observed, while curvatures over this threshold are addressed by bracing (over 13 hours per day for a duration of 2.5 years) in hope of preventing the curve progression to the point of surgery [10]. The effectiveness of bracing has been controversial and subject to more heterogeneity based on the type of curvature, age of the patient, duration of brace wearing and the model of the bracing [11]–[14]. Last therapeutic option is spine fusion surgery that aims for preventing curve progression and long-term consequences of larger spine deformities such as pain, reduced pulmonary capacity and other functional consequences that profoundly reduce the quality of life in affected individuals. Like any other invasive surgical approaches, there is always some level of risk for complications, during or after surgery, such as loss of neurological response, early or late infections, implant failure and recurrence or additional deformity. Nevertheless, patients surveys and studies report satisfactory short-term outcomes for

scoliosis correction surgery, while not much data is available regarding its long-term outcomes [10].

1.1.4 Etiology

Despite decades of research, there is no consensus among the experts regarding the etiology of AIS nor its pathogenesis. Nevertheless, the existence of a genetic component using both familial and population-based approaches, is well recognized [2], [15]. Moreover, abnormalities in central nervous system, bone metabolism and spinal growth, metabolic pathways and biomechanics have also been proposed as the etiological factors of AIS [16]–[18]. Cheng J.C *et al.* [2] have recently published a comprehensive review of the current understanding of AIS etiology.

1.1.4.1 AIS complexity and clinical heterogeneity

Adolescent Idiopathic Scoliosis is a complex disease with a wide range of clinical heterogeneity in several levels including age at onset, curve phenotype and the progression of spinal curvature. This makes timely diagnosis and early interventions very difficult. The aforementioned female bias further adds to this complexity.

AIS heritability is widely accepted through genetic findings from classic familial linkage studies to vast population studies using relatively recent technology-oriented methods such as GWAS and whole exome sequencing. Genetic variations and mutation have been reported to be associated to the disease in certain populations or families that perhaps could explain the heritability in some patients. But these findings do not converge into a causative gene with putative role and a classic mode of Mendelian inheritance [15], [19]. The emerging view favours a complex polygenic model with considerable heterogeneity [15], [20]–[22].

1.1.4.2 Several tissues are involved in AIS

Due to association of scoliosis with neurological/neuromuscular disorders, neuropathological mechanisms have long been suggested to play a role in AIS. Surgically

induced small brain lesions in laboratory animals and the removal of the pineal gland from chicken, fish or bipedal rats reportedly caused AIS resembling curvatures [16]–[18]. Moreover, coexisting abnormalities in oculo-vestibular and proprioceptive functions in AIS patients were observed in several investigations [23]–[27].

It is not yet fully known how the primary changes in the nervous system can affect spinal curvature; however, it is believed that sensory nerves effects in bone homeostasis and cross talks between muscle, bone and connective tissue may be involved [28]. An interesting investigation by Fukuda *et al.* [29] showed that nerve specific knockout of the axon guidance gene, Sema3A, in mice caused low bone mass due to reduced bone formation. Removal of the same gene from osteoblasts did not affect the bone mass in the animal, suggesting the involvement of sensory nerve independent of the local alterations [29].

Fibers disarrangement in the ligamentum flavum [29] or reduced glycosaminoglycan content of intervertebral discs have also been reported in AIS patients [18]. AIS patients have shown relative hypertrophy and increased electromyographic signalling in the paraspinal muscles surrounding the scoliotic curves which are suggested to be the result of curve progression [27], [29]. Cartilage tissue abnormalities such as calcification of the cartilage end plate and the adjacent disc have also been reported in AIS [30]. A conditional gene targeting in the mouse showed loss of *GRPR126* protein in cartilage affected normal spinal column development, resulting in a scoliosis phenotype [31].

Despite all the evidence on the involvement of nervous system, muscle, cartilage and bone in the development of AIS the existing data is insufficient to support a primary causal role for any of these tissues. In this research project we focus on bone.

1.1.5 Cellular-Molecular abnormalities in AIS

1.1.5.1 Bone metabolism factors

Investigating the cause of low bone mineral density (BMD) in AIS, Suh *et al*. [32] reported an elevation of RANKL and RANKL/OPG ratio in the serum of 72 AIS patients. This finding later was confirmed by others [33], [34]. Osteoblasts from 20 AIS patients

with low BMD showed an increase of RANKL in both mRNA and protein levels [35]. An association between a polymorphism in OPG gene and low BMD in lumbar spine has also been reported [34]. Antiosteoporosis treatments were suggested to help prevent AIS curve progression by restoring the balance of RANKL-OPG-RANK system and improving bone strength [36].

Osteocalcin is involved in both bone formation and resorption and is one of the hormones secreted from osteoblasts. Increased levels of osteocalcin in blood serum of AIS patients [33], [34] could be due to higher rate of bone remodeling and abnormal bone metabolism.

MATN1 protein forms filamentous structures in several tissues such as cartilage and helps in the organization of extracellular matrix (ECM). Several studies reported an association between SNPs in different regions of MATN1 and AIS [15], [19]. Recent meta-analysis concluded that some of these association might be restricted to specific ethnic backgrounds [37]. Reduced plasma levels of MATN1 protein are suggested to be a possible biomarker for disease progression [38]. Cartilage oligomeric matrix protein (COMP) is another ECM involved protein which is associated with skeletal disorders including scoliosis [39]. Reduced COMP levels in serum [40] and significant COMP mRNA downregulation in osteoblasts[41] were shown in AIS patients. It is of note that several recent studies showed interesting evidences supporting the contribution of rare variants enrichment in ECM genes to disease risk [42], [43].

1.1.5.2 Hematological factors (Platelets)

The similarity of platelet and muscle in their actin-myosin contractile apparatus, has led researchers to look for similar abnormalities in these two cell types in AIS. Since the early 1980s, a number of anomalies in platelets, calmodulin, and Ca transport in AIS have been documented in the literature (refer to [44] for a more comprehensive review). Calmodulin (CaM), binds to calcium, playing a role in platelet and muscle contraction through interactions with actin and myosin [44]. CaM concentration is increased in the platelet of AIS patients and this appears to be associated with disease progression. Non-progressive stabilized curves and healthy controls showed no difference in CaM

concentration. Also curve stabilization following therapeutic interventions reduce the increased CaM levels, suggesting a biomarker role for this protein [45], [46].

1.1.5.3 Systemic factors

G protein family is involved in transmitting extracellular signal to the cell, through interaction with a family of membranous receptors called GPCRs (G protein-coupled receptors). Based on the fact that melatonin receptors are GPCRs, Moreau *et al.* [47] studied the response of AIS osteoblasts to melatonin and found reduced response patterns compare to controls. They measured the cAMP concentration as a secondary messenger and reported an elevation of cAMP in AIS osteoblasts due to melatonin failure in reducing cAMP accumulation. Although this reduced response was shared among all tested AIS samples, the reduction pattern was not the same. The authors were able to classify AIS patients into three distinct groups based on their osteoblast response to melatonin [47], [48]. They were able to confirm their findings in another study using the cellular dielectric spectroscopy technique by direct measurement of the cellular response to Gi stimulation and reproducing three distinct patterns in AIS cells [49]. Reduced performance of Gi-coupled receptor signaling in AIS patients was later reported to be rather a systemic impairment and not restricted to downstream melatonin pathways. They found the same impairment in other cells (skeletal myoblasts and peripheral blood mononuclear cells) obtained from AIS patients which were also grouped in three differential groups or endophenotypes [49]. AIS complex nature and high levels of phenotypic and genotypic heterogeneity is one of the biggest challenges in understanding the disease. Endophenotypes can improve the stratification of the patients at a molecular level, potentially help with a better prognosis. The detailed procedure of the used methodology in AIS patients classification is available in JoVE visual journal [50].

Osteopontin (OPN) is another systemic factor that its association with idiopathic scoliosis is well documented. This multifunctional glycoprotein is expressed in all body fluids as well as in ECM of mineralized tissue [50]. Higher levels of circulating OPN in plasma of AIS patients is reported to correlate with curve severity [51]. Mice model studies

confirmed the increased OPN to be associated with disease development and severity. OPN depletion also showed to help improve the skeletal deformity [52]–[54].

1.1.5.4 Hormonal factors

Growth abnormalities are usually observed in AIS and they have been shown to specifically associate with the pubertal stage (reviewed in sub-section 1.1.6). Therefore growth hormone (GH) has been an interesting area to study for AIS researchers since the 1970s [52]. Elevated levels of GH [55]–[57] or its downstream players [58], [59] were showed to be associated with AIS. Genetic studies however failed so far to find a consensus correlation. The findings are conflictive and reported AIS associated SNPs concluded to be limited to an ethnic area or a proportion of the patients [60]–[64].

Estrogen has been assumed to play a role in AIS due to the biased prevalence in female and association of age at menarche with scoliosis development. Later age at menarche is parallel with higher AIS prevalence [65]. Estrogens influence growth, bone remodeling and bone gain, all of which are affected in AIS. There are some inconclusive data on blood estrogen levels [66]–[68], however its role in AIS is not concentration dependent, rather appears to be associated with the activity on their target cells [65], [69]. Estrogens suggested to have a key role in triggering the melatonin signaling dysfunction and bone remodeling in AIS patients [70]. A recent study on bipedal rats confirmed that estrogen increase the scoliosis incident and severity. Zheng et *al.* in this study suggested a loss of coupling of endochondral ossification between the anterior and posterior columns to be the underlying cause [71]. There has been extensive research trying to find an estrogen related genetic association with AIS in an effort to explain the higher prevalence in female. In result, multiple polymorphisms in estrogen receptors or other related genes have been reported, reviewed in [15]. Unfortunately, due to high discrepancy in the results, the estrogens genetic correlation with AIS remains debated. In essence estrogens may not be directly involved in AIS etiology, but still impact the disease through to its effects on many AIS etiopathological factors such as bone remodeling, growth factor and melatonin pathway [44].

Leptin is another hormone suggested to be involved in AIS. This energy regulating hormone plays also an important role in bone metabolism. Reduced levels of leptin in blood samples of AIS patients is reported in many studies [72]–[74]. Reduction in bone mass, bone strength and growth abnormalities have been listed to be associated to leptin bioavailability [75]. Hypothalamic hypersensitivity to circulating leptin levels, led to development of a double neuro-osseous theory that claims a role for both autonomic and somatic nervous systems in the development of IS [76]. AIS Osteoblast cells were shown to have significantly lower response to leptin stimulations compared to controls [75]. It is of note that melatonin [75] and cytosolic cAMP [75] can inhibit leptin synthesis. As mentioned above, there is an impairment in AIS cells involving cAMP and melatonin signaling pathways [47], [49].

1.1.6 Bone abnormalities in AIS

1.1.6.1 Growth and metabolism

Adolescence is a period of rapid skeletal growth, with skeletal mass doubling by the end of adolescence [77]. AIS occurs during pubertal growth spurt in children and curve progression is stabilized at skeletal maturity. Rapid growth phase is associated with the curve development and progression [78]. Taller and leaner children have been reported to show higher risk for AIS development [79], [80]. In addition to abnormal body height, asymmetries in the limb and segmental length were also reported [79], [80]. Whether these observed skeletal differences at the time of diagnosis will be resolved by skeletal maturity or remain present in adulthood is controversial [81], [82].

Since 1982, when Burner et *al.* [83] first reported lower BMD in patients with acquired back deformity, several studies have found a higher prevalence for osteoporosis in AIS compared to the general pediatric and adolescent population [84]–[86]. Lee *et al.* [87] reported an inverse relationship between curve severity and BMD in a cross-sectional study on 919 AIS girls. The causes of osteoporosis in AIS patients are unknown and whether poor bone quality is an etiological factor remains controversial. Bracing, due to partial immobilization of the body, has been postulated to cause a permanent loss of bone mineral mass, predisposing to adult osteoporosis, but this presumption has been refused in

several extensive studies[86]. The BMD measurement at the time of diagnosis might also serve as an additional objective indicator of curve progression, suggesting osteopenia to be an important risk factor with a prognostic value [88].

1.1.6.2 Structure and morphology

Structural factors, such as the cortical bone thickness and the trabecular bone micro-architecture, have been suggested to be of paramount importance for the determination of bone quality and strength [89]–[91]. Yu *et al.* [92] reported lower cortical thickness in AIS cases after the assessment of 214 AIS girls in comparison to 187 healthy age matched controls. They suggested AIS abnormal bone profile to be the result of altered endocortical modeling, deranged trabecular bone structure and disturbed bone mineralization.

Bone strength is a function of both BMD and bone quality. NIH reinforced this statement by defining osteoporosis as a skeletal disorder with compromised bone strength which features bone density and bone quality [93]. In 2017, Wang *et al.* (71) confirmed reduced mineralization and predominant trabecular changes in AIS patients. Interestingly, the tissue level of mRNA expression for RUNX2 was found to be lower in AIS bone biopsies, while SPP1 (OPN) and TRAP mRNA were found to be higher [94].

Despite decades of research, the etiology of AIS remains a mystery. Among all the studies on the etiology of AIS that have been carried out so far, cellular and molecular findings are among the least reported. Having access to a cellular bank from AIS patients we had the opportunity to investigate the etiology of AIS from a cellular-molecular perspective.

1.2 Bone cell mechanobiology

1.2.1 Introduction

Bone as a bio-ceramic composite features unique mechanical properties that have always attracted engineers. These mechanical features are mostly attributed to complex multilayer structures that are arranged in a hierarchical manner (Fig. 1-2).

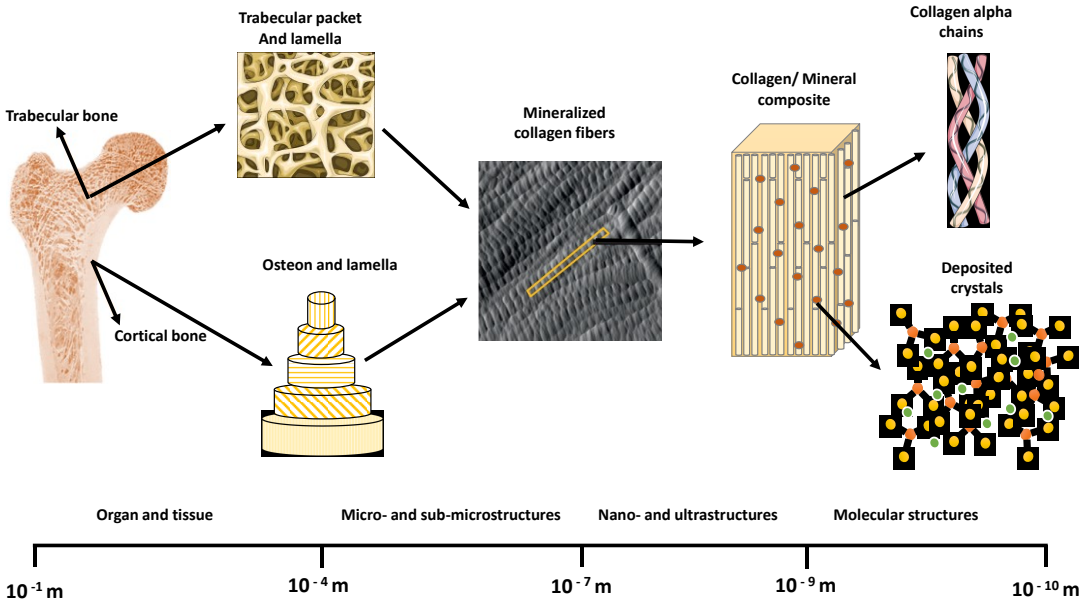

Figure 1-2 Levels of structural hierarchy in bone.

The composite of bone includes a hard cortical shell that covers the spongy cancellous bone inside. Cortical bone microscopic structure is composed of many secondary haversian systems (osteons) that are the product of remodeling process. Both trabecular and cortical bone are lamellar with a different microstructure. Collagen fibers with plates of minerals compose the ultra- and nano-structural layers. Figure is inspired and redrawn from, Burr. D.B and Akkus O. Bone morphology and organization, 2014 (DOI: http://dx.doi.org/10.1016/B978-0-12-416015-6.00001-0). Some of the motifs are downloaded from smart servier medical art website.

Bone cells are tightly attached to their extracellular environment in a complex dynamic fashion. Environmental stimuli such as gravity, strains, shear, compression, stretch, and fluid flow have the ability to trigger cellular response and influence the whole bone tissue. In addition, components of these stimuli such as magnitude, frequency and strain rate also affect this cellular response [95]. The relationship between bone formation, remodeling and the surrounded mechanical environment is presented in Frost's "mechanostat" theory [96]. This theory describes a homeostatic mechanism in bone that is responsible for sensing the applied mechanical changes and modifying the mass and conformation of bone to meet the mechanical demands in an optimal condition. He hypothesized that below a certain physiological threshold, bone reduces excess mass through increased remodeling. When strains exceed the upper physiological boundary, he argued, bone formation occurs through increased modeling to provide the needed strength [96]. Mechanostat defines a nonreplaceable role for mechanical forces to guide the effect

of physiological factors such as cellular interaction, hormones, etc. on bone adaptation mechanisms [95].

1.2.2 Bone cells

Bone tissue consists of three different cells, namely osteoblasts, osteoclasts and osteocytes. To carry out the diverse functions of skeletal maintenance, including bone formation, resorption, mineral homeostasis and bone repair, bone cells develop specialized morphology, function and characteristic locations. Some of them originate from the line of mesenchymal stem cells, which consist of pre-osteoblasts (undifferentiated cells), osteoblasts and bone lining cells. The rest rise from hematopoietic stem cell line including circulating or marrow monocytes, preosteoclasts and osteoclasts [97].

Cellular structure of the bone is mainly composed of osteocytes and osteoblasts as support cells plus osteoclasts as remodeling cells. Osteoblasts are responsible for osteogenesis through the deposition of bone matrix and regulation of bone resorption. Osteocytes are terminally differentiated osteoblasts that are trapped in their own bone matrix. They form a network through the extensions of their plasma membrane and are the most abundant cells in a bone [98]. The only cells that are capable of resorbing bone are Osteoclasts which are typically multinucleated cells.

1.2.2.1 Undifferentiated mesenchymal cells

Pre-osteoblasts or potent mesenchymal cells live inside the bone canals, endosteum, periosteum and bone marrow waiting for a stimulus to proliferate and differentiate into mature osteoblasts. They are mononuclear, irregular cells with minimum cytoplasm that respond to growth factors, hormonal changes, biomechanical stimulations among other factors. These cells have crucial role in healing a fracture or depositing more bone where needed [97], [99].

1.2.2.2 Osteoclasts

Osteoclasts are quite different from other bone cells in their morphology, function and origin. Unique in the entire body, these cells have impressive power for local digestion which makes bone resorption to be their primary role.

Unlike other bone cells, osteoclasts are derived from hematopoietic monocyte-macrophage lineage. The mononuclear precursor cells fuse to form the mature multinucleated osteoclasts. Multinucleation is an important feature of these cells that together with other adapted ultrastructural changes provide them with the bone resorption ability. The precursor cells are available in the marrow or blood stream and factors such as calcium gradient, secreted cytokines from osteoblasts and osteocytes, and matrix metalloproteinases can stimulate their recruitment to bone resorption sites [97].

The large multinucleated osteoclasts can have between three to twenty nuclei with numerous numbers of lysosomes and elongated mitochondria. The specific brush or ruffled border of osteoclasts adjacent the target area in the bone is perhaps the most complex and distinctive feature of these cells [100].

Beside bone resorption, osteoclasts also play a role in the regulation of minerals such as calcium and phosphate in the body alongside parathyroid and thyroid glands, osteocytes and renal hormones. Upon the discovery of osteoclasts activation by inflammatory stimuli, osteoimmunology was coined as a scientific term to explain the tight relationship between skeleton and immune system.

The most well-known regulators of osteoclastogenesis, the RANK/RANKL/OPG axis, were discovered through osteoimmunology studies. The Receptor Activator of NF-KapaB transcription Factor (RANK) is expressed by committed osteoclast precursors. Responding to its ligand (RANKL), RANK stimulates various intracellular pathways that lead to osteoclasts formation and activation. Secreted by osteocytes, Osteoprotegrin (OPG) on the other hand inhibits osteoclastogenesis by binding to RANK and competing with RANKL. In both osteocytes and osteoclasts, OPG secretion is regulated by the Wnt/beta-catenin pathways [100].

1.2.2.3 Osteoblasts

Although not terminally differentiated, osteoblast are mononucleated cells that are specialized mainly in bone matrix deposition and osteoclast regulation [101]. They coat the surface of bone packing tightly against each other [97]. Following bone formation completion, osteoblasts are destined for one of these three fates: some mature into their matrix and turn to entrapped osteocytes, some adapt a more flat form to cover the surface of the bone forming bone lining cells and the rest disappear from the site of bone formation by apoptosis [97]. Osteoblasts secrete large quantities of collagen type I and other specialized matrix proteins forming osteoid which later becomes a base for mineral deposition. They also express high levels of Alkaline phosphatase (ALP) and osteocalcin. In fact, these proteins are indicators of osteoblast existence [102].

Osteoblasts interact with each other, bone marrow and bone lining cells through adherent, tight and gap junctions. They also bind closely with extracellular matrix through their cytoskeleton and cellular junctions. In fact, osteoblast form a continuous network connecting the mineralized matrix to the bone surface, then to the bone marrow, and finally to the endothelial cells of the blood supplying vessels [102].

1.2.2.4 Osteocytes

Osteocytes are spider-shaped former osteoblasts that have been buried into the deposited bone matrix. They compose more than 90% of the bone material, and are among the most long-lived cells with up to 25 years life span [103]. The distinct positioning of the osteocytes into the bone tissue makes them easy to identify and observe, but it limits the functional studies due to difficulties in isolating them [104]. Osteocytes feature many long cytoplasmic projections (up to 50 per cell) that extend through the network of interconnecting bone canaliculi providing cell to cell communication that facilitate signal transduction. This network, filled with interstitial fluid that flows inside the osteocyte's canaliculi, coordinating the response of bone to biological and mechanical signals [103].

During bone formation, some osteoblasts are transformed to osteocytes which result in dramatic changes in osteoblasts morphology and functions. Osteocytes are considered to be the mechanosensory cells of a mature bone. Following the translation of

mechanical sensation to chemical signal, osteocytes affect function and differentiation of osteoblasts and osteoclasts, leading to bone formation or resorption [105], [106].

Osteocytes effects on the regulating function of osteoblasts and osteoclasts are well documented [107]. Different hormonal and mechanical cues trigger osteocytes production of regulatory factors such as OPG, RANKL and sclerostin. These regulatory factors in turn can stimulate other bone cells through paracrine or autocrine mechanisms [107].

Given the access of osteocytes to the mineralized material, they play a prominent role in mineral hemostasis. Osteocytes-mediated osteolysis are stimulated by changes that need a quick release of minerals in a short span of time, such as lactation [104].

Similar to osteoblasts, the osteocytes also have hormone releasing ability. These cells also can secret the FGF23 hormone which regulates serum phosphate levels through affecting the metabolism in distant organs such as kidney. Endocrine roles have also been recently attributed to osteocytes such as regulating lymphopoiesis which in turn affects the immune system and fat metabolism [108].

1.2.3 Cellular Mechanotransduction

All bone cells directly or indirectly respond to their local strains. The process of translating the mechanical stimulus into biological signals is called mechanotransduction [95]. Osteocytes viability depends on mechanical stimulation [106], [109], [110]. Strain induced osteocyte's apoptosis also has been found to correlate with percentage of bone resorption surfaces [111]–[113]. Osteocytes seem to be the main cells responsible for unloading-induced bone loss, as osteocyte-ablated mice are shown not to develop osteoporosis in the absence of mechanical stimuli [114]. Fluid flow is a well-known player in micronutrient and molecular transportation in bone as diffusion alone proven to be not sufficient to cover the entire lacunar-canalicular system [114].

The only other serious cellular candidate for mechanical sensation in bone is osteoblast. As the progenitors of osteocytes, it can be anticipated that osteoblast have some mechanosensory capacity. In fact, the major body of in vitro studies have been performed on osteoblasts with interesting findings that confirm osteoblasts' sensitivity to mechanical

stimulation [95]. Compressive stress has been suggested to regulate osteoblastic differentiation [115]. Mechanical induction has been shown to affect osteoblasts proliferation, differentiation, migration and mineralization, in addition to triggering actin rearrangement and the Wnt signaling pathway [116]–[121].

It is important to note that there are strong evidence and scientific arguments that are in favor of osteocytes being the primary and main cellular recipient of bone mechanotransductory signals. The placement and distribution of osteocyte in the three-dimensional structure of the bone is architecturally well suited to sense the surrounding movements. In fact, these cells are extremely sensitive to microfluidic flow changes [122]. In some cases, osteoblasts and osteocytes have been found to show the same mechanical sensitivity [114]. Fortunately, the results of in vitro studies on these "bone derived cells" in culture have been in agreement with what is reported by in vivo results [122].

1.2.4 Cilia

The primary cilium is a non-motile microtubule-based organelle present on the surface of most mammalian cell types. Primary cilia transduce different types of extracellular stimuli into cellular responses through well-known signalling pathways such as Wnt, Hedgehog and platelet-derived growth factor. Through these pathways, cilia play a regulating role in cell differentiation, proliferation, migration and polarity, and are therefore essential in tissue morphogenesis [123].

The ciliary proteins are synthesized in the cytoplasm and must be transported to the cilium as an outward projected organelle. This tightly regulated task is performed through an active process called intraflagellar transport (IFT) that requires IFT complexes [124].

The importance of primary cilia has only been known for the last decade and ciliary machinery already have been implicated in several human disorders. Although ciliopathies share common clinical features they can target different organs or tissue including kidney, limbs, brain, retina, liver and bone [125]. Interestingly, skeletal anomalies are among common clinical features in most of human ciliopathies (Fig. 1-3).

The presence of cilia has been reported in most of bone cells including, osteocytes, osteoblasts and MSCs [123], [126]–[128]. Bone cell cilia are required for osteogenic differentiation, and mechanically induced bone remodelling and adaptation. Several studies showed that cilia disruption leads to impaired cellular bone functions such as osteoblasts differentiation, bone formation and even regulation of bone resorption through osteocytes [123], [129]–[134] (reviewed in Table 1-I). Disruption of an essential gene for cilia formation (Kif3A) led to the significant reduction of mechanically induced bone formation in mouse [135]. Espinha *et al.* [136] showed that oscillatory fluid flow induces an increase in microtubules around primary cilia in a time- and shear-rate-dependent manner. He showed also that primary cilia are essential for this load-induced cellular response.

The primary cilia are adaptive mechanosensors and possess a specific mechanism that can regulate the sensitivity of a cell to mechanical stimulation [95]. For example, cilium stiffness changes in response to mechanical and chemical stimuli. The sensory adaptation happens in a short span of time making cilia good candidates for targeted therapeutic approaches in disorders with impaired mechanosensitivity [137].

Table 1-I. Phenotypic consequences of ciliary protein disruption in bone cells.

Adapted from Kaku M. and Komatsu Y, Curr Osteoporos Rep (2017) 15:96–102.

Model	Target cells	Cilia phenotype	Bone phenotype	Signaling pathway	Reference
Mouse Kif3a$^{Prx1\text{-}cre}$	Mesenchymal skeletal progenitors	Cilia loss	Shortening of the limb	Hh	[138], [139]
Mouse Kif3a$^{Wnt1\text{-}cre}$	Cranial neural crest cells	Cilia loss	Craniofacial abnormalities, both endochondral and intramembranous skeletal structures	Hh	[139], [140]
Mouse Kif3a$^{Col\alpha1(I)2.3\text{-}cre}$	Osteoblasts	ND	Impaired mechanoresponse but normal development	ND	[141]
Mouse Kif3a$^{Oc\text{-}cre}$	Mature osteoblasts	Reduced cilia number	Osteopenia	Hh and Wnt	[142]
Mouse Ift80$^{Prx1\text{-}cre}$	Osteoblast progenitors	Cilia loss	Decreased bone mass	Canonical Hh-Gli and non-canonical Hh-Gαi-RhoA	[143]
Mouse Ift80$^{Prx1\text{-}cre}$	Mesenchymal skeletal progenitors	Cilia loss	Defect in endochondral bone	Shh and Ihh	[138]
Mouse IFT88$^{Oc\text{-}cre}$	Mature osteoblasts	ND	Decreased bone density in mixed background mouse. Increased bone volume in C57BL/6	ND	[142]
Mouse Ift88^{Tg737Rpw} (ORPK)	Global	Malformed cilia	Craniofacial abnormalities including cleft palate	PDGF	[144]
Mouse Pkd1$^{Oc\text{-}cre}$	Mature osteoblasts	Reduced cilia number	Reduced bone mineral density	Hh and Wnt	[145], [146]
Mouse Pkd1$^{Dmp1\text{-}cre}$	Osteocytes	ND	Impaired mechano-response	ND	[147]
Mouse IFT20$^{Wnt1\text{-}cre}$	Cranial neural crest cells	Cilia loss	Impaired intracellular collagen transport	PDGF	[148]
Zebrafish zygotic Ptk7^{hsc9}	NA	ND	Late onset 3D spinal curvature and vertebral wedging	Non-canonical Wnt pathway	[22], [149]

Ciliopathy	Skeletal deformity	Reference
Alström syndrome		**PMID: 15795345**
Asphyxiating thoracic dystrophy		**PMID: 17468754**
Bardet–Biedl syndrome		**PMID: 18443298** **PMID: 14676542**
Ellis–van Creveld syndrome		**PMID: 10700184**
Joubert syndrome		**PMID: 17558409**
Mainzer–Saldino syndrome		**PMID: 22503633** **PMID: 20856047**
Meckel–Gruber syndrome		**PMID: 17389183**
Nephronophthisis		**PMID: 1008585** **PMID: 1008584**
Oral–facial–digital syndrome		**PMID: 9249769** **PMID: 13900550**
Polycystic kidney disease		**PMID: 8320707**
Senior–Loken syndrome		**PMID: 8486308**
Simpson Golabi Behmel syndrome		**PMID: 6490008**

Figure 1-3 Human ciliopathies with skeletal deformities.

The icons respectively represent abnormalities in the extremities, including polydactyly and phalangeal cone-shaped epiphyses, craniofacial defects, short stature or skeletal dysplasia and spinal abnormalities, including scoliosis and kyphosis. Reconstructed and adapted from Nguyen A.M., Jacobs C.R., Bone 54 (2013) 196–204.

1.2.5 Bone mechanotransduction involved pathways

1.2.5.1 Wnt signaling

The canonical Wnt or Wnt/beta-catenin pathway is based on stabilizing beta-catenin. The Wnt proteins (such as Wnt10b, Wnt3a) attach to the LPR5/6 and Frizzled (FRZ) transmembrane receptors, activating a downstream signal that suppresses the activity of Glycogen Synthase Kinase 3 beta (GSK3beta), and inhibits beta-catenin phosphorylation [150]. A stable unphosphorylated beta-catenin molecule then translocate to the cell nucleus where it regulates the transcription of Wnt target genes. In the absence of Wnt initial signaling, GSK3beta remains active, destabilizing beta-catenin with phosphorylation, and eventually causing the ubiquitination and removal of this protein and thus Wnt signaling turns off [151], [152].

The canonical Wnt pathway is necessary for a healthy bone mass development and plays a major role in controlling skeletal patterning, development and homeostasis. This importance underscored by the number of human bone diseases associated with errors in this pathway [153]–[155]. Wnt pathway involvement in bone development starts at early stages by controlling the pattern in which bone material is laid.

Osteoblasts are one of the major cellular targets of the Wnt pathway in bone [151]. It has been reported that beta-catenin is an essential factor in determining whether mesenchymal progenitors become osteoblasts or chondrocytes, highlighting the role of Wnt signaling in osteoblast commitment [156], [157]. LRP5 loss- or gain-of-function mutations in humans or mice alter bone formation without affecting the resorption process [156]–[158]. This indicates that osteoblasts are indeed the main cellular targets of Wnt pathway in bone.

Loss and gain of functions in human Wnt co-receptor LRP5 are shown to lead to low and high bone mass syndromes, respectively [159], [160]. Wnt5a has also been implicated in bone, using an animal model study [161], which showed the reduction of bone mass following its genetic ablation, likely due to a decrease of osteoblast number.

In addition to osteoblast commitment and proliferation, Wnt signaling also affects osteoblast differentiation and function. Several Wnt signaling antagonists such as Sfrp2, Wif1, Dkk1 or FrzB, are strongly up-regulated during the late phase of osteoblast

differentiation. This fact suggests the involvement of a negative Wnt feedback loop throughout the last stages of osteoblast maturation. Expression of a constantly active mutant beta-catenin in osteoblasts led to an increase in expression of collagen in those cells [131], [151]. Wnt pathway also indirectly controls osteoclasts differentiation through its effects on osteoblasts and RANKL/OPG ratio.

In the case of transmitting mechanical signaling in bone, the wnt pathway plays an important role by activating or deactivating several signaling cascades [162]. Beta-catenin heterozygous deletion in mice osteocytes significantly mitigated the loading induced-anabolic response in bone [163]. Both Lrp5 and -6 play regulatory roles in loading-induced Wnt canonical signaling in bone. The loss of function mutation in Lrp5 have been shown to reduce or eliminate the load induced osteogenic response through reduction in mechanical-induced bone matrix deposition [164].

The positive effect of loading on bone formation could presumably be a consequence of an increase in Wnt stimulatory molecules or a reduction of Wnt inhibitory factors. For instance, the expression of Sclerostin (from Sost gene) as an Lrp5/Lrp6 antagonist is dramatically reduced in response to mechanical loading, and increased by skeletal disuse [165]. Despite similarities in structure and sequence between Lrp5 and -6, they seem to be different in their downstream load induced signalling. Lrp-5 affects bone formation while Lrp-6 regulates bone resorption. Lrp-6 effects are observed earlier in developmental phase than those of Lrp5 [150].

Beta-catenin is one of the major downstream targets of both Lrp5 and -6, and its inactivation in osteoblasts has been shown to cause osteopenia. The associated low bone mass phenotype in mice has been reported to be due to the increased number and activity of osteoclast thus affecting bone resorption rather than formation[166]. Interestingly, both beta-catenin alleles are proved to be necessary for mechanotransductory response in osteocyte and/or late stage osteoblasts [163].

1.2.5.2 Kinase signaling

Mitogen activated protein kinase (MAPK) pathways are activated in many cell types following an extracellular force induction. The MAPKs are among serine/threonine protein

kinases with fundamental roles in the differentiation, proliferation and cell survival. Physical forces can activate extracellular signal regulated kinases (ERK1/2) through a calcium dependent mechanism in bone cells, causing RANKL downregulation and decreased osteoclastic activity [167]. Akt kinase is another serine/threonine kinase which is activated by fluid shear stress in bone cells affecting MSCs differentiation process. This results in an increase in osteoblasts commitment and bone mass. Focal adhesion kinase (FAK) forms a network with other signaling proteins such as Src and the PIK3 kinases. This kinases network in response to mechanical activation of integrins stimulates downstream signals that lead to osteoblast proliferation. FAK also promotes the expression of osteopontin, osteocalcin, COX2, RUNX2 and Osterix (Osx) in mature osteoblasts which are among key osteogenesis regulators [168], [169].

1.2.5.3 Calcium signaling

Changes in intracellular levels of calcium affects cellular proliferation, differentiation and mobility. Mechanical stimulation of bone cells has been shown to follow up with a rapid rise in intracellular levels of calcium in bone cells through calcium channels [170]. Calcium movements can cause cytoskeleton rearrangement and activate various protein kinases such as PKA or MAPK, or trigger ATP and nitric oxide pathways in osteoblasts [171], [172].

1.2.5.4 G-Protein mediated signaling

G-protein coupled receptors are activated following mechanical induction causing rises in intracellular calcium, cAMP and cGMP levels[95]. Fluid shear stress application on osteocytes causes a temporary decrease in cAMP, which is catalyzed from ATP by adenylate cyclase (AC). AC isoform 6 has been shown to colocalize with cilium. Transient decrease in cAMP following shear stress is found to be AC6 dependent[173]. Primary cilium-mediated AC6 activation in osteocytes cells affects COX2 gene expression and PGE2 signaling [123]. Phospholipase C activation by fluid flow also initiates IP3 signaling, through a G-protein mediated mechanism, which in turn causes COX2 expression. RhoA GTPase is another important player in cellular response to mechanical strain. Mechanical

induced RhoA activity not only affects the MSC lineage commitment but also plays a role in the organization of cellular actin cytoskeleton to stress fibers. These contractile stress fibers are thicker structures that equip the cells to accommodate the applied mechanical challenge [119].

1.2.5.5 Prostaglandins

Prostaglandins are enzymatically derived from arachidonic acid that are implicated in bone remodeling. Therefore, they act as a vital element in healing processes and in bone tissue adaptation to stress responses [174]. Prostaglandin receptors are G-Protein coupled receptors. These receptors have a crucial role in regulating the functions of prostaglandins in bone [175]. Prostaglandin E2 (PGE2), in particular, plays a regulatory role in various processes of inflammation and bone metabolism [174]. Different types of mechanical induction have been reported to increase PGE2 levels in skeleton, such as hypergravity [175], fluid flow [176] and weight bearing [177].

Arachidonic acid transformation to prostaglandins is regulated by two cyclooxygenase (COX) isoenzymes, COX-1 and COX-2. They both affect the bone tissue but COX2 is the dominant one in osteoblasts [174]. COX2 protein is among the osteogenic factors that their expression in osteoblasts are induced by mechanical induction [127], [178], [179].

1.2.5.6 Estrogens

Declining levels of circulating estrogens in aging females and its direct correlation with post-menopausal osteoporosis suggest that estrogen receptors (ERs) are involved in bone mechanical induced adaptation. Both alpha and beta forms of ERs are facilitators of pathways functions in strain stimulated bone cells (osteoblasts and osteocytes) proliferation and osteogenesis. ER-alpha mostly contributes to the load-induced osteogenic response through the promotion of anabolic influences in osteoblasts and their progenitors. ER-beta is more involved in the strain-related responses induced in resident cells such as osteocytes. Activation of TGF1 receptors and COX2 expression or severe down regulation of sclerostin are among downstream effects of the ER stimulation following a mechanical

signal[180], [181]. Bone cell mechanotransduction pathways are summerized in figure 1-4.

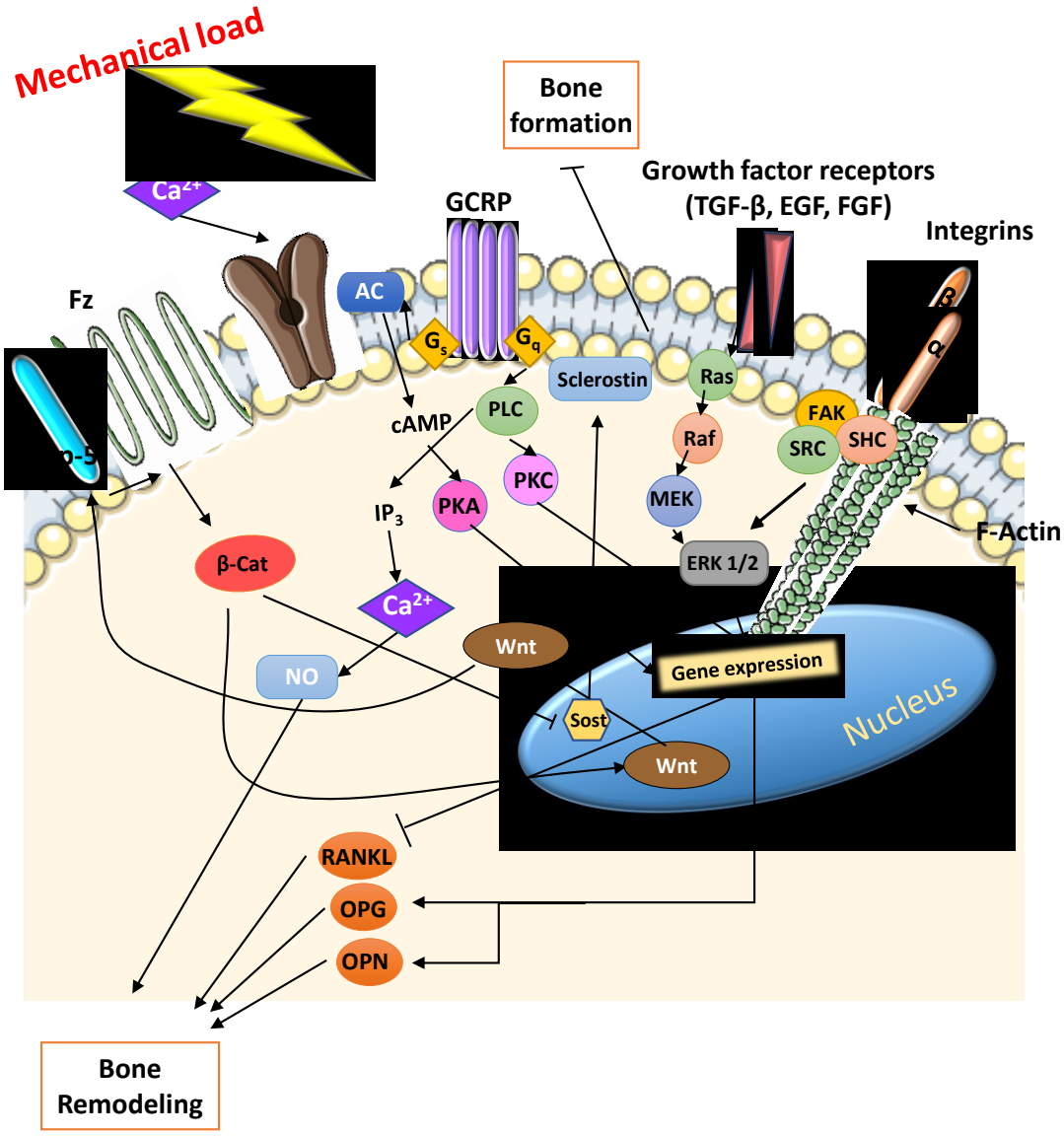

Figure 1-4 Bone cell mechanotransduction

Mechanical loading induces a complex cascade of events through several membrane bound sensors in bone cells. Here we show some of the more important players in osteoblasts and osteocytes. Inspired and redrawn from J Musculoskeletal Neuronal Interact 2016; 16(3):221-236.

1.3 Biomechanics and AIS

1.3.1 The challenge of modeling AIS in laboratory animals

One of the recalcitrant challenges in understanding the biological basis of scoliosis is the limitation of relevant animal models. The absence of spontaneous scoliosis in nature lies in the fact that humans are the only vertebrate walking in a fully erect position. Therefore, the upper body's center of mass is positioned directly above the pelvis in humans which is not the case in quadrupeds neither in other bipeds. The biped vertebrates walk with flexed hips and knees which put the spine in a more horizontal position, moving the upper body's center of mass in front of the pelvis (Fig. 1-5) [182].

Rodents that are conventionally used as laboratory animals are quadrupedal with different spinal structure and different center of gravity compared to human [54], [183]. Quadrupeds only become susceptible to spinal curvature when they are forced to walk upright, usually using drastic surgical or systemic interventions. This further confirms the importance of biomechanics in AIS development [183].

Gorman *et al.* [184] in 2007 for the first time used the biomechanical similarities between fish and human to conclude that non-induced idiopathic-type scoliosis is not exclusive to human nor bipedalism. She introduced the "Curve back" guppy as a model for

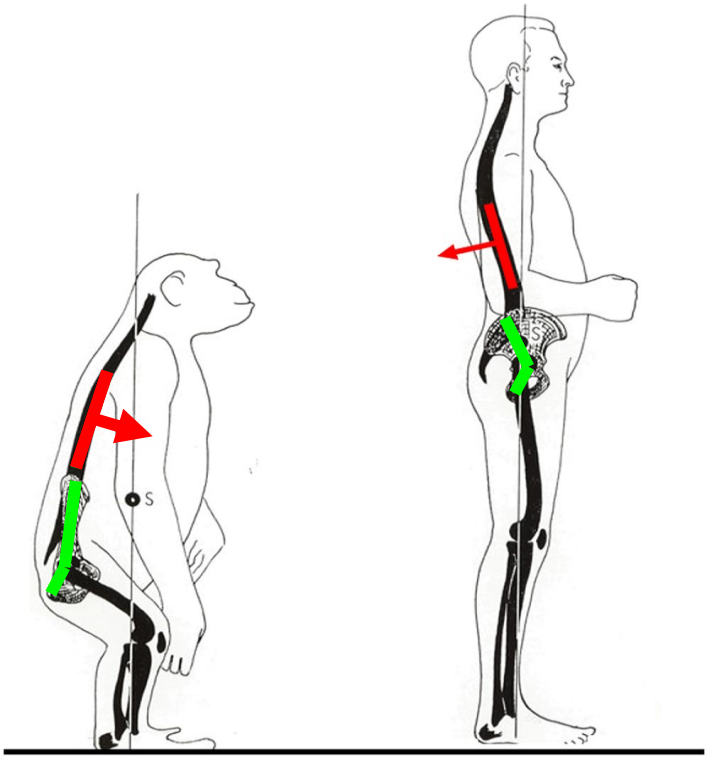

Figure 1-5 Biomechanical differences of human with other bipeds.

Pelvic axis in human and ape are shown by green lines. Bent-knee and bent-hip stature of the ape pushes the center of gravity in front of pelvis. The unique sagittal alignment of human spine, in comparison with the ape spine causes some area of the human spine to be subjected to posterior shear loads (red lines) which have been shown to reduce rotational stability of the spine. Adapted from Schlösser *et al.*, The Spine Journal 17 (2017) 1202–1206. Doi: https://doi.org/10.1016/j.spinee.2017.03.016

human idiopathic scoliosis with a strong genetic component and similar onset, variability and progression (Fig. 1-6). In a following paper in 2008, Gorman and Breden [182] proposed that AIS development depends on the interactions between normal spinal loading along the cranio-caudal axis with an unknown predisposing factor.

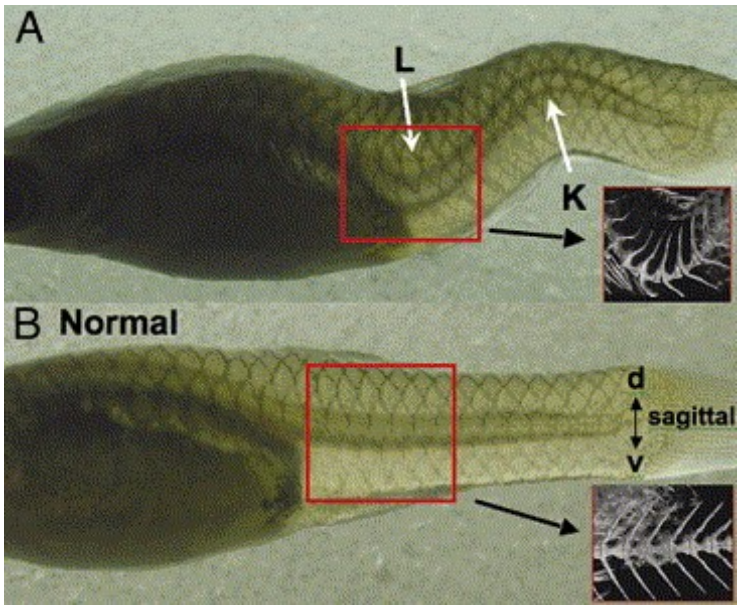

Figure 1-6 The Curveback guppy as a model for human idiopathic scoliosis.

A) The *curveback* phenotype is a primary anterior lordosis (L) and a secondary posterior kyphosis (K) occurring on the sagittal plane. CT scan image shows no vertebral breaks or fusion associated with curvature. B) Normal fish with sagittal plane and dorsal/ventral axes shown. Adapted from Gorman and Breden, Comparative Biochemistry and Physiology, Part C 145 (2007) 28–38, Doi: https://doi.org/10.1016/j.cbpc.2006.10.004

Ciruna *et al.* [22] later, generated a zebra fish model for skeletal curvature based on a sequence variant in a single AIS patient that disrupts ciliary protein, Ptk7. Zebrafish ptk7 mutants developed late-onset-spinal curvature that modeled AIS [22]. It is interesting to note that Ptk7 and cilia are both players in the Wnt pathway. Ptk7 plays a key role in non-canonical Wnt/planar cell polarity (PCP) signaling that coordinates the movement of polarized cells to shape the body axis during development [185]. Ptk7 also negatively regulates the activity of canonical Wnt/beta-catenin pathway [149]. Cilia also play a role in restraining Wnt/beta-catenin signalling [186].

Biomechanical similarities between fish and human and introduction of fish as an only non-induced AIS model confirms the importance of biomechanics in AIS development.

1.3.2 AIS biomechanics

The importance of biomechanics and bodily responses to mechanical stimuli in both development of AIS and its non-surgical therapy is well established within the scientific community. Understanding the biomechanics holds a great promise for the development of novel personalized therapeutic options for AIS [187].

There is a growth disparity between the anterior and posterior elements of vertebral bodies in idiopathic scoliosis patients. The diminished rate of growth in dorsal plane affects the ventrally located vertebral bodies, inhibiting them from growing vertically, forcing them to rotate and thus contribute to the curvature. Furthermore, recent studies have reported growth disparity between the spinal cord and vertebral column or a disproportional growth between the skeletal and neural systems in some scoliotic patients [188]–[191].

Another aspect of AIS biomechanics is the altered nature of forces that applies to an erect posture compared to the rest of primates. Castelain *et al.* [192] suggested that humans being bipedal results in dorsal shear forces that contribute to the rotational instability of spine. The spinal rotational instability in turn results in asymmetrical loading which cause asymmetrical growth of the spine and leads to scoliosis.

The negative effect of these unique dorsal shear forces on human spine has been confirmed to make the human spinal column more susceptible to rotational instability even in comparison with other bipedal animals [193]–[196]. In fact, neuromuscular anomalies have been observed in a portion of “idiopathic” cases of scoliosis as mentioned before. Several investigations reported the existence of an intraspinal syrinx (a fluid filled cavity) [187], [197], [198] or pathological somatosensory anomalies in some cases of typical idiopathic thoracic adolescent scoliosis [199].

Understanding biomechanics of scoliosis is of crucial importance to development of effective treatment strategies. Any attempt to mechanically correct the spine inevitably involves exerting some load or force. The corrective forces are variable in amplitude, frequency, flexibility, duration and mode of application. Developing accurate mathematical models such as Finite-Element Method to simulate the mechanical loading on the spine and the development and progression of the disease is an active area of research. Such models are sought to better understand the disease progression and optimise the best therapeutic approach for each patient based on their individual deformity [187].

Available knowledge on the biomechanics of AIS have been mostly limited to description of the deformity, gross mechanical forces and developing mathematical models for simulations. Unfortunately, the existing biomechanical theories and models fail to predict why, where and when the initial deformity commences.

1.4 **Hypothesis and accomplished objectives**

Skeletal abnormalities have been documented in many human ciliopathies (Fig. 1-3). The well documented role of cilia in bone mechanotransduction and gross skeletal biomechanical abnormalities that are associated with scoliosis phenotype suggest that cilia in particular and mechanotransduction in general are important in the etiology of AIS. The main hypothesis of the present dissertation was to answer this question: Does biomechanical impairment play a role in adolescent idiopathic scoliosis? We studied this hypothesis from three different angles, therefore the objectives were to investigate the mechanotransduction impairment in genetics, cellular and molecular aspects of AIS osteoblast samples compared to controls.

This hypothesis is addressed in two manuscripts that are presented in this dissertation. In the first article, we introduced a relationship between cilia abnormalities and AIS for the first time using osteoblasts. We showed that cilia abnormalities affect downstream mechanical induced molecular changes and signalling pathways in AIS osteoblast cells. To confirm the cilia involvement, we manipulated the morphology of cilia in control cells and observed similar molecular abnormalities seen with AIS cells in those cells as well. Finally, we investigated the genetic component using whole exome

sequencing and presented genetic evidence supporting the role of an impairment of the cellular mechanotransduction machinery in AIS development.

In the second manuscript, we further characterized the disturbed cellular mechanotransduction of AIS osteoblasts following mechanical induction. We showed that cilia do not sense nor response to the mechanical signals normally. We then presented novel evidence for mechanical-induced cytoskeleton abnormalities in AIS osteoblasts. Finally, we showed that disturbed mechanotransduction in AIS cells affect their overall behaviour in response to mechanical induction.

In this doctorate research we attempted to introduce and establish a role for cellular mechanotransduction as a novel etiological factor for adolescent idiopathic scoliosis.

Chapter II

Article One;

Identification of Elongated Primary Cilia with Impaired Mechanotransduction in Idiopathic Scoliosis Patients

Identification of Elongated Primary Cilia with Impaired Mechanotransduction in Idiopathic Scoliosis Patients

Published: Scientific reports 7, Article number: 44260, March 2017. DOI: 10.1038/srep44260

Niaz Oliazadeh[1,2], Kristen F. Gorman[3], Robert Eveleigh[4], Guillaume Bourque[5] and Alain Moreau[1,2,6*]

[1]Viscogliosi Laboratory in Molecular Genetics of Musculoskeletal Diseases, Saint Justine Children's Hospital Research Center. Montreal, QC, Canada.

[2]Department of Biochemistry, Faculty of Medicine, University of Montreal, QC, Canada.

[3]Department of Biological Sciences, California State University, Chico, CA 95929, USA.

[4]Genome Quebec Innovation Center, McGill University, Montréal, Quebec, H3A 0G1, Canada.

[5]McGill University, Montréal, QC, Canada.

[6]Department of Stomatology, Faculty of Dentistry, Université de Montréal, Montreal, QC, Canada.

[*]Corresponding author: Alain Moreau, PhD, E-mail: alain.moreau@recherche-ste-justine.qc.ca

Author contributions:

Niaz Oliazadeh: Conceived the study, designed, performed and analyzed the experiments, and wrote the manuscript as the lead author.

Kristen F. Gorman: Evaluated exome data, discussed and provided critical consultation during the study, and participated in writing of the manuscript.

Robert Eveleigh: Performed bioinformatic analyses of the whole exome sequences and SKAT-O analysis and participated in writing of the manuscript.

Guillaume Bourque: Supervised all bioinformatics.

Alain Moreau: The principal investigator who has secured the funding of this research project, supervised and supported the study and participated in writing of the manuscript.

2.1 **Abstract**

The primary cilium is an outward projecting antenna-like organelle with an important role in bone mechanotransduction. The capacity to sense mechanical stimuli can affect important cellular and molecular aspects of bone tissue. Idiopathic scoliosis (IS) is a complex pediatric disease of unknown cause, defined by abnormal spinal curvatures. We demonstrate significant elongation of primary cilia in IS patient bone cells. In response to mechanical stimulation, these IS cells differentially express osteogenic factors, mechanosensitive genes, and signalling genes. Considering that numerous ciliary genes are associated with a scoliosis phenotype, among ciliopathies and knockout animal models, we expected IS patients to have an accumulation of rare variants in ciliary genes. Instead, our SKAT-O analysis of whole exomes showed an enrichment among IS patients for rare variants in genes with a role in cellular mechanotransduction. Our data indicates defective cilia in IS bone cells, which may be linked to heterogeneous gene variants pertaining to cellular mechanotransduction.

2.2 Introduction

Idiopathic scoliosis (IS) is a complex pediatric syndrome that manifests primarily as an abnormal three-dimensional curvature of the spine. Eighty percent of all spinal curvatures are idiopathic, (MIM 181800) making IS the most prevalent form of spinal deformity. With a global incidence of 0.15% to 10% (depending on curve severity) [6], IS contributes significantly to the burden of musculoskeletal diseases on healthcare (http://www.boneandjointburden.org). Children with IS are born with a normal spine, and the abnormal curvature may begin at different points during growth, though adolescent onset is the most prevalent [200]. Idiopathic scoliosis is diagnosed by ruling out congenital defects and other causes of abnormal curvature, such as muscular dystrophies, tumors, or other syndromes.

The etiology of idiopathic scoliosis is unknown largely because of phenotypic and genetic heterogeneity. Curve magnitude is highly variable and the risk for severe curvature is not understood beyond the observed female bias. Although a genetic basis is accepted, genetic heterogeneity has been implicated in several familial studies [201], [202] and numerous genome-wide association studies (GWAS) have detected different loci with small effects [15]. Despite such genetic correlations, no clear biological mechanism for IS has emerged. It is likely that IS phenotypic heterogeneity is a consequence of genetic variations combined with biomechanical factors that are influenced by individual behavioral patterns. As a musculoskeletal syndrome, biomechanics are thought to have an important role in the IS deformity. Pathological stressors applied to a normal spine or normal forces on an already deformed spine have been studied for a role in curve predisposition and progression [203]. For example, factors that contribute to spinal flexibility, sagittal balance, shear loading on the spine, and compressive or tension forces may contribute to the 'column buckling' phenotype associated with IS [187], [204], [205]. Furthermore, therapeutic options available for IS, bracing and corrective surgery, approach the disease from a mechanical perspective, and successful outcomes depend on understanding the complex biomechanics of the spine. In this paper, we report evidence supporting an association between IS and mechanotransduction through the non-motile microtubule-based signaling organelle known as cilium.

Primary cilia are antenna-like organelles that transmit chemical and mechanical signals from the pericellular environment [133], [206]. They are found in the cells of all human tissues (except blood), including bone, cartilage, tendons, and skeletal muscle (a comprehensive list of tissue types and cell lines with primary cilia can be found at: http://www.bowserlab.org/primarycilia/ciliumpage2.htm). In addition to functions linked to olfaction, photo and chemical sensation, recent studies have established a mechanosensory role for primary cilia in tissues, such as the kidney, liver, embryonic node, and bone structure (the mechanosensory role of cilia in bone is reviewed by Nguyen, et al., 2013) [123]. As the most recent established role for cilia, mechanisms for mechanosensation are not yet entirely understood. For example, the involvement of calcium channels, in response to cilia bending following a fluid movement, is yet a matter of debate and might vary depending on the tissue examined [207], [208].

As a mechanosensor in bone, the primary cilium can transduce fluid flow induced shear stress occurring within the canaliculi that interconnect osteocytes as well as strain-related mechanical stimuli in pre-osteoblasts [209]. The load-induced fluid flow in bone canaliculi is recognized to play a role in maintaining bone homeostasis through bone resorption and formation cycles (i.e. bone tissue remodelling) [210]. Cilia mediate the transduction of this fluid flow to mesenchymal stem cells (MSCs), and is implicated in osteogenic gene expression and lineage commitment [127]. Mechanical loading modulates the incidence and length of primary cilia in cells, such as chondrocytes, in which cilia direction affects the direction of growth in growth plates [211]. Mechanical loading has also been shown to induce bone cell proliferation through a cilia-dependent mechanism [209]. Interestingly, skeletal disorders are a common feature in several human ciliopathies, such as Jeune syndrome and short rib-polydactyly [212].

Considering the role of primary cilia in mechanotransduction, our hypothesis was that idiopathic scoliosis is a ciliopathy-like condition and that the genetic architecture of IS may involve enrichment of pathogenic variants in ciliary genes. To explore this idea, we reviewed established ciliary genes for an association with spinal curvature and the function of validated IS genes for connections to cilia. We found that numerous ciliary genes present a spinal curvature phenotype when knocked down in animal models, and that scoliosis is associated with many human ciliopathy syndromes [213], [214]. Additionally, the majority

of confirmed IS associated genes are connected to cilia structure or function (Table 3.1). To test our hypothesis, we examined bone-derived cells and exomes of patients and controls.

Confocal images of primary osteoblast cultures, derived from bone fragments obtained intraoperatively at the time of the spine surgery, revealed that IS patients have longer primary cilia and an increased density of cells with elongated cilia. To investigate functional consequences of the IS cilia phenotype, we applied controlled mechanical strain to bone cell cultures and examined the expression of osteogenic, mechanosensitive, and Wnt signaling genes at several time points. To explore a direct genetic correlation between cilia and IS in our French-Canadian cohort, we used SNP-set Kernel Association Test – Optimal Unified approach, or SKAT-O [215] to analyze exomes of 73 IS patients and 70 controls. The results suggest that IS may be caused by variants in genes related to cellular mechanotransduction but is not restricted to ciliary genes.

2.3 **Results**

2.3.1 Osteoblasts of IS patients have longer cilia.

To assess whether there is an observable defect associated with primary cilia in IS patients, we chose to look at osteoblast cells derived from bone specimens obtained during surgery. All samples were from age matched adolescent female subjects. FBS deprivation was used to promote ciliogenesis and differentiation. We examined cilia morphology using anti-acetylated α-tubulin immunofluorescence staining prior to and after 24, 48, and 72 hours (h) starvation in primary osteoblasts from 4 IS patients and 4 non-scoliotic trauma patients used as controls (Fig. 2-1a). The fraction of ciliated cells and cilia length were quantified in fixed and stained cells. Measurements were acquired from 5 x 5 stitched tile images per sample, in duplicate (50 fields). We found that the cilia in IS-derived cells were approximately 30% to 40% longer than cilia in control cells (Fig. 2-1b, Table 2-II). We also observed that IS cells showed a reduced incidence of ciliated cells compared to controls, although the difference did not reach the statistical significance (Fig. 2-1c). To validate the staining of cilia, double immunostaining was performed on fixed IS osteoblasts

using anti-Ninein, as the basal body marker or anti-IFT88 to stain the length of cilia alongside the anti-acetylated α-Tubulin (Supplementary Fig. 2-1).

2.3.2 IS and control cells grow at the same rate.

Cilia assembly, disassembly, and length have been associated with cell cycle and control of cell proliferation [216]. To investigate if there is a correlation between longer cilia in IS patients and a differential growth rate, we assayed proliferation by counting viable cell (Trypan Blue stained) number as a function of time. Cell proliferation rate was various in all the samples as it is visible in the error bars (Fig. 2-2). It seems that IS cells increase in number slightly faster than controls, but the difference does not pass the significant threshold at any of the three time points analyzed (24, 48 and 72 h).

2.3.3 Lithium Chloride (LiCl) increases the length of primary human osteoblasts.

Lithium chloride has previously been used to induce longer cilia in some cell types [217]. To examine whether the LiCl induced elongated cilia is similar to the long cilia phenotype observed in IS cells, we treated the control cells with three different concentrations of LiCl (1mM, 10 mM and 50mM) [217] and examined their cilia with confocal microscopy. Primary human osteoblasts died after 24h of exposure to 50mM LiCl. However, we measured a significant increase in the cilia length at both 1mM (3.94 ± 1.24 μm) and 10mM (5.81 ± 1.72 μm) LiCl treated cells compared to non-treated cells (2.18 ± 0.48). LiCl treatment did not affect the percentage of ciliated cells (Supplementary Fig. 2-2).

2.3.4 LiCl affects the expression of Wnt signaling indicators and osteogenic factors.

To investigate the possibility of inducing an IS-like phenotype in control cells using LiCL, we tested the expression of several osteogenic and signaling factors in IS cells and LiCl-treated controls in comparison with non-treated controls (Table 2-III). Primary human osteoblast cells from the control group were treated with 10 mM LiCl, for 24h (Based on work by Thompson et al 2016) [217]. As expected [217], LiCl caused a decrease in GSK3B

expression. Inhibition of GSK3B is associated with the activation of canonical Wnt signaling, and in both LiCl treated cells and IS cells there was an increase in beta-catenin expression (3.4-fold and 5.8-fold respectively). However, IS patients did not have altered basal expression for GSK3B, instead they showed a 2-fold decrease in AXIN2 expression, which was not the case in LiCl-treated control cells. Both IS and LiCl treated cells had significantly decreased levels of RUNX2. LiCl treated cells had a 3.9-fold increase in PTGS2 (COX2) expression that was not observed among IS cells. Idiopathic scoliosis cells had a 2-fold overexpression of SPP1 compared to controls but treated cells showed a 2.7-fold decrease in expression.

2.3.5 IS cells have impaired biomechanical response.

We evaluated the functional response of IS cells having long cilia by monitoring changes in expression for several mechanoresponsive genes under fluid flow, at four time points (0, 4 h, 8 h, 16 h). We applied a 1 [Pa] shear stress (the magnitude at the center of the dish) in 1 [Hz] frequency, which corresponds to a Womersley number of 8, equations (1, 2 and 3). The biomechanical parameters were chosen to be physiologically relevant based on the reported frequency spectra of forces affecting the human hip during walking, (1-3 Hz) [218], and the Womersley number (5-18) estimated for cerebrospinal fluid motion in the spinal cavity [219].

Differential gene expression was compared for IS vs. controls at each time point, and then the whole response profile of each gene was examined. For each gene, after normalization to two endogenous controls (GAPDH and HPRT), the baseline expression level at 0h (before treatment) of every sample was defined as its own calibrator. The gene expression for all time points for each sample was compared to its own 0h (which has a RQ value of 1). The results have been shown as fold changes compared to the calibrator (Fig. 2-3). We asked one question per gene: is there any difference between IS and control at each time point? For three genes (ITGB1, CTNNB1 and POC5) that showed a different overall expression pattern in IS vs. controls, we asked a second question: is there a significant difference in gene expression before and after flow? Each gene has been analyzed independently using a pair wise t-test for each question followed by a post hoc

Bonferroni. Concordant with previous findings regarding biomechanical induction and the expression of osteogenic factors [123], [127], [220], our assay showed a dramatic increase in Bone morphogenetic protein 2 (BMP2) and Cyclooxygenase-2 (COX2) expression in IS and controls, following 4 and 8 hours of fluid flow induction. However, for both genes, the IS response was significantly less than controls (Fig. 3-3). The response for Runt-Related Transcription Factor 2 (RUNX2) in IS patients, while not significant, is also less than what we observed in controls. We also tested the expression of Secreted Phosphoprotein 1 (SPP1, also known as Osteopontin or OPN) as an osteogenic factor in bone and did not observe a biomechanical response in IS or control cells (Fig. 3-3). The modified responses to mechanical stress observed in this study corroborate those previously reported in human mesenchymal stem cells (MSCs) [127]. Expression of integrin beta 1 (ITGB1) and integrin beta 3 (ITGB3) were monitored due to their possible role in transmitting mechanical signals in bone [221]. The expression of ITGB1 did not notably change during 16 h of flow application in controls, while a significant decrease in expression was observed in IS cells ($p = 0.025$) at 4 hours post flow. ITGB3 expression did not significantly change in IS or control cells. Cilia are well known for their regulatory effect on the Wnt signaling pathway [129]. Beta-catenin, a main player in the Wnt pathway [118], [129], [222], is localized to the cilium [223]. We found the expression of beta-catenin (CTNNB1) did not change in control osteoblasts as it has been shown previously [118], while IS cells showed a significant continual rise in CTNNB1 expression in response to flow application (p at 4 h = 0.03, 8 h = 0.008). To further explore the role of Wnt signaling in IS, we also tested the expression of Axin2, GSK3B (Glycogen Synthase Kinase 3 Beta), and INVS (Inversin), after exposure to flow. Although pairwise comparisons between IS and controls did not show a significant difference in Axin2 expression, IS cells showed a reduced response to mechanical stimuli. This was most apparent after 4 hours of flow application, where control cells had a significant reduction in expression but IS cells did not. Inversin and GSK3B responses were not significantly different between IS and controls. To examine the possibility of Hedgehog pathway involvement in the IS mechanical response, we measured the activity of PTCH1 (patched) and Gli1 as established indicators of HH pathway activity [217]. PTCH1 expression decreased among both IS and controls at all times, although after 4 hours we observed a more significant response among IS patients (Supplementary Fig.

2-3). GLI1 expression was not detected after 35 cycles in two attempts of RT-qPCR (data not shown).

Fuzzy planar cell polarity (FUZ), Protein Of Centriole 5 (POC5), and Ladybird homeobox 1 (LBX1) genes were added to the experiment following our exome analysis, and recent published scoliosis genetic studies [201], [224], [225]. For FUZ, response profiles were not different among IS and controls (data not shown). Although, we did not see any significant differential expression between IS and controls for POC5, it is worth mentioning that its expression decreased almost by half at the 4-hour point in both IS and controls ($p < 0.05$), suggesting a role in early stages of mechanotransduction response (Fig 3). LBX1 expression was not detected after 35 cycles in two attempts of RT-qPCR (data not shown).

2.3.6 LiCl treated control cells also show impaired biomechanical response.

We examined the mechanosensory response of control osteoblasts treated with LiCl for comparison to the non-treated control and IS patient cells. An ANOVA was used to compare gene expression levels among the three groups and a Tukey test was used for post-hoc analysis of significant results. In LiCl treated control cells the three osteogenic genes (BMP2, PTGS2, RUNX2) showed a dramatic decrease in expression in response to flow that was significant for BMP2 and PTGS2. This response had a similar but exaggerated pattern compared to that observed in IS cells (Fig. 2-4). Of the other genes tested, none showed a significant differential response (Supplementary Fig. 2-3).

2.3.7 Whole Exome Sequencing (WES) results.

We used whole exome sequencing to test the hypothesis that rare variants in ciliary genes might be causal for IS. We performed exome sequencing on peripheral blood DNA sampled from 73 IS and 70 matched controls using the Agilent SureSelect Human All Exon 50 Mb v3 capture kit and the Life Technologies 5500 SOLiD Sequencing System. Variants were called and annotated using a customized bioinformatics pipeline including SAMTOOLS, GATK and Picard program suites [226]. To reduce the number of likely variants, we subsequently filtered the total variant set to remove those with a minor allele

frequency greater than 5%, as well as variants not in or adjacent to protein-coding exons. After filtering, our dataset included 73 IS patients, 70 controls, 8544 genes, and 16,384 variants. We used SKAT-O to survey our exome data under two different weighting parameters: in favor of lower frequency variants (Madsen Browning weighting, Set I), and in favor of variants with projected deleterious effects and pathogenicity (Combined Annotation Dependent Depletion: CADD weighting, Set II). Since the underlying biology of idiopathic scoliosis is not understood, an omnibus test such as SKAT-O is considered more powerful than a burden test because it does not make assumptions regarding direction or size of variant effect [227]. Analysis using Madsen Browning weighting (Set I) identified 259 genes and analysis using CADD weighting (Set II) identified 240 genes that are significant ($p \leq 0.01$) after correction for multiple testing. The Sets were compared and genes that were significant in both (n = 120; Supplementary Table 2-1) were considered candidates for idiopathic scoliosis. This list was examined for ciliary genes using the SYS`CILIA gold standard list [228] and the Kim *et al.* 2010 [229] list as references, along with inquiries using Google search engine. Fuzzy planar cell polarity protein (FUZ) is the only known ciliary gene in both data lists. However, there is a greater number of variants in controls compared with cases (12 controls with at least one variant vs 1 patient). Of the candidate genes, the 25 most significant ($p < 0.001$) were further examined to determine the number of patients and controls having at least one variant. Seven of these genes have greater variant enrichment among patients: CD1B, CLASP1, SUGT1, HNRNPD, LYN, ATP5B, AL159977.1 (Supplementary Table 2-1).

We also looked at the variant profile for each of the four IS patients used in our cellular analyses, to see if there are shared genes with variant enrichment. Controls could not be examined because the cohort used for molecular work differs from the genotyped control cohort. Control bone tissue was obtained intraoperatively from non-scoliotic trauma patients whereas the genotyped controls were from a non-surgical cohort. None of the genes identified in our combined SKAT-O table were shared among all the four tested patients, but they all have variants in either CD1B, CLASP1, or SUGT1. The CDK11A gene is represented among three patients, but in the exome cohort, nearly all patients and controls have at least one variant for this gene (Supplementary Fig. 2-4).

2.4 Discussion

In the current study, we provide experimental evidence that correlates idiopathic scoliosis (IS) with morphological and functional abnormalities in cilia. Elongated primary cilia in IS patient osteoblast cells is a novel observation that may be linked to the etiology of the disease. We examined the possibility of inducing IS like phenotype in control osteoblasts by increasing their cilia length with LiCl treatment. Using SKAT-O to survey IS and control exomes, we suggest that idiopathic scoliosis is a result of heterogeneous defects in genes pertaining to the cellular mechanotransduction machinery. Currently, idiopathic scoliosis is exclusively defined by its clinical phenotype and genetic studies have failed to identify a consensus ontology. Therefore, this study introduces an important biological context to understand mechanisms associated with the disease.

We found that cilia in IS cells are significantly longer across all measured time points, but the most conspicuous length differences are visible before starvation and at 24 hours after starvation (Fig. 2-1b), suggesting an abnormality in cilia formation at early stages of cilia growth. Although we did not see any significant differences in the percentage of ciliated cells before starvation, long cilia (up to 13 μm in few cells) were visible in pre-starved IS bone cells and not controls. This could suggest actin organization impairment, considering that actin polymerization inhibitors induce longer cilia and facilitate ciliogenesis independently of starvation [229]. Irregularity in the control of cilia length has been associated with cytoskeletal disruption and actin dynamics, either due to genetic mutation [229] or in response to mechanical stress [230]. While there is no statistically significant difference in the incidence of cilia between controls and IS, there does seem to be a trend of IS cells having a lower incidence than control at every time point. This might be an indicator of cell cycle irregularities, considering the tight correlation of cilia differentiation to cell cycle progression. Our proliferation assay confirmed that the IS cilia phenotype is independent of cell proliferation, but we did not rule out the existence of any impairment in different phases of cell cycle. In an attempt to induce an IS like phenotype we treated control osteoblasts with LiCl, which significantly increased the length of their cilia. The primary cilium participates in cell signaling, cell cycle regulation and mechanotransduction during development, homeostasis, and regeneration. The length of the primary cilium has an important effect on the quantity of forces transmitted to internal

cell components, with longer cilia inducing higher strains compared with shorter ones [133]. In addition, the higher deflection of a long cilium will affect the regulation of certain molecular responses, such as stretch-sensitive channels, and transporter proteins, plus key pathways such as Hedgehog, Wnt, and platelet-derived growth factor signaling [133], [134], [221], [231]–[233].

Cilia have been shown to play important roles in both the canonical Wnt/beta-catenin and non-canonical Wnt/planar cell polarity pathways [129], although these roles are not well understood. The Wnt/beta-catenin pathway controls gene expression through the stability of beta-catenin [223]. Cilia are known to restrain canonical Wnt signaling [223] by beta-catenin regulation [234]. The absence of cilia alters beta-catenin activity and increases Wnt signaling, while multiciliated cells show an inhibited Wnt response [234]. The effect of elongated cilia on Wnt activity is not fully understood. In both IS cells with naturally longer cilia and LiCl treated cells with induced elongated cilia we observed an elevation in basal levels of CTNNB1 (beta-catenin 1) gene expression. LiCl treatment is known to mimic canonical Wnt activation through the inhibition of GSK3B, and subsequent prevention of beta-catenin protein degradation. Although we did not observe altered expression of GSK3B among IS cells, there was a decrease in basal expression of AXIN2, another negative regulator of canonical Wnt signaling. Furthermore, in both induced and IS elongated cilia phenotypes there was a decrease in basal levels of RUNX2 expression. This is consistent with LiCl induced inactivation of GSK3B, and the fact that GSK3B and Wnt are among RUNX2 regulators [235]. We assayed Inversin (INVS) as an indicator of non-canonical Wnt activity while PTCH1 and GLI1 were chosen as players in Hedgehog signaling, based on the previous works by Simons (2005) [236] and Thompson (2016) [217], respectively. We did not observe significant basal expression differences among IS, LiCl-treated, and controls for INVS or PTCH1. GLI1 showed a slight decrease (0.6-fold) in IS cells compared to controls, but its expression was not detected in LiCl treated cells. In summary, the basal gene expression profile of the IS cells with elongated cilia has similarities to the LiCl induced elongated cilia in control cells, suggesting altered canonical Wnt signaling (Table 3).

Bones are under constant mechanical stimulation that is transferred to cells through cilia. Changes in mechanical loading have a regulatory effect on bone cell turnover through

changes in gene expression [210], [237]. We applied physiologically relevant mechanical stimulation to bone-derived cells and surveyed gene expression to investigate the effect of IS elongated cilia on cellular mechanotransduction. Bone morphogenic protein 2 (BMP2), Runt related transcription factor 2 (RUNX2) and Cyclooxygenase-2 (COX2) are involved in several interconnecting pathways that lead to osteoblastogenesis and bone formation [238]. Considering their established mechanosensitivity, the fact that all these genes showed a reduced response to mechano-stimulation in IS cells might explain why almost half (38% to 65% in different cohorts) of IS patients suffer from osteopenia and/or osteoporosis [239], [240]. When we treated control cells with LiCl, we increased the length of their cilia and they also showed a dramatically decreased response for osteogenic factors upon mechanical stimulation (Fig. 2-4). Our results suggest that the lower bone mass density reported for IS patients could be the result of abnormalities in late stages of bone formation and mineralization, or perhaps as a consequence of their poor response to mechanical stimulation, which could be associated to the elongation of their cilia. COX2 (also known as Prostaglandin-Endoperoxide Synthase 2, PTGS2) is a cilia-dependent mechanosensitive gene in bone and the key enzyme in prostaglandin biosynthesis. Addition of prostaglandin has been associated with irregularity of cilia length in IMCD3 cells, and COX2 knockdown caused curved body axis in zebrafish (31%; n = 110) [241]. Interfering with beta 1-integrin signaling can reduce the normal upregulation of COX2 that occurs after mechanical stimulation in osteocytes [242]. Integrins are localized to the primary cilium [243] and mechanical stimuli modulates integrin-mediated signals that are transmitted through focal adhesion sites and actin bundles [244]. In the case of the two integrins that we tested, beta 1 and beta 3, the response pattern to flow were found to be different between IS cells and controls. These trends further demonstrate the existence of an altered mechanosensation in IS cells, and reflect the *in silico* work of Khayyeri *et al.* 2015 [133], where elongated cilia were modeled to show hypersensitivity to mechanical stimuli. Figure 2-5 illustrates how our tested genes are related through pathways that link ciliary mechanotransduction to bone formation. In response to mechanical stimulation, IS cells having elongated cilia showed an immediate elevation in CTNNB1 (beta-catenin) expression that increased throughout the 16-hour profile (Fig. 2-3), which was not seen in controls or LiCl treated cells. The mechanical response profiles for the other signaling

molecules did not significantly differ among IS, control, or LiCl treated groups (Supplementary Fig. 2-3).

Bone mass homeostasis is the outcome of constant regulation of complex interactions between several systems including growth factors, hormones and mechanical loading. Wnt signaling has been shown to regulate bone remodeling, although different studies suggest different roles. *In vivo* administration of LiCl has been shown to increase bone mass in mouse models [245] but not in supplemented chickens [246]. *In vivo*, inhibition of beta-catenin degradation in osteoblasts resulted in a high bone mass phenotype [131]. In addition, several studies suggest an inhibitory role for the Wnt pathway on osteoblastic differentiation [247], [248]. Jansen *et al.* (2009) show that the role of Wnt in bone homeostasis is experimentally dependent on the type of cell examined, the stage of differentiation, interactions with other mechanosensitive pathways, and the duration of mechanical loading [130]. Our LiCl treated control cells showing a reduced biomechanical response for osteogenic factors similar to IS cells, could be the results of disturbed Wnt signaling which is required for later stages of osteoblast differentiation and matrix mineralization [247].

Elongated cilia can be caused by decreased intracellular calcium, increased cyclic AMP, cyclic AMP-dependent PKA activity [249], and modulation of the target-of-rapamycin (TOR) growth pathway [250]. Interestingly, increased cAMP levels were reported previously in IS osteoblasts and seems to be caused by a hypofunctionality of G inhibitory proteins [47], [48]. The cilium is highly dynamic in its capacity to respond to extracellular stimulation and induce downstream intracellular changes. It is important to remember that we counted the number of ciliated cells and measured their lengths while they were in a stationary phase. We do not know how the cilia length changes in response to flow. Considering the dynamic nature of cilia, this could be interesting to study. Varying levels and duration of mechanical loads have an important role in cilia length regulation via an adaptive signaling mechanism [251]. Further insights could be gained from future studies investigating the IS cilia phenotype under different mechanical stimulations.

Ciliopathies comprise a large number of human genetic disorders that are defined by the causative or predisposing gene being related to cilia structure, function, sensory

pathways, or localization. To examine whether the IS cilia phenotype is linked to ciliary genes, we reviewed established cilia gene lists for associations to spinal curvature and surveyed well defined IS genes in human and animal studies for a functional link to cilia. From our review using the SYSCILIA gold standard list of 303 verified ciliary genes, we found that 55 genes are associated with a human syndrome having clinical reports of scoliosis. Two of these genes, SUFU (Suppressor of fused homolog) and AJAP1 (Adherens junctions associated protein 1) are in loci that are associated with IS through linkage studies [252], [253], and 19 have both clinical (human) and experimental (animal model) associations with scoliosis. Furthermore, we found an additional 13 published animal model studies in which manipulation of the ciliary gene caused spinal curvature. In summary, 22% of these well-established cilia genes are associated with spinal curvature. In addition, from the study by Kim *et al.* 2010 [229], we found 3 other genes that modulate ciliogenesis or cilia length and feature a clinical syndrome with reported scoliosis. Supplementary Table 2-2 is a list of ciliary genes that are associated with a scoliosis phenotype.

All well supported IS genes, and several genetic animal models with a similar curve phenotype, are linked to cilia (Table 1-I). We tested two of the IS genes, Ladybird homeobox 1 (LBX1) and POC5, for differential mechanotransduction in our functional assay. We were unable to amplify LBX1 from our bone cells (data not shown), but POC5 showed a dramatic response after 4 hours of stimulation suggesting a role in mechanotransduction, although not exclusive to IS. POC5 in mammalian cells plays a role in stages coupled to cell cycle progression. POC5 is essential for centriole assembly and procentriole elongation. Procentriols can eventually mature to serve as the base of cilia [254]. Considering the initial depletion of POC5 expression in our results and the apparent recovery at later stages of flow application, it would be interesting to study the dynamics of cilia growth in response to shear stress in coordination with POC5 expression and localization.

Considering that many ciliary genes are associated with spinal curvature, and that IS genes are implicated in ciliary function or structure, we expected to find an enrichment of rare variants in ciliary genes in our French-Canadian cohort. From our exome analysis, the only ciliary gene among our candidates is FUZ, encoding a planar cell polarity protein

that is involved in ciliogenesis and cell mobility. However, FUZ has a greater number of variants among controls, and we did not see a biomechanical response in its gene expression (among patients or controls). Among the 25 most significant genes in our list of candidates, we identified seven that have a greater number of variants among patients compared to controls. Interestingly, the majority of these genes are involved in elements of cellular mechanotransduction machinery. For example, Cytoplasmic linker associated protein 1 (CLASP1) not only interacts with actin filaments and regulates microtubules, but also is essential for maintaining spindle position and correct cell division axis [255]–[257]. CD1B and LYN also interact with actin [258]. LYN plays an important role in integrin signaling and regulates cell proliferation, migration, and differentiation [259]. SUGT1 and HNRNPD have roles in cell cycle and cell proliferation [260], [261]. SUGT1 is also required for centrosome organization [260]. Our examination of variant profiles for patients used in our cellular analyses depict that all have variants in at least one of the following: CD1B, CLASP1, SUGT1 (Supplementary Fig. 2-4).

Although our reviews support a direct role for ciliary genes in IS, our exome data suggests that elongated cilia result from cellular processes affecting cilia indirectly. This is reinforced by our observations of elongated cilia prior to and during early cell cycle events. It is possible that idiopathic scoliosis is a result of heterogeneous gene defects pertaining to the cellular mechanotransduction machinery in general. Independent support for this idea comes from a recent IS exome study that reports rare variants in extracellular matrix (ECM) genes strongly contributing to disease risk [42] Cilia extend outward from cells and protrude into the ECM environment to sense substrate changes. It has been shown that ECM molecules such as collagen are closely associated with primary cilia in chondrocytes, in which several well-known ECM receptors colocalize with primary cilia [233], [243].

This study identifies elongated cilia in idiopathic scoliosis patient bone cells as a new observation connected to the phenotype, and demonstrates functional consequences related to cellular mechano-responsiveness. Although validated IS genes are functionally or structurally linked to cilia, exome results suggest that the genetic architecture is more broadly related to biomechanics. Differential basal gene expression in IS cells compared to control cells treated with LiCl and untreated, suggest altered canonical Wnt signaling. Wnt signaling is known to affect bone homeostasis and biomechanical responsiveness

[105], [262]. We demonstrated an impaired biomechanical response in both IS cells and LiCl treated cells. However, gene expression differences between the IS and LiCl induced elongated cilia phenotypes reflect a unique mechanism for the IS phenotype. Further studies are required to elucidate the signaling pathway(s) altered in IS and how these relate to genetic studies.

2.5 Methods

2.5.1 Study cohort

This study was approved by the institutional review boards of The Sainte-Justine University Hospital, The Montreal Children's Hospital, The Shriners Hospital for Children in Montreal and McGill University, as well as the Affluent and Montreal English School Boards. Parents or legal guardians of all the participants gave written informed consent, and minors gave their assent. All the experiments were performed in accordance with the approved guidelines and regulations. All the subjects are residents of Quebec and are of European descent. Each IS patient was clinically assessed by an orthopedic surgeon at the Sainte-Justine University Hospital. The inclusion criteria for this study was a minimum Cobb angle of 10 degrees and a diagnosis of idiopathic scoliosis. Cobb angle is the clinical parameter used for quantification of curve magnitude where a larger angle denotes a greater magnitude. For cellular experiments, we used bone samples from a subset of patients who required corrective surgery. Control bone samples were from surgical non-scoliotic trauma patients recruited at the Sainte-Justine University Hospital. All patients used for cellular studies were adolescent females (Table 2-IV). The medical files of controls were reviewed to exclude the possibility of scoliosis. For exome sequencing, control blood samples were collected from non-IS participants that were first screened by an orthopedic surgeon using the forward-bending test (Adam's test) [263]. Any children with apparent spinal curvature were not included in the control cohort.

2.5.2 Cell culture

Primary osteoblasts were derived from bone specimens obtained from IS patients and trauma patients (as controls), intraoperatively. For all IS cases, bone specimens were

surgically removed from affected vertebrae (the sampled vertebrae varied from T3 to L4) as a part of correctional surgery. For non-scoliotic control cases, bone specimens were obtained from other anatomic sites (tibia or femur) during trauma surgery. Using a cutter, bone fragments were manually reduced to small pieces under sterile conditions. The small bone pieces were incubated in αMEM medium containing 10% fetal bovine serum (FBS; certified FBS, Invitrogen Life Technologies, ON, Canada) and 1% penicillin/streptomycin (Invitrogen) at 37°C in 5% CO_2, in a 10-cm^2 culture dish. After one month, osteoblasts emerging from the bone pieces were separated from the remaining bone fragments by trypsinization. Bone cells were characterized using alizarin red (Supplementary Fig. 2-5) and ALP staining (data not shown). In addition to the expression of osteoblast markers (RUNX2, SPP1 and BMP2) used in our qPCR experiment, we also confirmed the expression of Alkaline Phosphatase, Bone Sialoprotein II and Osteocalcein, using RT-PCR, as osteoblast specific genes in our primary cultures (Supplementary Fig. 2-5). For serum starvation and to promote ciliogenesis, cells were washed in PBS upon confluency and incubated in media supplemented with 1% FBS for the desired time periods (0 h, 24 h, 48 h, and 72 h). For shear stress experiments, cells were washed with PBS after starvation and incubated in regular media right before fluid flow application.

2.5.3 Immunofluorescence

Cells were seeded in 8-well chamber slides (Falcon, Corning Incorporated, AZ, USA) at a density of 9×10^5 cells per well. Upon reaching 80% confluence, the cells were washed with PBS and starved to induce cilia differentiation. At each time point during starvation, the cells were washed with PBS, fixed with 4% PFA in PBS buffer for 10 minutes at room temperature, washed (1% BSA in PBS), and then permeabilized with 0.1% Triton-X-100 in PBS for 10 min at room temperature. After two washes, the cells were blocked in 5% BSA in PBS for 1 h at room temperature. Mouse anti-acetylated α-tubulin (Invitrogen; 32-2700) diluted (1:1000) in 3% BSA-PBS was the primary antibody to detect cilia. Cells were incubated with this primary antibody overnight at 4°C. The following day, after 3 washes, the cells were incubated for 1 h at room temperature with Alexa Fluor® 488 conjugated goat anti-mouse secondary antibody (Invitrogen; A11029). After 3 washes, 1µg/ml dilution of Hoechst (Sigma-Aldrich, ON, Canada; 94403) in 1% BSA-PBS was

used to stain the nucleus at room temperature for 10 min. Alexa Fluor® 555 Phalloidin dilution (1:40) in 1% BSA-PBS incubation at room temperature for 20 min was used to stain the cytoskeleton. The images were captured on a Leica Confocal TCS-SP8 or Zeiss Confocal 880 using × 63 (oil) objective with 1,024 × 1024 pixels resolution. Each sample has been examined in stitched 5x5 tile images, in duplicate (50 fields of view). Maximum projections of the Z-stacks were used for primary cilium measurement and counting was done in Image J (NIH). Two separate double staining with anti-Ninein antibody (Millipore, CA, USA, ABN1720) as the cilia base marker and anti-IFT88 (Proteintech, IL, USA, 13967-1-AP) were performed to co-stain the cilia alongside anti-acetylated α-tubulin to confirm the method.

2.5.4 Proliferation assay

Bone cells acquired from IS patients were cultured, as previously described in the methods regarding cell culture. Upon reaching 90% confluence, cells were harvested by adding Trypsin-EDTA (0.25%) and phenol red (Thermo Fisher Scientific Inc.,NY, USA 25200-072) for subculture (P3 to P5). Cells were washed and counted (Trypan Blue staining of viable cells) using the Vi-cell® XR (Beckman Coulter, Inc., CA, USA) automated cell counter and then seeded in 12 well plates (100,000 per well in triplicate for each sample). Cells were allowed to grow at 37°C in 5% CO_2 and each well was counted at different time points (24 h, 48 h, 72 h, 96 h and 120 h post culture). Bone cells from age- and gender-matched trauma surgical patients were used as controls.

2.5.5 *In vitro* fluid flow stimulation

For each sample, the cells were divided equally between 4 vented 75 cm^2 tissue culture flasks and cultured in 21 ml medium (αMEM + 10% FBS + 1% penicillin/streptomycin). Upon reaching 80% confluence, the medium was removed, the cells were washed with warm PBS and then transferred to starvation medium for 48 h. After 48 h cells were washed again and transferred back to 20 ml regular medium immediately before they were subjected to oscillatory fluid flow using a double-tier rocking platform, with some modification of the rocker method described by Robin M.

Delaine Smith *et al.* [210] with a maximum tilt angle of ± 20 degrees, and a speed of 1 tilt per second (equal to 1 Hz). The entire unit was housed in a cell culture incubator held at 37°C and 5% CO_2 for the duration of the flow experiments (4h, 8h, and 16h). No flow 0h cells were housed in the same incubator and harvested at 8h.

Fluid shear stress patterns were applied to cells in a predictable, controlled, and physiologically relevant manner through the whole experiment. From a biomechanical point of view, one expects that the cilia-related gene expression to be a function of time elapsed, t, and the shear stress exerted on the cells, which in turn depends on the fluid viscosity, *v*, the frequency of flow oscillations, *f*, and the thickness of the fluid film, *h*. Designing an experiment in which all these parameters match the physiological conditions can be prohibitively challenging, and in fact unnecessary. Fortunately, the design of the experiment can be simplified using the π-Buckingham theorem [264] that is widely used in engineering and physics. The π-Buckingham theorem states that the dynamics of a problem (e.g. fluid flow) can be completely described and measured by a set of nondimensional quantities.

Here we define ϕ to be the ratio of gene expression measured at a given time, t , to its expression at 0 h. Noting that ϕ is a nondimensional quantity, one can use the π-Buckingham theorem to show that ϕ is a function of two other nondimensional numbers, equation (1):

$$\phi = \phi(\alpha, t*) \qquad (1)$$

Where α is the Womersley number defined as

$$\alpha = h\sqrt{(\frac{2\pi f}{v})} \qquad (2)$$

and t^* is a nondimensionalized time

$$t^* = t f. \qquad (1)$$

The Womersley number takes into account the effect of viscosity and shear stress exerted on the cell and is widely used in biomechanical studies involving pulsating fluid flow, equation (2) [265]. The value of Womersley number ranges from 5 to 18 in fluid motion of cerebrospinal fluid in the spinal cavity [219]. We designed our experiment such

that the Womersley number experienced by the cells is equal to 8, which is well within the expected range in vivo. This value corresponds to an average shear stress at the center of the dish with a magnitude of 1 [Pa] in our experiment (see Zhou *et al.* 2010 [266] for details of calculation).

2.5.6 RNA extraction

All RNA was extracted using Trizol (Invitrogen-Thermo Fisher Scientific, 15596-026), according to the manufacturer's instructions. Briefly, cell culture dishes containing adherent bone cells (passage 2 or 3) were washed with PBS before trypsinization, then transferred to a 15 ml tube and after centrifugation, the cell pellet was stored immediately at -80° C. All the cells went through RNA extraction the following day and were lysed in 1ml Trizol. RNeasy MinElute Cleanup Kit (Qiagen Inc., ON, Canada; 74204) was used to purify RNA, according to the manufacturer's instructions.

2.5.7 Quantitative RT-PCR

Reverse transcriptase quantitative PCR (RT-qPCR) was used to assay gene expression levels. All the primer design, validation, and gene expression were performed at the Genomics core facility of Institute de Recherche en Immunologie et Cancérologie (IRIC), University of Montreal, Quebec. All RNA was run on a bioanalyzer using a Nano RNA chip to verify its integrity. Total RNA was treated with DNase and reverse transcribed using the Maxima First Strand cDNA synthesis kit with ds DNase (Thermo Fisher Scientific). Before use, RT samples were diluted 1:5. Gene expression was determined using assays designed with the Universal Probe Library from Roche (www.universalprobelibrary.com). For each qPCR assay, a standard curve was performed to ensure that the efficacy of the assay is between 90% and 110%. Quantitative PCR (qPCR) reactions were performed in triplicate with 2 internal controls (GAPDH and HPRT) using PERFECTA qPCR FASTMIX II (Quanta Biosciences, Inc., MD, USA), 2 μM of each primer, and 1 μM of the corresponding UPL probe. The Viia7 qPCR instrument (Thermo Fisher Scientific) was used to detect the amplification level and was programmed with an initial step of 20 second at 95˚C, followed by 40 cycles of: 1 sec at 95˚C and 20

second at 60˚C. Relative expression (RQ = 2-ΔΔCT) was calculated using the Expression Suite software (Thermo Fisher Scientific), and normalization was done using both GAPDH and HPRT. The baseline expression level at 0h (before treatment) of every sample was defined as its own calibrator. The calibrator has a RQ value of 1 because it does not vary compared to itself. For each gene, the two groups (control and IS) were compared at each time point using a pairwise t-test. In this way, we asked one question per gene and we did three comparisons to answer (three comparisons per family of test). After looking at the results of these tests, we asked another question for three of the genes that seemed to show an overall expression profile that was different between IS and controls (ITGB1, CTNNB1 and POC5). For these genes we added three more comparisons: the expression at 0h for IS was compared to each of the other time points (4h, 8h and 16h) using 3 separate pairwise t-tests. We also examined gene expression values for IS, controls and LiCl treated controls at baseline, by using the delta Ct mean (expression level normalized with endogenous controls) of every sample at 0h. The control cells were considered as the calibrator and the changes in gene expression of the other two groups were calculated as the fold changes in relative quantity (RQ) as explained above. A greater than ± 2 -fold gene expression change relative to control was considered significant.

RT–PCR primer sequences are as follows:

BMP2 F: 5′-cagaccaccggttggaga-3′; R: 3′-ccactcgtttctggtagttcttc-5′

SPP1 F: 5′-gcttggttgtcagcagca-3′; R: 3′-tgcaattctcatggtagtgagttt-5′

ITGB3 F: 5′-gggcagtgtcatgttggtag-3′; R: 3′-cagccccaaagagggataat-5′

PTGS2 F: 5′-gctttatgctgaagccctatga-3′; R: 3′-tccaactctgcagacatttcc-5′

RUNX2 F: 5′-ggttaatctccgcaggtcac-3′; R: 3′-ctgcttgcagccttaaatga-5′

ITGB1 F: 5′-cgatgccatcatgcaagt-3′; R: 3′-acaccagcagccgtgtaac-5′

POC5 F: 5′-aacaactgtgtaatcagatcaatgaa-3′; R: 3′-tgcctatggcatgagacaag-5′

LBX1 F: 5′-tcgccagcaagacgttta-3′; R: 3′-gccgcttcttaggggtct-5′

FUZ F: 5′-tcacctccacgcacttcc-3′; R: 3′-gggcctggtagacctcatct-5′

GAPDH F: 5′-agccacatcgctcagacac-3′; R: 3′-gcccaatacgaccaaatcc-5′

HPRT F: 5′-tgatagatccattcctatgactgtaga-3′; R: 3′-caagacattctttccagttaaagttg-5′

AXIN2 F: 5′- ccacccttctccaatcc-3′; R: 3′-tgccagtttctttggctctt-5′

INVS F: 5′-tgataacttatttcgaaccccact-3′; R: 3′-acaatctgtgcatggcctaa-5′

GSK3B: 5′-ttggagccactgattatacctct-3′; R: 3′-tcccctggaaatattggttg-5′

PTCH1: 5′-catcaactggaacgaggaca-3′; R: 3′-gcgacactctgatgaaccac-5′

GLI1: 5′-tgaaactgactgccgttgg-3′; R: 3′-ggatgtgctcgctgttgat-5′

2.5.8 Induced phenotype via Lithium Chloride (LiCl)

To examine the effect of LiCl on cilia length of primary osteoblasts, we exposed the previously tested controls to 1mM, 10mM and 50 mM LiCl (Sigma-Aldrich, ON, Canada;203637). Osteoblast were starved for 48 hours and treated for 24 hours before measuring the length of their cilia (Supplementary Fig. 2-2). Cells that were treated with 50 mM LiCl did not survive. Cells undergoing mechanical stimulation were treated with 10mM LiCl.

2.5.9 Exome and Sanger sequencing

Genomic DNA was extracted from the whole blood of 73 IS patients and 70 controls using the PureLink® Genomic DNA extraction kit (Thermo Fisher Scientific). Library preparation and exome sequencing was performed at GENESE (Génomique de la Santé de l'Enfant, Sainte-Justine University Hospital Research Center). Selected variants were confirmed using Sanger sequencing technologies at the Genome Quebec Innovation Centre. Samples were barcoded and captured using libraries of synthetic biotinylated RNA oligonucleotides (baits) targeting 50 Mb of genome (Agilent SureSelect Human All Exon 50 Mb v3) and sequenced on the 5500 SOLiD Sequencing System (Thermo Fisher Scientific). Trimmed FASTQ formatted sequences were aligned to the exome target sequence using Bfast+bwa (version 0.7.0a) in the paired-end alignment mode [267]. Mapped reads were refined using GATK and Picard program suites [226] to improve

mapped reads near indels (GATK indel realigner) and improve quality scores (GATK base recalibration) and to remove duplicate reads with the same paired start sites (Picard mark Duplicates). Variants were called using SAMTOOLS batch calling procedure referenced against the UCSC assembly hg19 (NCBI build 37). Variants were additionally filtered to remove variants that are present with minor allele frequencies (MAF) > 0.05 (dbSNP, 1000 genomes, ExAC and/or Exome variant server (ESP). Variants were annotated using the GEMINI framework [268] that provides quality metrics and extensive metadata (e.g. OMIM, clinVar, etc.) to help further prioritize variants. To optimize the querying criteria for the GEMINI database, we performed bidirectional Sanger sequencing for more than 100 different variants. Using an optimized threshold (Coverage DP >10x, Genotype quality GQ > 80, Call rate > 90%, Alternate quality (QUAL) > 50, Map quality > 20), the results show 85% genotype correlation between the sequencing methods. This threshold was used to filter our data prior to analysis.

2.5.10 Statistical analyses

To test for accumulation of rare variants in genes associated with IS, we used the Sequence Kernel Association Optimal unified test algorithm SKAT-O [227]. SKAT-O is a region-based omnibus test that increases a study's power to detect rare variants. Because there is no model for the genetic basis underlying IS, SKAT-O is optimal over SKAT or burden testing alone, since it is a robust technique to detect variable effect rare polymorphisms [215]. Variants that passed our filtering criteria, with a dataset minor allele frequency ≤ 5% were analyzed in two different sets (a complete list of variants is presented in Supplementary Table S3 available online at: https://www.nature.com/articles/srep44260#s4). Additionally, high quality variants with membership to the Illumina HumanExome Chip were extracted from the Gemini database for population structure analyses using R package SNPRelate. The top two components were used as covariates in the SKAT-O analysis. The first set used the manual recommended settings for rare variants: SKATBinary with SNP weighting based on Madsen and Browning weights (i.e. less frequent are more impactful) (B1 = 0.5, B2 = 0.5). The second set weighted-SNPs are based on Combined Annotation Dependent Depletion (CADD) scores (i.e. functional, deleterious, and disease-causing variants have greater

impact) [269]. For both sets, we generated a null model of no association between genetic variables and outcome phenotype adjusting for covariates. Covariate analysis confirmed that there was not population stratification in our dataset. The gene-level significant thresholds were determined by the efficient resampling (ER) method and the conservative minor allele count (MAC) threshold of ≤ 40 [270]. To examine the number of ciliary genes in our datasets, we used two reference lists that define a ciliary function based on experimental evidence: 1) the SYSCILIA gold standard list of genes containing 303 ciliary genes verified by independent publications [228] ; 2) a list of 52 genes (51 novel genes because one is in the SYSCILIA list) from a functional genomic screen that used RNA interference to identify genes involved in the regulation of ciliogenesis and cilia length [229].

2.5.11 Review of ciliary genes associated with spinal curvature

If idiopathic scoliosis is a genetically heterogeneous ciliopathy-like condition, then we expect a large number of known ciliopathies have spinal curvature as a comorbidity. We reviewed the SYSCILIA gold standard gene list and the Kim *et al.* 2010 list [228], [229] to ascertain how many ciliary genes were associated with spinal curvature phenotypes in either a human syndrome or an animal model. For each of the 303 genes, the search terms in Google included the gene name with “spinal curvature” and “scoliosis”. Additionally, if the gene was known to be associated with a syndrome in the OMIM database, we also searched the syndrome name with “scoliosis”.

2.6 Acknowledgements

We thank the patients and families who participated in this study, and the orthopedic surgeons and nursing teams at Sainte-Justine University Hospital, The Montreal's Children Hospital, and The Shriners Hospital for Children in Montreal. The authors would also like to thank Prof. Alireza Najafi-Yazdi, from Mechanical Engineering Department of McGill University for useful discussions regarding the design of the biomechanical experiment. We also thank Ms. Anita Franco, project coordinator, for her technical assistance. We are also thankful to the members of Moreau's lab for their supports, specifically Dr. Cedric Julien and Dr. Jean-François Lavoie as well as Dr. DaShen Wang, Mr. Saadallah Bouhanik, Ms. Qilin Tang and Ms. Dina Nada. The authors are grateful to Prof. Mark E. Samuels, from the Biochemistry and Molecular Medicine Department of Université de Montréal for reviewing the paper. We thank Dr. Smitha S. Dutt who participated in the technical editing of the manuscript. This work is supported by grants to A. Moreau from La Fondation Yves Cotrel de l'Institut de France, Paris, France, Paradigm Spine LLC/Fourth Dimension Spine LLC (NYC, USA), and Génome Québec (Montreal, Canada). Similarly, the work is supported by scholarships awarded to N. Oliazadeh from Fondation CHU Sainte-Justine and Network of Applied Medical Genetics (RMGA). K.F. Gorman is a recipient of the CHU Sainte-Justine Research Centre/CIHR MENTOR Training Program Postdoctoral Award for Excellence in Musculoskeletal Research.

Author contributions. N.O. conceived the study, designed, performed and analyzed the experiments. K.F.G. evaluated exome data, discussed and provided critical consultation during the study. N.O. and K.F.G wrote the manuscript together. R.E. performed bioinformatic analyses of the whole exome sequences and SKAT-O analysis and participated in writing of the manuscript. G.B. supervised all bioinformatics. A.M. is the principal investigator who managed, supported the study and participated in writing of the manuscript.

Competing financial interests: The authors declare no competing financial interests.

2.7 Figure legends

Figure 2-1. Morphology of primary cilia in osteoblasts from IS and controls. (a) Immunofluorescence micrographs of IS and control osteoblasts at 0, 24, 48, and 72 hours following serum-starvation. Cells were stained for acetylated α-Tubulin (green), F-Actin (red), and Hoescht (blue). Long cilia (green) are visible in IS patients, at all time-points. (b) Elongated primary cilia appear more frequently in IS bone cells (4 IS vs. 4 controls assayed in duplicate, from 5 x 5 stitched tile images (50 fields) per sample). (c) Percentage of ciliated cells is not significantly different between IS and control cells ($n \leq 1{,}000$ count per individual). Error bars are constructed using 1 standard error from the mean. Statistical analysis was performed with t-test using JMP-11®, $*P < 0.005$.

Figure 2-2. Similar growth rates among IS and control cells. There is no significant difference in the average cell number between control and IS patient cells at any given time point (n = 8: 4 IS vs. 4 controls). Plates were seeded with 100,000 osteoblast cells per well in AMEM media, in triplicate, for each patient and control. Each error bar is constructed using 1 standard error from the mean.

Figure 2-3. Biomechanical response profile of human primary osteoblast from IS patients with elongated cilia vs. control. We used RT-qPCR to examine the effect of oscillatory fluid flow on gene expression after 4, 8, and 16 hours of stimulation. Gene expression in every sample has been normalized to two endogenous controls (GAPDH and HPRT). The 0h of every sample has been defined as its calibrator. The graphs represent the fold changes at each time point, compared to the calibrator. For each gene, the two groups (control and IS) were compared at each time point using a pairwise t-test. In addition, the expression at 0h for IS was compared to each of the other time points (4h, 8h and 16h) using separate pairwise t-tests. For a post hoc Bonferroni analysis, the maximum number of comparisons per gene is 6, three comparisons per question (i.e. three comparisons per family of test). Even if we consider each gene as a family (i.e. six comparisons), using this formula ($FWER = 1 - (1 - \alpha)^M$ [271]) the family-wise error rate (FWER) would be: $1 - (1\text{-}0.05)^6 \approx 1 - 0.73 \approx 0{,}26$. Solving the Bonferroni (0.26 / 6) new

α would be 0.043 which does not affect our findings. For example, CTNNB1 results at 4 ($p = 0.03$) and 8 hours ($p = 0.008$) will still be significant. It is the same case for POC5 4h ($p = 0.01$) but ITGB1 with a $p = 0.047$ will not pass the test. Overall, the multiple test error is not significant in our analysis and it will not change the results. Genes were chosen based on the following characteristics: Biomechanically responsive genes in bone tissue: BMP2, PTGS2 (COX2), RUNX2, SPP1 (OPN); role in mechanotransduction through cilia: ITGB1, ITGB3; indicator of Wnt pathway activity: CTNNB1; GSK3B, AXIN2, INVS; indicator of Hedgehog signaling: PTCH1; or implicated in an IS study: POC5. Each error bar is constructed using 1 standard error from the mean. n = 8, (4 IS vs. 4 controls) for all genes except CTNNB1, where n = 4 (2 IS vs. 2 controls).

Figure 2-4. Osteogenic factors response profile of primary human osteoblasts from control, IS and LiCl treated controls under mechanical stimulation. We used RT-qPCR to examine the effect of oscillatory fluid flow on gene expression after 4, 8, and 16 hours of stimulation. Gene expression in every sample has been normalized to two endogenous controls (GAPDH and HPRT). The 0h of every sample has been defined as its calibrator. The graphs represent the fold changes at each time point, compared to the calibrator. Three groups were compared using Anova and followed by post-hoc Tukey test to analyze the significant results. 10 mM LiCl treatment for 24 h significantly suppresses the expression of tested osteogenic factors under mechanical stimulation compared to non-treated controls ($p < 0.0001$). The response pattern of LiCl-Control group follows what is observed in IS but is dramatically exaggerated. It is of note that response is not completely lost Statistical analysis was performed with Anova, followed by Tukey test using JMP-12®.

Figure 2-5. Molecules are connected through pathways linking ciliary mechanosensation to bone formation. The molecules that we show to be differentially affected in IS (marked by an arrow) are related through multiple interconnected pathways, summarized in this figure. The results of our gene expression studies are confirmed by

expected responses through these pathways. For example, BMP2 expression directly affects RUNX2, which in turn affects COX2 expression.

2.8 Figures

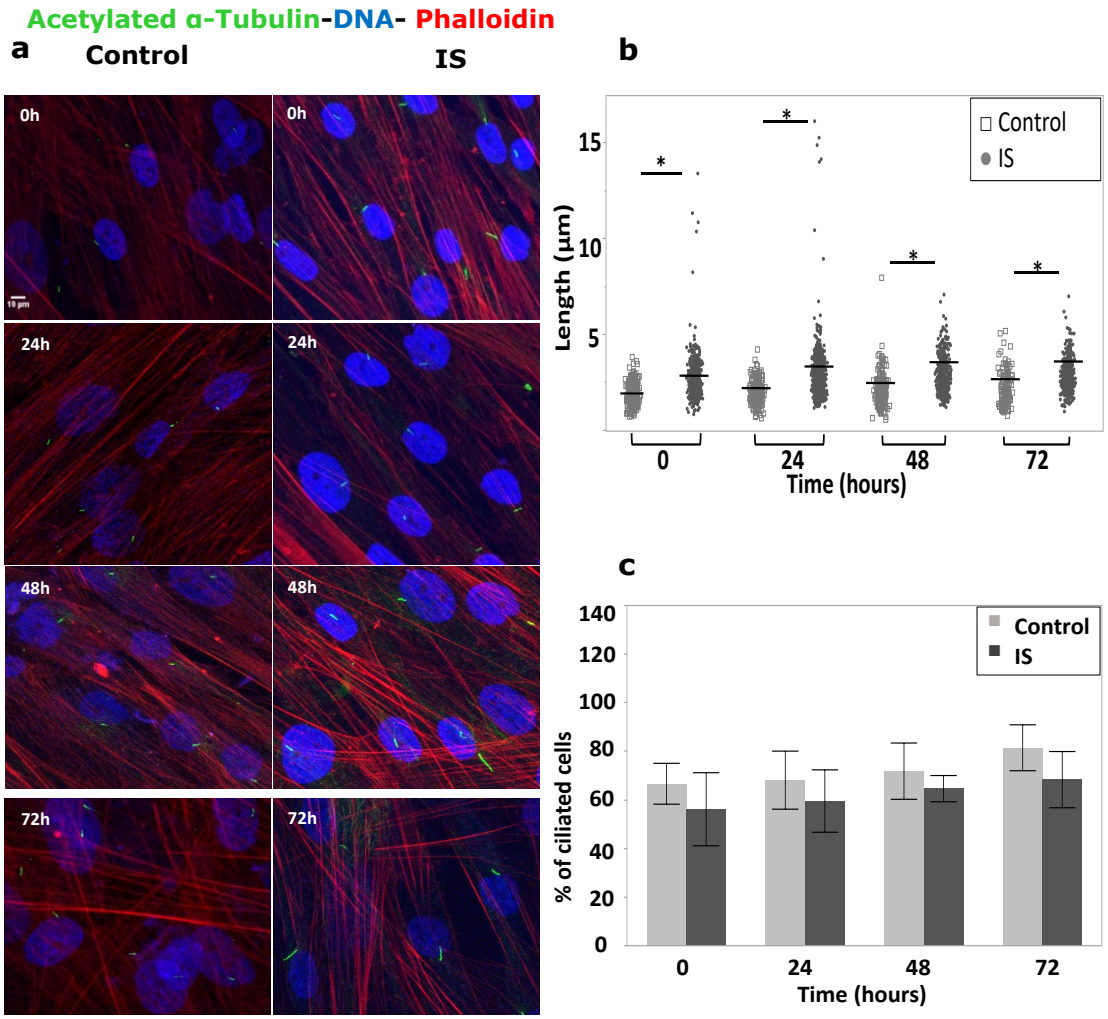

Figure 2-1 Morphology of primary cilia in osteoblasts from IS and controls.

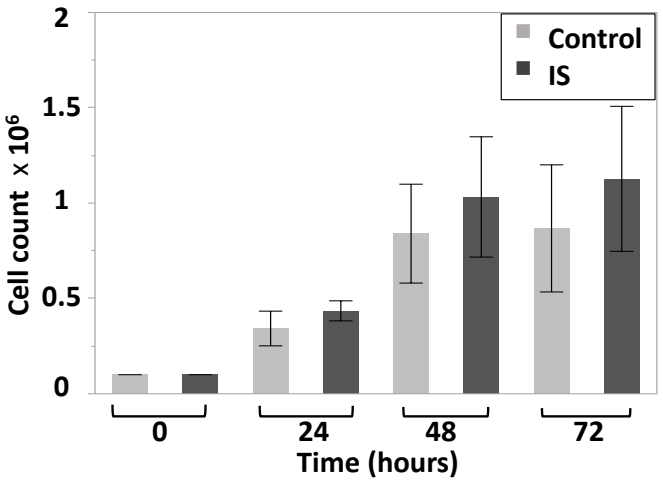

Figure 2-2. Similar growth rates among IS and control cells.

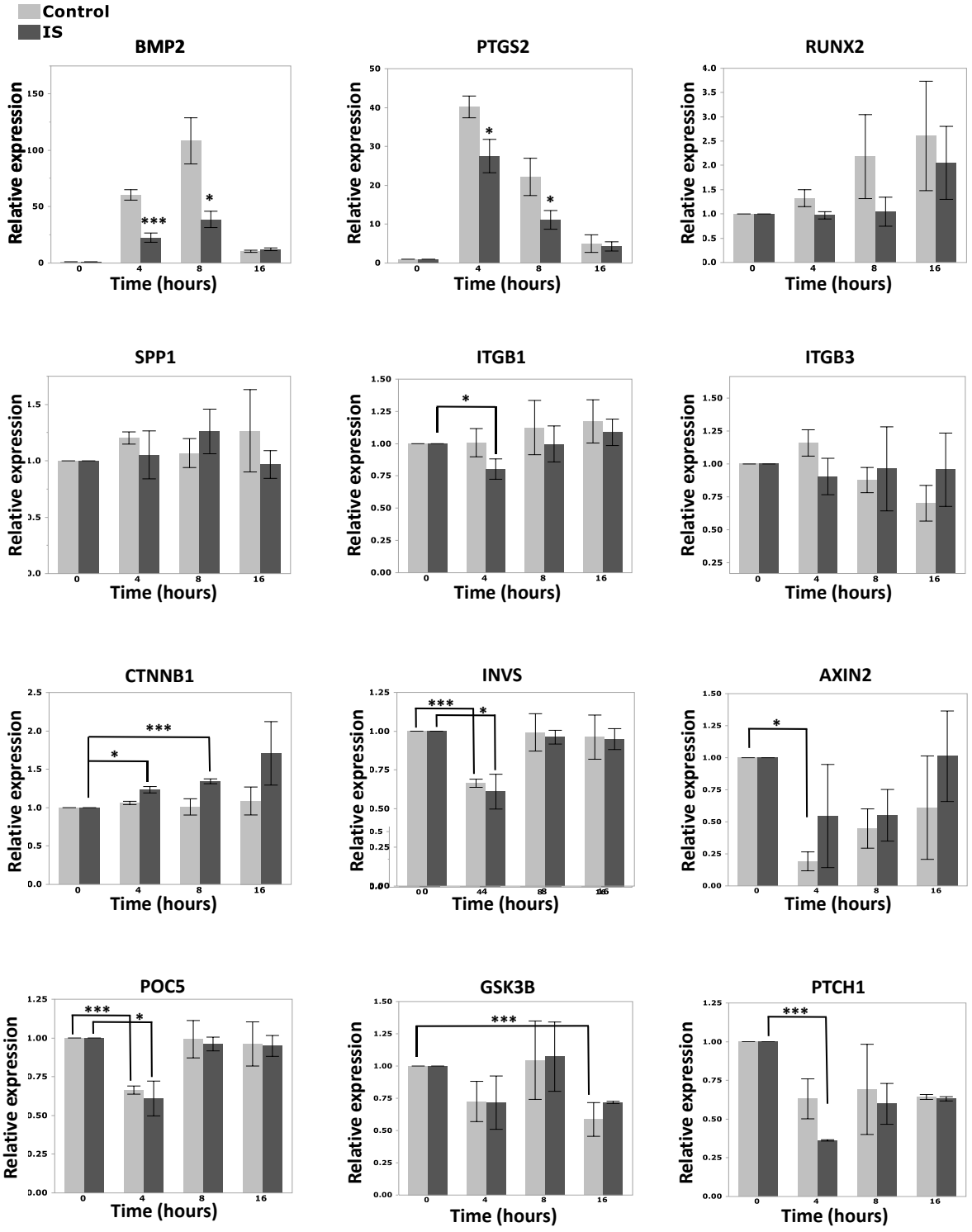

Figure 2-3. Biomechanical response profile of human primary osteoblast from IS patients with elongated cilia vs. control.

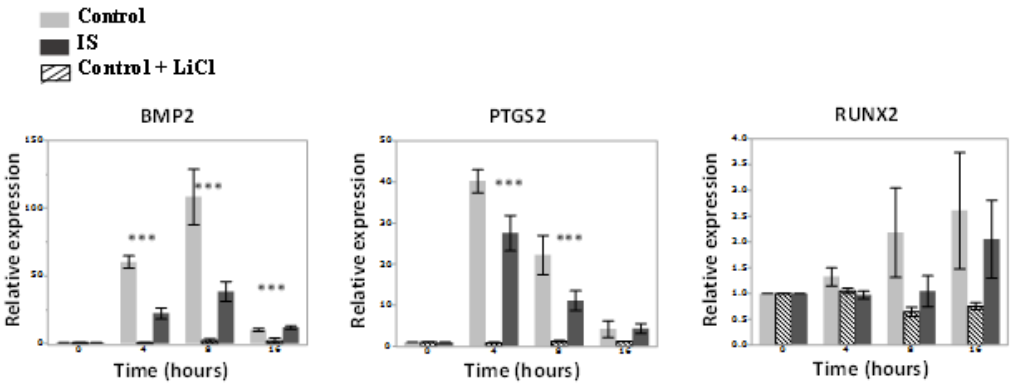

Figure 2-4. Osteogenic factors response profile of primary human osteoblasts from control, IS and LiCl treated controls under mechanical stimulation.

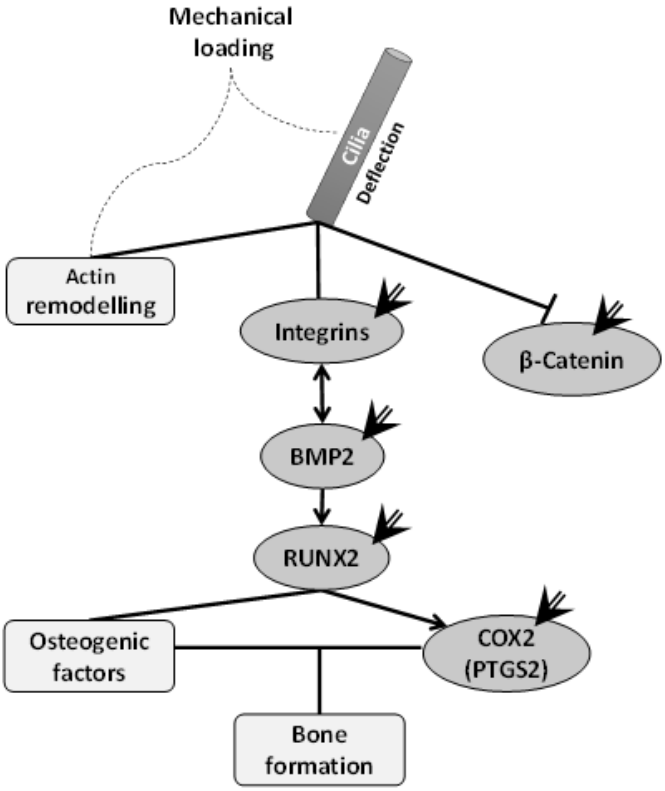

Figure 2-5. Molecules are connected through pathways linking ciliary mechanosensation to bone formation.

2.9 **Tables**

Table 2-I. IS-associated genes in humans and/or animal models, which are also associated with cilia.

Gene	Scoliosis Association	Cilia Association
TBX6	PMIDs: 26120555, 20228709 (Congenital and idiopathic scoliosis in humans)	PMIDs: 18575602 & 17765888 (Affects morphology and motility of nodal cilia in mice & zebrafish)
LBX1	PMIDs: 26394188, 25987191, 25675428, 24721834 (Idiopathic scoliosis association in several ethnic groups, confirmed using different approaches)	PMIDs: 18541024 (deleted in a mouse model of the primary ciliary dyskinesia gene)
GPR126	PMIDs: 25954032, 25479386, 23666238 (Idiopathic scoliosis in humans and mice)	PMIDs: 16875686, 24227709 (No direct relation to cilia. Essential for the development of myelinated axons in zebrafish and mice)
PAX1	PMIDs: 25784220, 19080705, 16093716 (Congenital and idiopathic scoliosis in humans and mice)	PMIDs: 19517571, 23907320, 24740182 (Other family members are associated with cilia signaling pathways or ciliated tissues)
POC5	PMID: 25642776 (Idiopathic scoliosis in humans)	PMID: 23844208, 19349582 (interacts with cilia and is essential for centriole structure in humans and Drosophila)
KIF6	PMID: 25283277 (idiopathic-type curvature in zebrafish)	PMID: 16084724 (Predicted to be involved in ciliary function or structure)
PTK7	PMID: 25182715 (idiopathic-type curvature in zebrafish)	PMID: 20305649 (Role in cilia orientation in zebrafish)
FGF3	PMID: 25852647, 24864036 (Idiopathic scoliosis in a KO mouse model; Scoliosis in a human case report carrying loss-of-function mutation in the gene)	PMID: 26091072 (Affecting the organization of chondrocyte primary cilia in the growth plate in mice)

Table 2-II. Significantly longer cilia in IS-derived bone cells.

	0 h	24 h	48 h	72 h
Controls	1.94 ± 0.35	1.99 ± 0.32	2.05 ± 0.66	2.16 ± 0.78
IS	2.66 ± 1.14	2.87 ± 1.84	2.82 ± 0.81	2.80 ± 0.65
P Value	2.62632 E-22	1.00327 E-20	2.49 E-25	1.03284 E-14

The average length of cilia in μm ± variance at four starvation time points (0, 24 h, 48 h, 72 h). To compare the length of cilia between IS and non-IS controls, we combined measurements of up to 1000 cilia for each sample (25 fields per sample, in duplicate), at each time point, then used a t-test to compare the mean lengths of cilia in IS vs. control pools. The difference in length was significant across all the time points for IS patients ($P \leq 0.005$), n = 8 (4 IS vs. 4 Controls).

Table 2-III. The basal level of gene expression in LiCl-treated control and IS compared to non-treated control osteoblasts.

	RQ (Fold change)		
	Control	**LiCl-Control**	**IS**
BMP2	1	1.045	0.754
PTGS2	1	3.942*	1.481
RUNX2	1	0.202*	0.299*
SPP1	1	0.366*	2.020*
CTNNB1	1	3.367*	5.762*
GSK3B	1	0.296*	1.007
INVS	1	0.746	1.127
AXIN2	1	0.821	0.508
PTCH1	1	0.721	0.528
GLI1	1	Not Determined	0.687
ITGB1	1	1.670	1.169
ITGB3	1	0.692	0.829
POC5	1	0.499	1.133

The expression of several signaling and osteogenic factors were compared in human primary osteoblast samples from controls, LiCl treated controls and IS groups. The control cells are considered as the calibrator and the changes in gene expression of the other two groups are shown as the fold changes in relative quantity (RQ). LiCl-Controls were treated with 10 mM LiCl for 24 h. 2-fold change in gene expression compared to controls is considered significant and marked with an asterisk.

Table 2-IV. Clinical features of patients tested for ciliary morphology.

Patient ID	Cobb Angle (degree)	Curve Type
1	42°-66°-38°	lTrTlL
2	21°-50°-67°-31°	lTrTlTLrL
3	50°-56°	lTrL
4	50°-89°	rTlTL

All samples (patients and controls) are from female subjects. Mean age for controls is 15 ± 3, mean age for patients is 15 ± 1. Cobb angles in degrees, multiple angles reflect multiple curves. Curve types - T: Thoracic; L: Lumbar; TL: Thoracolumbar; l: left and r: right.

2.10 **Supplementary materials**

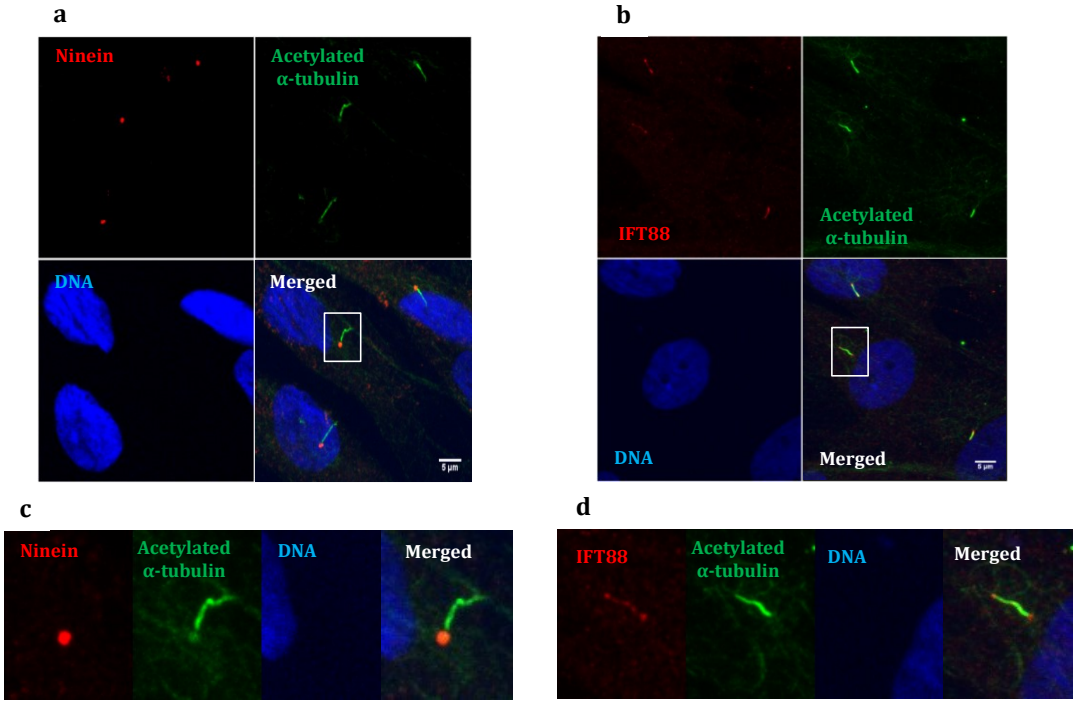

Supplementary Figure 2-1. Cilia Immunofluorescence co-staining.

To validate the staining of cilia, double immunostaining was performed on fixed IS osteoblasts using Anti-acetylated α-Tubulin and a) anti-Ninein, as the basal body marker or b) anti-IFT88 to stain the length of cilia. Lower parts of each panel show the magnified version of the area framed in white rectangles from the upper part. Three different channels of staining are shown side by side the merged image. The images were captured on a Leica Confocal TCS-SP8 using × 63 (oil) objective and Maximum projections of full Z-stacks.

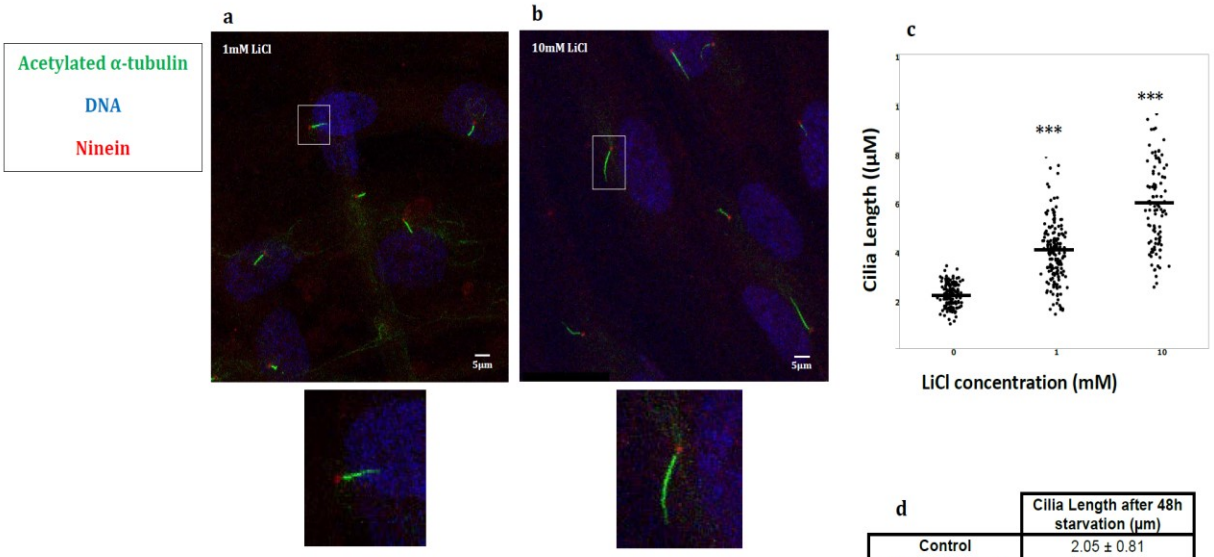

d

	Cilia Length after 48h starvation (µm)
Control	2.05 ± 0.81
Control-1mM LiCl	3.94 ± 1.24
Control-10mM LiCl	5.81 ± 1.72
IS	2.82 ± 0.90

Supplementary Figure 2-2. LiCl increases the length of cilium in primary human osteoblasts.

Human primary osteoblasts (OB) were transferred to differentiation media (1% supplemented media) upon confluency, after 24h media was changed to differentiation media plus indicated concentrations of LiCl (1, 10 and 50 mM). The increased length of cilia is visible in immunofluorescence stained cilia of cells after **a)** 1mM LiCl and **b)** 10 mM LiCl. **c)** Both concentrations of LiCl significantly increase the length of cilia ($p < 0.0001$). The horizontal bars indicate the average value for each sample. Samples assayed in duplicate in 3 x 3 stitched images (18 fields) per sample. Statistical analysis was performed with Anova, followed by Tukey test using JMP-12®. **d)** The average length of cilia in µm ± variance.

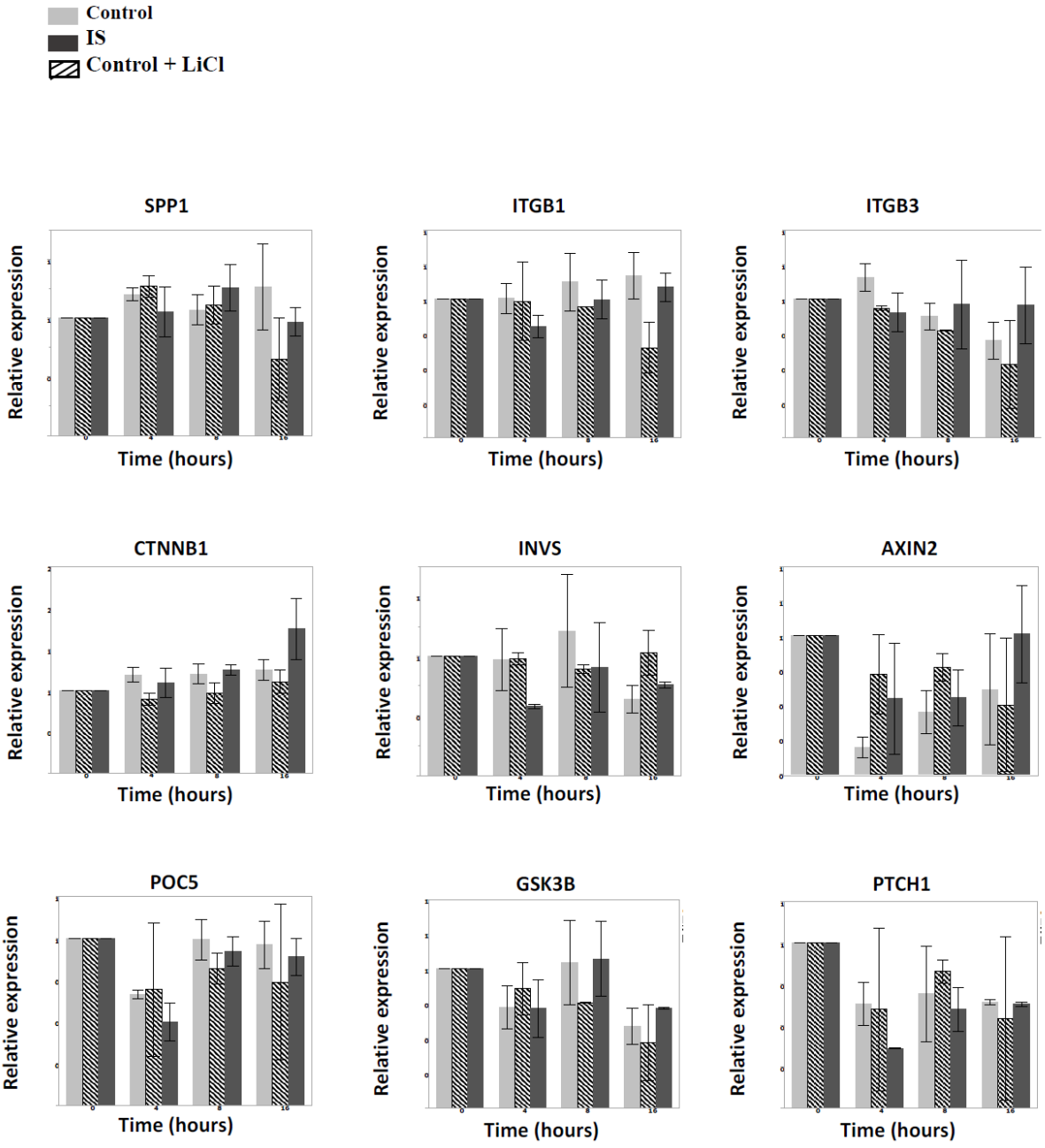

Supplementary Figure 2-3. Effect of 10 mM LiCl treatment on biomechanical response profile of control cells.

Changes in gene expression following 10mM LiCl treatment for 24h in human primary osteoblasts in controls compared to not treated controls and IS cells is shown after 4, 8 and 16 hours of fluid flow mechanical stimulation. The 0h of every sample has been defined as its calibrator. The graphs represent the fold changes at each time point, compared to the calibrator. 10 mM LiCl significantly suppress the expression of BMP2 and PTGS2 ($p < 0.0001$). Statistical analysis was performed with Anova, followed by Tukey test using JMP-12®. Further details are exactly similar to Fig. 2-3 in the body of the paper.

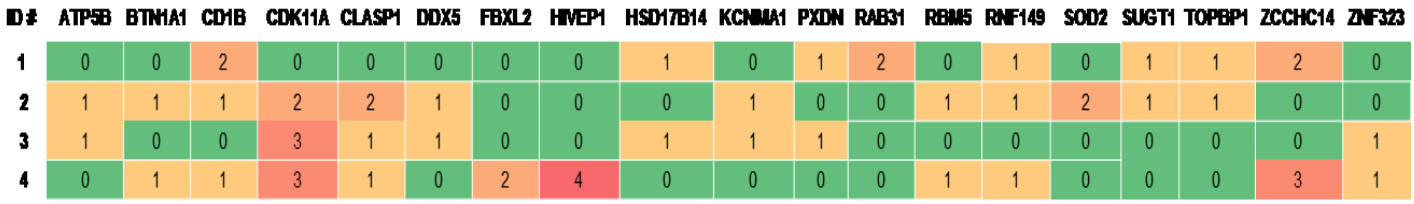

ID #	ATP5B	BTN1A1	CD1B	CDK11A	CLASP1	DDX5	FBXL2	HIVEP1	HSD17B14	KCNMA1	PXDN	RAB31	RBM5	RNF149	SOD2	SUGT1	TOPBP1	ZCCHC14	ZNF323
1	0	0	2	0	0	0	0	0	1	0	1	2	0	1	0	1	1	2	0
2	1	1	1	2	2	1	0	0	0	1	0	0	1	1	2	1	1	0	0
3	1	0	0	3	1	1	0	0	1	1	1	0	0	0	0	0	0	0	1
4	0	1	1	3	1	0	2	4	0	0	0	0	1	1	0	0	0	3	1

Supplementary Figure 2-4. Mutation profile of the tested IS patients.

Patients used in our cellular assays were surveyed for variants in genes listed in Supplementary Table 2-I (significant genes from our SKAT-O analyses). Patients are listed as rows and each column is a gene. This heat map illustration shows a color-coded profile of the number of variants per patient for a given gene. Only genes with a total of more than 1 variant are listed.

a

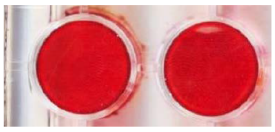

b

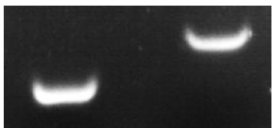

c

ALP	Primer-F	CTGCAAGAAAGGGGACCCAAGAAA
	Primer-R	TGGGAGGGTCAGATCCAGAATGTT
BSP	Primer-F	TGTCACTGGAGCCAATGCAGAA
	Primer-R	CGAAAATGGTAGCCGGATGCAAAG

Supplementary Figure 2-5. Characterization of osteoblast cells.

We derived osteoblasts from surgical bone specimens. To confirm that these cells are osteoblasts, **a)** we show the results of Alazarin red staining. Mineralization was induced on confluent mono layer by addition of Ascorbic acis (50 µg/ml), Beta-glycerophosphate (2.5 mM) and Dexamethasone (10 nM). After 4 weeks of treatment cell were fixed with formaldehyde and stained with Alizarin red. Also, in addition to the RT-qPCR performed in this study using osteoblast genes (RUNX2 and SPP1), **b)** We performed RT-PCR on Alkalin phpsphatase (ALP) and Bone Sialoprotein II (BSP) to demonstrate the expression of bone markers in our cultured cells. **c)** Shows the sequence of the primers used for RT-PCR.

Supplementary Table 2-I

Gene	Set I p-Value	Set II P-Value	Total # of variants	# of patients with at least 1 variant in the gene		% of carrier in each cohort	
				Ctrl	IS	Ctrl	IS
FEZF1	9.15E-11	2.65E-19	5	66	32	97.05	48.48
CDH13	2.57E-10	3.25E-17	19	60	33	88.23	47.82
FBXL2	2.56E-08	9.36E-16	12	61	33	89.7	47.82
TRIM13	1.26E-15	1.40E-12	4	66	24	97.05	34.78
CD1B	**3.01E-10**	**9.56E-11**	**8**	**9**	**39**	**13.23**	**56.52**
VAX1	1.88E-06	1.03E-10	2	68	33	100	47.82
CLASP1	**8.91E-11**	**2.40E-08**	**20**	**20**	**40**	**29.41**	**57.97**
SUGT1	**1.46E-06**	**7.2616E-05**	**4**	**3**	**24**	**4.41**	**34.78**
MIPEP	0.0014094	0.0000836	10	15	15	22.05	21.73
FAM188A	0.0000002	0.0001427	6	55	18	80.88	26.08
TAF6	0.0014127	0.0002192	5	19	13	27.94	18.84
WHSC1	0.0071833	0.0002409	10	13	13	19.1	18.84
GPR158	0.0002783	0.0002783	6	10	0	14.7	0
HNRNPD	**0.0017598**	**0.0005109**	**2**	**9**	**27**	**13.23**	**39.13**
RUNX1T1	0.0023515	0.0005488	7	9	6	13.23	8.69
GRIK3	0.0006117	0.0006117	8	10	0	6.8	0
FUZ	0.0008073	0.0006782	2	12	1	17.64	1.44
LYN	**0.0008863**	**0.0007450**	**8**	**15**	**31**	**22.05**	**44.09**
DDX5	0.0001886	0.0010911	10	21	21	30.88	30.43
PODXL	0.0013684	0.0011242	8	29	19	42.64	27.53
ATP5B	**0.0000845**	**0.0011539**	**2**	**39**	**58**	**57.35**	**84.05**
PIGK	0.0013620	0.0013620	1	8	0	11.76	0
AL159977.1	**0.0014244**	**0.0014244**	**1**	**7**	**20**	**10.29**	**28.98**
09-Sep	0.0022854	0.0016437					
TMEM87A	0.0032928	0.0017381					
CDYL	0.0024058	0.0018024					
SPINT3	0.0052096	0.0019710					
SERTM1	0.0021402	0.0021402					
FOLR3	0.0066193	0.0021883					

FCER2	0.0089662	0.0022807
MAEA	0.0045425	0.0024208
PXT1	0.0024448	0.0024448
UVRAG	0.0020578	0.0026755
SPPL3	0.0034537	0.0027288
IGHV3-50	0.0028372	0.0028372
HIVEP1	0.0083740	0.0028738
SMAD5	0.0029845	0.0029845
PPP1R21	0.0049157	0.0031375
SEC62	0.0037166	0.0032281
TOPBP1	0.0032396	0.0033324
HIPK3	0.0026868	0.0038810
KRTAP12-2	0.0065859	0.0042138
FYB	0.0050317	0.0042320
PXDN	0.0065021	0.0042866
CDV3	0.0033835	0.0044761
RP3-344J20.2	0.0045058	0.0045058
RP11-405L18.2	0.0045353	0.0045353
MRPL18	0.0045444	0.0045444
SOD2	0.0032723	0.0046861
FOXP2	0.0121444	0.0052680
REEP1	0.0077257	0.0053911
C1orf106	0.0149906	0.0055753
DNASE1L1	0.0060096	0.0060096
BTN1A1	0.0038913	0.0061222
MLST8	0.0061333	0.0061333
HMP19	0.0061466	0.0061466
OR8B4	0.0061994	0.0061994
AC105901.1	0.0061994	0.0061994
OR5F1	0.0062091	0.0062091
GLE1	0.0062309	0.0062309
OR5P3	0.0062688	0.0062688
SCFD1	0.0046767	0.0063033
CDK11A	0.0070020	0.0065103
HSD17B14	0.0065478	0.0065478

NFU1	0.0047800	0.0067241
GTF2H3	0.0094774	0.0067495
RAB7A	0.0103840	0.0067820
HOXA3	0.0089285	0.0069693
ZC3H4	0.0142957	0.0078344
DDX55	0.0091711	0.0078680
FBXW10	0.0131410	0.0082482
OSBPL2	0.0151770	0.0084846
POLR1A	0.0064189	0.0084922
NOP58	0.0011558	0.0085539
RAB31	0.0059917	0.0085944
EFNB2	0.0087664	0.0087664
ZCCHC14	0.0061474	0.0088272
GLP1R	0.0027424	0.0090174
RNF149	0.0018573	0.0091609
OR1J2	0.0030637	0.0092475
WI2-81516E3.1	0.0092702	0.0092702
GAPDHP27	0.0094020	0.0094020
SFTA3	0.0094162	0.0094162
ACSF3	0.0049349	0.0094399
POU2F2	0.0094536	0.0094536
MIR345	0.0095567	0.0095567
SNPH	0.0095929	0.0095929
MATR3	0.0096761	0.0096761
RP11-73B8.2	0.0098988	0.0098988
SNORA48	0.0143542	0.0100947
PATZ1	0.0112660	0.0100977
RBM5	0.0129867	0.0103482
HMGA1	0.0107856	0.0107856
ATP1A3	0.0072792	0.0107874
ACTG1P1	0.0110246	0.0110246
PAIP1	0.0076500	0.0117165
KCNMA1	0.0061465	0.0117956
PALB2	0.0070721	0.0121181
PLEKHG5	0.0030211	0.0123985

C11orf2	0.0045615	0.0124733
MT1DP	0.0127363	0.0127363
CYC1	0.0130029	0.0130029
DTD1	0.0130405	0.0130405
CREB3L3	0.0130488	0.0130488
RPL23A	0.0131062	0.0131062
CD164L2	0.0131438	0.0131438
PCCB	0.0131462	0.0131462
GIMAP7	0.0131582	0.0131582
AHCYL1	0.0131586	0.0131586
TNNT2	0.0131632	0.0131632
ZNF134	0.0131638	0.0131638
AC079612.1	0.0131750	0.0131750
MTA2	0.0132229	0.0132229
RP11-672F9.1	0.0132263	0.0132263
CLEC5A	0.0132773	0.0132773
C1orf222	0.0088940	0.0139165
CD96	0.0128161	0.0140861
PPFIBP1	0.0057785	0.0142691
ZNF323	0.0009831	0.0147700
SUPT3H	0.0144813	0.0152422

After analyses by SKAT-O we compared the genes statistically significant (at $p < 0.01$) in Set I and Set II. There are 120 genes shared from these approaches. The top 25 genes were examined in our cohort to determine the distribution of variants among case and control. Seven genes have variant enrichment among patients (bold).

Supplementary Table 2-II

Gene Name	Source	Human clinical association	Animal model studies	References
AHI1	SCGS v1	Joubert syndrome (type 3) OMIM 608894	NA	PMID: 20301500
ALMS1	SCGS v1	Alstrom syndrome (type 1) OMIM 606844	NA	PMID: 20301444, 11941369, 11941370
ARL6	SCGS v1	Mutated in Bardet-Biedl syndrome (type 3) and retinitis pigmentosa (type 55) OMIM 60884	NA	PMID:19956407, PMID:15314642, PMID:20207729, PMID:20603001
ATXN10	SCGS v1	Defects cause spinocerebeller ataxia 10 OMIM 603516	NA	PMID:26077168,
B9D1	SCGS v1	Meckel syndrome (type 9) OMIM 614144, and Joubert syndrome (MIM213300)	NA	PMIDs: 15473174, 20301500
B9D2	SCGS v1	Meckel syndrome (type 10) OMIM 611951	NA	PMIDs: 15473174, 20301500
BBS1	SCGS v1	Bardet-Biedl syndrome (type 1) OMIM 209901	NA	PMID:14676542
BBS10	SCGS v1	Bardet-Biedl syndrome (type 10) OMIM 610148	NA	PMID:14676542
BBS12	SCGS v1	Bardet-Biedl syndrome (type 12) OMIM 610683.	NA	PMID:14676542
BBS2	SCGS v1	Bardet-Biedl syndrome (type 2) OMIM 606151	NA	PMID:14676542
BBS4	SCGS v1	Bardet-Biedl syndrome (type 4) OMIM 600374	NA	PMID:14676542
BBS5	SCGS v1	Bardet-Biedl syndrome (type 5) OMIM 603650	NA	PMID:14676542
BBS7	SCGS v1	Bardet-Biedl syndrome (type 7) OMIM 607590	NA	PMID:14676542
BBS9	SCGS v1	Bardet-Biedl syndrome (type 7) OMIM 607968	NA	PMID:14676542
CC2D2A	SCGS v1	Meckel syndrome (type 6), Joubert syndrome (type 9) ,COACH syndrome, OMIM 612013	NA	PMID: 14676542, 20301500 and https://rarediseases.info.nih.gov/gard/1410/coach-syndrome/resources/9
CCDC103	SCGS v1	Primary ciliary dyskinesia (type 17) OMIM 614667	Curved body axis in MO zebrafish larvae	PMIDs:22581229, 23796196
CCDC114	SCGS v1	Primary ciliary dyskinesia (type 20) OMIM 615038	NA	PMIDs: 23796196, 17449765, 8414746
CCDC164	SCGS v1	Primary ciliary dyskinesia (type 20) OMIM 615288	NA	PMIDs: 23796196, 17449765, 8414746
CCDC28B	SCGS v1	Bardet-Biedl syndrome 1 OMIM 610162	Curved and shortened body axis in MO zebrafish	PMID: 23015189, 14676542
CCDC39	SCGS v1	Primary ciliary dyskinesia (type 14) OMIM 613798	NA	PMIDs: 23796196, 17449765, 8414746
CCDC40	SCGS v1	Primary ciliary dyskinesia (type 15) OMIM 613799	Curved body axis in MO zebrafish	PMID:21131974
CEP290	SCGS v1	amaurosis (type 10), Meckel-Gruber syndrome (type 4), nephronophthisis (type 6) and Se	Curved body axis in MO zebrafish	PMIDs:21257638, 14676542, 20301500
CEP41	SCGS v1	Joubert syndrome (type 15) OMIM 610523	Curved body axis in MO zebrafish	PMIDs:22246503, 20301500
CLUAP1	SCGS v1	NA	Kyphosis phenotype in KO mouse model	PMID: 25348401
DCDC2	SCGS v1	Joubert syndrome in human OMIM 605755	Curved body axis and kinky tail in MO zebrafish	PMIDs: 25557784, 19066617
DNAAF2	SCGS v1	Primary ciliary dyskinesia (type 10) in human OMIM 612517	NA	PMIDs: 23796196, 17449765, 8414746
DNAAF3	SCGS v1	Primary ciliary dyskinesia (type 2) OMIM 614566	Curved body axis in MO zebrafish	PMIDs:22387996, 23796196, 17449765, 8414746
DNAH5	SCGS v1	Primary ciliary dyskinesia (type 3) with or without situs inversus OMIM 603335	NA	PMIDs: 23796196, 17449765, 8414746
DYNC2H1	SCGS v1	Short-rib thoracic dysplasia 3 with or without polydactyly (type 3) OMIM 603297	NA	PMIDs: 12637423, 23456818, 19361615
DYX1C1	SCGS v1	Ciliary dyskinesia, primary OMIM 608706	Curved body axis in MO zebrafish larvae	PMIDs: 23650548, 23796196, 17449765, 8414746
EVC	SCGS v1	Ellis-van Creveld syndrome and Weyers acrodental dysostosis OMIM 604831	NA	PMIDs: 22344360, 2380047
EVC2	SCGS v1	Ellis-van Creveld syndrome OMIM 607261	NA	PMIDs: 22344360, 2380047
HSPB11	SCGS v1	NA	Curved body axis in MO zebrafish larvae	PMID: 22205996
IFT122	SCGS v1	NA	Curved body axis in MO zebrafish larvae	PMID:20493458
IFT140	SCGS v1	Short-rib thoracic dysplasia 9 OMIM 614620	NA	PMIDs: 12637423, 23456818, 19361615
IFT172	SCGS v1	Short-rib thoracic dysplasia 10 OMIM 607386	Curved body axis in MO zebrafish larvae	PMID: 19517571, 12637423, 23456818, 19361615
IFT27	SCGS v1	NA	Spinal curvature in KO mouse	PMID: 25446516
IFT57	SCGS v1	NA	Curved body axis in MO zebrafish larvae	PMID: 19517571
IFT80	SCGS v1	NA	Curved body axis in MO zebrafish larvae	PMID: 17468754
IFT88	SCGS v1	NA	Curved body axis in MO zebrafish larvae	PMID: 19517571
KIF17	SCGS v1	NA	ccasional slight curvature of the tail in MO zebrafi	PMID: 18304522
KIF3B	SCGS v1	NA	Curved body axis in MO zebrafish larvae	PMID: 22308397, 19384852
MKKS	SCGS v1	Bardet-Biedl syndrome 6, McKusick-Kaufman syndrome OMIM 604896	NA	PMID:14676542 and https://www.socialstyrelsen.se/rarediseases/bardet-biedlsyndrome
NEK8	SCGS v1	Nephronophthisis 9 OMIM 609799	Curly tail down in MO zebrafish	PMID: 19644333, 22687244
NPHP3	SCGS v1	Meckel syndrome 7, Nephronophthisis 3, OMIM 608002	Curved body axis in MO zebrafish larvae	PMID: 20462968, 14676542
OFD1	SCGS v1	Retinitis pigmentosa 23, Joubert syndrome 10 OMIM 300170	Curved body axis in MO zebrafish larvae	PMID: 18971206, 20301500, 22927466
ORC1	SCGS v1	Meier-Gorlin syndrome 1 OMIM 601902	Curved body axis in MO zebrafish larvae	PMID: 21358633, 22333897
PAFAH1B1	SCGS v1	Lissencephaly 1 OMIM 601545	NA	PMID: 19136950
PCM1	SCGS v1	NA	Curved body axis in MO zebrafish larvae	PMID: 22767577
PKD1	SCGS v1	Polycystic kidney disease, adult type I OMIM 601313	Curved body axis in MO zebrafish larvae	PMID: 20335443 and Catapano F. et al. Case Reports in Nephrology, 2012
PKD2	SCGS v1	Polycystic kidney disease 2 OMIM 173910	Curved body axis in MO zebrafish larvae	PMID: 16770799, 20335443,17360770
RP2	SCGS v1	Retinis pigmentosa, OMIM 300757	Slight to sever curved tail in MO zebrafish larvae	PMIDs: 16770799, 21282572
RPGR	SCGS v1	Retinis pigmentosa 3 OMIM 312610	Curved body axis in MO zebrafish larvae	PMIDs: 16770799, 22927466
RPGRIP1L	SCGS v1	COACH syndrome, Joubert syndrome 7 and Meckel syndrome 5 OMIM 610937	Curved tail in MO zebrafish larvae	1500, 15473174, 22927466, 19955120 and https://rarediseases.info.nih.gov/gard/1410/coach-syndrome
RTTN	SCGS v1	Polymicrogyria with seizures OMIM 610436	NA	PMID: 24507697
SDCCAG8	SCGS v1	Bardet-Biedl syndrome 16, OMIM 613524	rved and shortened body axis in MO zebrafish lar	PMID: 20835237, 14676542
SUFU	SCGS v1	Identified in the locus associated with IS triple curves	NA	PMID: 20358593
SYNE2	SCGS v1	Emery-Dreifuss muscular dystrophy 5 OMIM 608442	NA	PMID: 19589462
TTC21B	SCGS v1	Short-rib thoracic dysplasia, Nephronophthisis OMIM: 612014	NA	PMIDs: 12637423, 23456818, 19361615
TTC26	SCGS v1	NA	Curved body axis in MO zebrafish larvae	PMID: 22718903
TTLL3	SCGS v1	NA	Curved body axis in MO zebrafish larvae	PMID: 21262966
TTLL6	SCGS v1	NA	Curved body axis in MO zebrafish larvae	PMID: 21262966
TUBA1A	SCGS v1	Isolated lissencephaly sequence (ILS) OMIM 602529	NA	PMID: 21410694
WDR19 (IFT144)	SCGS v1	Nephronophthisis 13, Short-rib thoracic dysplasia 5, Jeune syndrome OMIM 608151	NA	PMIDs:19644333, 22019273
KDM1A	SCGS v1	Kabuki syndrome OMIM 609132	NA	PMID: 25568573
HERC2	Kim et al 2010	Mutation of HERC2 causes developmental delay with Angelman-like features OMIM 60583	NA	PMID: 23243086
TRIM3	Kim et al 2010	Limb-Girdle Muscular Dystrophy (LGMD)	NA	PMID: 11822024
AJAP1	Kim et al 2010	Locus is associated with IS in a GWAS study	NA	PMID: 26394188

The ciliary genes that are associated with scoliosis phenotype in human and/or animal models are listed in Supplementary Table 2-2.

Chapter III

Article Two;

Altered Mechanotransduction in Adolescent Idiopathic Scoliosis: A Pilot Study

Altered Mechanotransduction in Adolescent Idiopathic Scoliosis: A Pilot Study

---

To be submitted to: The FASEB Journal

Niaz Oliazadeh[1,2], Kristen F. Gorman[3] and Alain Moreau[1,2,4*]

[1]Viscogliosi Laboratory in Molecular Genetics of Musculoskeletal Diseases, Saint Justine Children's Hospital Research Center. Montreal, QC, Canada.

[2]Department of Biochemistry, Faculty of Medicine, University of Montreal, QC, Canada.

[3]Department of Biological Sciences, California State University, Chico, CA 95929, USA.

[4]Department of Stomatology, Faculty of Dentistry, Université de Montréal, Montreal, QC, Canada.

*Corresponding author: Alain Moreau, PhD, E-mail: alain.moreau@recherche-ste-justine.qc.ca

Author contributions:

Niaz Oliazadeh: Conceived the study, designed, performed and analyzed the experiments, and wrote the manuscript as the lead author.

Kristen F. Gorman: Provided insightful discussion and revised the manuscript.

Alain Moreau: The principal investigator who has secured the funding of this research project, supervised and supported the study and participated in writing of the manuscript.

3.1 **Abstract**

Adolescent Idiopathic Scoliosis (AIS) is the most prevalent pediatric spinal deformity condition. Our previous works demonstrated the presence of longer cilia and altered molecular mechanosensory response in AIS osteoblasts. The aim of this study is to further characterize the mechanosensory defect in the bone cells of AIS patients. Under both short- and long-term flow applications, AIS cilia length adjustment in response to flow was significantly different from controls. Flow induced increase in secreted VEGF-A in control osteoblasts was not detected in AIS under flow-conditioned media. Confocal microscopy images showed that the strain-induced rearrangement of actin filaments was compromised in AIS osteoblasts. Unlike controls, AIS osteoblasts failed to position or elongate themselves in proportion to the bidirectional applied flow. Finally, fluid flow showed to have an inhibitory effect on cell migration contrasting with control osteoblasts that migrated significantly faster under flow. Collectively, our data, demonstrated that in addition to the observed primary cilium defects, there are also cytoskeletal abnormalities at the cellular level resulting in an impaired mechanotransduction in AIS. Thus, we propose that the AIS etiology is a result of a generalized defects in cellular biomechanotransduction. A growing spine is under constant stimulation for growth and bone remodeling in response to applied mechanical forces. Recognition of an altered mechanotransduction as part of AIS pathomechanism must be considered in the conception and development of more effective bracing treatments and could explain failures of bracing in progressive cases.

Keywords: cilia, osteoblasts, scoliosis, mechanotransduction, VEGF

3.2 Introduction

Adolescent Idiopathic Scoliosis (AIS) is a complex pediatric disease involving an abnormal three-dimensional spinal curvature of unknown cause. At the clinical level, AIS phenotypic heterogeneity is illustrated by a wide range of curve type patterns from mild spinal deformity to severe scoliosis. In the most severe cases, progressive scoliosis is accompanied with rib cage deformity that can cause serious health issues such as pulmonary and cardiac distress for the patient. Clinically, idiopathic scoliosis is broadly categorized by the age when a curve onset is first noted. Adolescent idiopathic scoliosis is the most prevalent type of idiopathic scoliosis affecting an average of 2% - 4% of children aged 10 to 16 years old with a potential of progression during the rapid phase of growth [5], [272].

Despite decades of research into the etiology of AIS, the exact root causality for the disease is still unknown [28]. Although a genetic basis is acknowledged, genetic heterogeneity coupled with the clinical heterogeneity has complicated efforts to understand the biological basis of AIS [15], [19], [273]. Genetic predispositions, hormonal imbalance, neurological disorders and environmental factors have all been suggested to play a role in disease onset and scoliosis progression as well as in the elaboration of specific spinal curve patterns (Reviewed in [2]).

Adolescent Idiopathic Scoliosis occurs at adolescents during pubertal growth spurt and curve progression usually stabilizes at skeletal maturity. Comparing AIS patients to healthy age-matched groups, researchers listed several growth or growth-related abnormalities among the patients. Abnormal age associated growth patterns, differences in body height and proportions, differential body composition such as lower bone mass and muscle index, lower bone mineral density, quality and strength, abnormal bone turnover and finally hormonal changes all have been reported either as a potential cause or a secondary side effect of the disease [274].

Because the deformity presents clinically in the tissues of bone, cartilage, and muscle, idiopathic scoliosis is considered primarily a musculoskeletal disease, although other physiological systems have been implicated [2]. Considering the fact that tissues of the musculoskeletal system are load bearing, biomechanics is an important factor in the

pathogenesis of the disease. Traditionally, biomechanics has been applied to AIS on the anatomical level. For example, how a growing scoliotic spine can lose its mechanical stability, resulting in the deformation of vertebral bodies, which could potentially encourage compensatory curves and thus deformity progression [275]. Independent of underlying etiological factor, the importance of biomechanics in AIS development as well as its non-surgical treatments (e.g. bracing, physical therapies) is well established [187]. Understanding the bodily responses to mechanical stimuli can provide novel angles regarding etiology and also holds many possibilities for improving the current therapeutic approaches and developing novel personalized options.

To understand the etiology of AIS, our approach is to examine biomechanics from a cellular level. Our previous work showed that the mechanosensory organelle, the primary cilium, from AIS patient derived osteoblasts is longer than the primary cilia in osteoblasts derived from non-patient bone. Furthermore, we demonstrated that the cells with elongated cilia are less responsive to mechanical stimulation [179]. Our comparative analysis of AIS patient versus control exomes indicated an enrichment for rare variants in genes involved in mechanotransduction and/or ciliogenesis among AIS patients [179]. Evidence that idiopathic scoliosis is associated with cellular biomechanical defects is further supported by several AIS genetic studies. These studies either corroborate a ciliopathy [276], [277], or implicate other mechanosensitive features such as the extracellular matrix [42]. Taken together, recent evidence supports a disturbed cellular mechanosensory system in AIS.

We previously demonstrated that AIS osteoblasts have elongated cilia, and that these cells differentially express mechanosensitive genes in response to shear force, compared to control osteoblasts. The primary cilium is a dynamic organelle that can change length under varying circumstances [249]. In this study we investigated whether osteoblasts from AIS patients display different ciliary dynamics in response to oscillatory fluid flow. Then we evaluated cellular behaviors such as migration, elongation and orientation in response to flow.

In our previous study we showed that the most dramatic difference in ciliary length between AIS patients and control derived osteoblasts was before cellular starvation and at 24 hours post starvation. Considering that actin polymerization inhibitors induce longer

cilia and facilitate ciliogenesis independently of starvation [229], we also investigated flow induced actin rearrangement and vascular endothelial growth factor (VEGF) secretion.

3.3 Materials and Methods

3.3.1 Cell culture

Primary osteoblast (OB) cultures were generated from intraoperatively obtained bone samples of AIS and trauma patients as previously reported [179]. Briefly, bone specimens were extracted from vertebrae (varied from T3 to L4) of AIS patients or other parts of skeleton (tibia or femur) of non-scoliotic trauma cases. After cutting the bone to smaller pieces, they were incubated in culture (αMEM medium, 10% fetal bovine serum, 1% penicillin/streptomycin (Invitrogen Life Technologies, ON, Ca) at 37°C in 5% CO2 for a month. Emerging primary osteoblasts were then separated by trypsinization and characterized using mineralization and osteoblast marker [179]. To promote ciliogenesis, cells were washed in sterile PBS upon confluency and incubated in differentiation media (reduced FBS to 1%) for 48h. We chose 48h to possibly minimize the differences between cilia length of controls and AIS, based on our previous results. Cells were washed with PBS after differentiation and incubated in regular media right before starting all our experiments.

3.3.2 *In vitro* fluid flow stimulation

For shear stress experiments, each sample were divided between two 1-well chamber slides (Thermo Fisher scientific, Nunc™ Lab-Tek™, MA, USA) at a density of 3×10^5 cells per well in complete medium (αMEM + 10% FBS + 1% penicillin/streptomycin). Upon reaching 80% confluency, the medium was removed, the cells were washed with warm, sterile PBS and then transferred to a starvation medium to promote cell differentiation and ciliogenesis. After 48h cells were washed again and transferred back to 2 ml regular medium immediately before they were subjected to oscillatory fluid flow using a double-tier rocking platform, as explained in our previous work [179]. In summary, a two-tier rocker with ± 20 degree of maximum tilt angle was housed in a cell culture incubator at 37 °C and 5% CO_2 for the duration of the flow

experiments. Flow samples were sat on the rocker moving at a frequency equal to 2Hz, while no flow control cells were kept in the upper shelf of the same incubator during the experiment. Fluid shear stress patterns were applied to cells in a predictable, controlled, and physiologically relevant manner in a magnitude of 1 Pa at the middle of the dish as we elaborated in our previous publication [179].

3.3.3 Immunofluorescence staining

Cells were washed with PBS, fixed with 4% PFA in PBS buffer for 10 minutes at room temperature, washed again (1% BSA in PBS), and then permeabilized with 0.1% Triton-X-100 in PBS for 10 min at room temperature. After two washes, the cells were blocked in 5% BSA in PBS for 1h at room temperature. For cilia staining, cells were incubated with anti-acetylated α -tubulin (Invitrogen Life Technologies, ON, CA) diluted (1:1000) in 3% BSA-PBS, overnight at 4° C. The following day, after 3 washes, the cells were incubated for 1h at room temperature with Alexa Fluor 488 conjugated goat anti-mouse secondary antibody (Invitrogen). After 3 washes, 1 μg/ml dilution of Hoechst (Sigma-Aldrich, ON, CA) in 1% BSA-PBS was used to stain the nucleus at room temperature for 10 min. F-actin was stained with Alexa Fluor 555 Phalloidin (Invitrogen), dilution (1:40) in 1% BSA-PBS incubation at room temperature for 20 min.

3.3.4 Scratch/wound healing test

Osteoblasts from both AIS and control groups (n=3 per group) were cultured in one chamber slide dishes (Thermo Fisher Scientific, Nunc™ Lab-Tek™, MA, USA). Upon reaching 80% confluency, and after 48h of ciliogenesis, three linear wounds were created in each slide, perpendicular to the long edge and equally distanced from each other by scratching the monolayer using a sterile 200 μl pipette tip [278]. Cells were then washed with PBS to remove floating cells and debris before being transferred to regular warmed media. The scratched areas in live cells were imaged using ENVOS FL Microscopy (ThermoFisher Scientific, MA, USA), objective 20x. These images were then used to calculate the T_0 area of the wounds in corresponding samples. After flow experiment, immunofluorescence staining and imaging, the degree of wound closure was measured

manually as the percentage of the area covered by migrating cells at T_{20} compared to the initial wound at T_0, using Fiji software[279]. We evaluated 3 wounds per sample, and 3 fields of view per wound.

3.3.5 Confocal microscopy and image analysis

Images were captured on a Leica Confocal TCS-SP8 using 63x (oil) or 10x objectives with 1024×1024 pixels resolution. Each sample has been examined in stitched 5×4 or 5×5 tile images, (covering 20 or 25 fields of view). Maximum projections of the Z-stacks were used for primary cilium length and actin intensity measurements, which was done in Image J (NIH). To be able to measure the intensity of fluorescent stained actin as an indicator of protein quantity, all related images were acquired using the same microscope under identical settings (i.e. laser intensity, acquisition time, resolution, etc.). Corrected total cell fluorescence (CTFC) was calculated by measuring actin intensity normalized to the background of each sample, using Fiji software. For cell alignment analysis, we used the longest axis of the nucleus as the major axis of the cell. The orientation of each cell was determined by measuring the angle (α) between the cell and the axis of flow application manually in Fiji software. We evaluated cellular orientation in 5×4 tile images, i.e. 20 fields of view per sample. The cells with round nucleus were omitted from evaluation.

3.3.6 Vascular endothelial growth factor (VEGF-A) measurement

Cell culture medium were collected from samples at the end of each fluid flow experiment, aliquoted, labeled and transferred to -80 freezer for later process. In the day of experiment, the samples were thawed on ice and centrifuged at 4^{o}C, 10 000xg for 10 minutes to remove possible cellular debris. VEGF-A levels were measured using the Human VEGF-A Platinum ELISA kit (ThermoFisher Scientific, Waltham, MA, USA), following the manufacturer's protocol. Absorbance was read at 450nm, using the DTX880 Multimode Detector (Beckman Coulter, Brea, CA, USA).

3.4 Results

3.4.1 Cilia length is differentially adjusted in AIS osteoblasts in response to fluid flow

Normal osteoblasts modify the length of their cilia in response to the intensity and duration of applied mechanical stimulation. This adaptive response is part of a biological regulatory process that allows the cells to adjust their mechanosensory structures proportionally to accommodate the mechanical challenge [210]. We investigated if the elongated cilia previously observed in AIS osteoblasts behaves differently when compared to similar cells obtained from healthy subjects after applying 1Pa fluid flow shear stress for a short (1.5 hour) or long (20 hours) period. We found out that control cells reduce the length of their cilia significantly after 1.5h of flow application (mean decrease of 8%, $P < 0.005$) while under long term flow application (20h) their cilia length increased significantly (mean increase of 13.2%, $P < 0.0001$). Conversely, in AIS osteoblasts, short-term flow application induced an increase in the length of their cilia (mean increase of 13.3%, $P < 0.0001$), while long-term flow application had no significant effect (Fig. 3-1). Of note, the length of cilia in absence of flow application for 1.5 and 20h (NoF 1.5h and NoF 20h) in AIS samples was shorter (respectively 2.26 ± 0.66 μm and 2.57 ± 0.75 μm) when compared to healthy osteoblasts (2.15 ± 0.70 μm and 2.08 ± 0.50) but only the 20h comparison reached a statistical significance ($P < 0.0001$). Previously, we reported an increased length in cilia of AIS osteoblasts that was consistent up to 72h of ciliary growth in ciliogenesis media. In the current experiments however, the cilia were measured post-ciliogenesis and after being transferred for 1.5h or 20h to the regular media. In both cases, the common observation is in support of an impaired regulation of cilia length in AIS that could contribute to the reported abnormal mechanosensory behaviours. Consequently, in order to minimize the effects of cilia length discrepancy at the starting point of our functional experiments, we chose the 48h starvation point for ciliogenesis that previously showed lesser length variations between the two groups as previously reported [179].

3.4.2 Flow induced actin remodeling is impaired in AIS osteoblasts

Mechanotransduction induced actin remodeling in bone cells has been previously reported [280]. Fluid shear stress in osteoblasts induces actin reorganization and changes

them into thicker structured contractile stress fibers [281], [282]. Disruption of actin cytoskeleton negatively affects the cellular mechanosensitive responses, while actin polymerization enhancement promotes osteogenic differentiation [282].

To test the response of actin filaments to fluid flow in primary osteoblasts, we measured the intensity of fluorescently stained actin relative to their corresponding background in both mechanically induced (flow, F) and in absence of mechanical stimulation (no flow, NoF) groups and compared the AIS cells to controls. Application of an oscillatory fluid flow induced F-actin remodeling and reorganization in control cells. This is consistently visible across images acquired from control cells subjected to flow, contrasting with AIS osteoblasts in the same condition, which actin response was not detected in them (Fig. 3-2A). Moreover, following flow application a significant increase in the F-actin intensity was observed in flow subjected osteoblast compared to no flow in controls (2.3-fold increase, $P = 0.009$), while the F-actin intensity in flow subjected AIS cells remained unchanged following the same flow application (Fig. 3-2B).

3.4.3 Fluid flow does not increase the rate of wound healing/cell migration in AIS cells

The orientation of primary cilia orientation changes in response to a wound healing stimulation, and it has been shown that cilia turns perpendicular to the leading edge of a migrating cell after 10 hr in culture [283] as if pointing towards the direction of migration [284]. This dynamic changes in cilia is a consequence of tightly regulated assembly and disassembly, which is mediated through F-actin dependent mechanisms [283]. Furthermore, using cells derived from a mouse model, mechanical stimulation was reported to accelerate wound closure by about 50% [119].

To assess whether AIS cells show impaired actin dynamics, we examined the rate of wound healing using a scratch test applied to the cultured osteoblast monolayer surface in IS and control cells, with and without the influence of fluid flow. We scratched each sample in 3 straight lines using a sterile p200 pipette tip, recorded images of the T0 scratched area for each sample and compared that to the same area after 20h (T20) of applying (F) or not applying fluid flow (NoF). The uncovered area of each T20 scratch was

measured in comparison with its baseline value (T0) to calculate the percentage of wound healing. Considering the natural variability of migration rates that is expected from human primary cells, we decided to compare each AIS or control cell only to its own static counterpart rather than comparing the whole AIS group vs. controls (Fig. 3-3). In osteoblasts obtained from healthy individuals, the cells in all T20, F and NoF samples were seen to migrate into the scratched area starting to heal the wound, and we observed a significant increase ($P < 0.05$) in the rate of wound healing among control cells in response to the fluid flow (56.6%, 52.4% and 84.2% wound closure) compared to their static counterparts (33.8%, 26.2% and 73.3% wound closure). While wound healing process was also visible in both T20, F and NoF samples of AIS osteoblasts, fluid flow application not only did not enhance the healing process, but rather reduced the rate of healing in all tested AIS samples (flow induced wound closures were 61.8%, 32.4% and 32.3% versus 74.8%, 77.2% and 45.3% without flow). Therefore, flow application on AIS osteoblasts did not promote cell migration as expected, on the contrary it showed to have an inhibitory effect. AIS osteoblasts migrated through the scratched gap faster in stationary conditions (NoF) and this increased rate was even significant in one AIS case (77.2% NoF vs. 32.4% F, $P < 0.005$) (Fig. 3-3).

3.4.4 AIS cellular orientation in response to directional flow is impaired

Nucleus positioning and orientation relative to the leading edge of a moving cell contributes to the polarized, asymmetrical task of cellular migration. Multiple cytoskeleton elements including cilia and actin filaments have been shown to associate to movement and orientation regulation of nucleus and the cell as a unit. Nuclear rotation and orientation have been hypothesized to be the consequence of cytoskeleton rearrangement [285].

It has been reported that directional mechanical stimulation could affect the orientation and morphology of the MSC cells in culture [286]. After observing the defects in cilia length adjustment and actin filaments rearrangement in response to flow, we decided to look at the orientation and positioning of cultured primary osteoblasts from AIS patients following 20h of oscillatory fluid application in comparison with osteoblasts from controls (Fig. 3-4A). We measured the angle between the long axis of the nucleus relative to the direction of applied flow (Fig. 3-4B) in 500-750 cells across 20 different fields of

view per sample. In theory, random cell orientation would result in one-third of the cells being oriented with their long axis ±30° from any random line drawn through the field of cells [281]. This means in static conditions, cellular population orientation relative to an arbitrarily selected line will be divided in 3 groups: ~ 33% between 0 - 30°, ~ 33% between 30°- 60° and ~ 33% between 60°- 90°. As presented in Table 3-I and Figure 3-4C, both no flow samples in AIS and control group are following the expected random distribution. After flow application (20h, 2Hz), control cells started orienting themselves perpendicular to the axis of strain. This shift of distribution is visible in the bar charts of Figure 4C. While flow application seems to also disturb and shuffle the normal orientation distribution of AIS cells, the pattern does not follow the observed shift in controls. At the end of 20h flow, 41.08% of control cells are positioned in angles between 60° to 90° relative to the axis of flow, while this value is only 19.49% in AIS cells. Our results show that AIS osteoblasts fail to align themselves normally in response to the axis of a bidirectional oscillatory flow, which is a prominent type of load induced force affecting bone cells *in vivo* [282].

3.4.5 Fluid flow does not induce VEGF secretion in the medium of cultured AIS osteoblasts.

Pathways involved in regulation of actin cytoskeleton and VEGF signalling are reported to be among the main activated pathways under mechanical induction in mouse osteoblastic cells [116]. This prompted us to investigate for possible changes in VEGF secretion in the medium of cultured AIS and control osteoblasts. Indeed, secreted VEGF was significantly increased by an average of 68.8% (p = 0.035) in control osteoblasts following fluid flow application (Fig. 3-5). Interestingly, the same mechanical stimulation did not increase the amount of secreted VEGF in AIS osteoblast medium, strongly suggesting an impaired mechanotransduction pathway.

3.5 Discussion

Despite decades of research on idiopathic scoliosis, there is not much understanding of the disease in the cellular level. Among 3773 publications listed on the PubMed database in English language with “Idiopathic Scoliosis” or “AIS” in their title, since the beginning

of 1990 till present date, only less than 40 papers used any cellular methods in their investigation of the disease (Fig. 3-6).

The relationship between mechanical strain and bone morphology is complex, with adaptive changes on molecular, cellular and tissue levels. In our previous work we identified impaired cellular biomechanosensation among AIS patients. Using osteoblasts derived from AIS bone, we reported elongated primary cilia, along with an altered molecular mechanosensory response profile [179]. In the current study we aimed to further characterize the AIS mechanosensory abnormalities that are observable under mechanical strain. These studies shed insight into the etiology of AIS from a dynamic perspective that incorporates both physics and cellular biology.

We found out that osteoblasts modify the length of their primary cilium in response to fluid flow application, in a time dependent manner. In control cells, short-term flow (1.5h) reduced the average length of cilia, while continuous application of the same flow regimen induced an increase in ciliary length. In contrast, AIS osteoblasts increased the length of their cilia following short-term fluid flow, while the continuous flow application had no significant effect on their average ciliary length. These results show that the previously reported cilia abnormality is dynamic according to mechanical circumstances. It is known that different types of mechanical stimulation can activate different molecular pathways; stretch, compression, gravity, vibration and fluid shear stress are all physiological forces but they differ in their effects and mechanisms (reviewed in [287]). Even the same type of stress can be applied with different magnitudes, durations and frequencies, which can induce different cellular responses. For example human fetal osteoblasts are responsive to pulsatile shear stresses but not to steady or oscillatory ones [288]. As a mechanosensory organelle, increase or decrease in the length of cilia, in response to mechanical stimulations, has been shown as a cellular attempt to adjust its mechanical sensitivity. Cultured osteoblasts stimulated with a long period of oscillatory fluid flow (up to 5 days) have been shown to shorten their ciliary length [210]. We have previously shown that AIS osteoblasts cultured in cilia differentiation media up to 72h can keep growing significantly longer cilia compared to controls, suggesting an abnormality in their cilia length regulation [179]. In the current experiments, we allowed the cells to grow their cilia for 48h before transferring them to regular media for mechanical stimulation,

because this was a time point when we observed less variability between case and controls for length [179]. Evaluating the length of cilia following the applied mechanical strain, we again observed an abnormal length adjustment pattern compared to controls. Cilia length adjustment in response to different flow application regimen and its importance on downstream cellular adaption have been shown before in several human cells including osteoblasts [210], [249].

Cilia length regulation and maintenance is the result of a precise balance between processes involved in its assembly and disassembly. Intraflagellar transport (IFT) is a tightly evolutionary conserved system, which is responsible for transferring molecules to and from the tip of the cilium as an organelle extended out of cytoplasm. The IFT system composed of two multi-protein complexes, IFT-A and IFT-B, localized at the cilia base, that are involved in retrograde and anterograde transportation respectively [289]. The accumulation or increased activity of the anterograde IFT system leads to elongation of cilia whereas reduced mobility of them results in shorter cilia [290]. Stimulation of cyclic AMP and subsequent increased activity of PKA has been shown to lengthen cilia in mammalian epithelial and mesenchymal cells, through increased trafficking of anterograde IFT complex [249]. Fluid shear-mediated deflection of the longer primary cilia then stimulates cAMP reduction inside the cell creating a regulatory feedback loop which shortens the cilia again [291]. Melatonin signalling dysfunction and the following disturbance of intracellular cAMP previously reported in AIS patients [47], [48], [70] might explain ciliary length abnormalities observed in AIS osteoblasts. AIS osteoblasts failure to adjust their ciliary length in proportion to applied mechanical stimulation (i.e. short- or long-term fluid flow) indeed points towards the possibility of ciliary defects underlying AIS pathogenesis. Incapable of adjusting the length of their cilia accordingly, AIS osteoblasts are not able to transfer proper information about the type and scale of the introduced mechanical stimulation to the cell, compromising the adaptive nature of bone to surrounding forces and perhaps leading to structural abnormalities in the bone. There could be a causative link between cilia length miss-regulation and AIS, as is the case in some types of cancers [283].

The cytoskeleton is comprised of microtubules, intermediate and actin filaments, and provides the means of perceiving and responding to mechanical signals. Fluid shear

stress application on osteoblast induces reorganization of actin filaments into contractile stress fibers [292], while disruption of the actin cytoskeleton reduces the response of bone cells to fluid shear stress [282]. Additionally, enhancement of actin polymerization increases osteogenic differentiation [293]. Consistently, oscillatory fluid flow (20h), induced actin rearrangement in our control osteoblasts, changing them to thicker and more intertwined fibrillar structures with significantly higher intensities as shown in confocal microscopy images, while this drastic change of actin filaments is completely missing in AIS osteoblast that underwent similar flow condition. Observed cytoskeletal changes following flow shear stress has been confirmed to be the result of increased crosslinking proteins such as filamin and α-actinin rather than increased amount of actin monomers in mouse and human fetal osteoblasts [294]. These alterations following a mechanical loading, cause rearrangement of actin filaments that enhance mechanical resistance of the whole cell [294].

The migratory potential of osteoblast lineage was first described in detail by Jones & Boyde [295]. During the process of bone remodeling, osteoblasts and their progeny are required to navigate through a complex three-dimensional bone structure with a remarkable spatial precision. They need to skilfully reach to their destination, depositing new material either into site of a fracture or a forming bone. Beside getting attracted towards or repelled from certain chemotactic cues, mechanical signals such as fluid flow, i.e. “flowtaxis”, also serve as landmarks for osteoblasts navigation [282], [296]. In fact, migration of MSCs, as osteoblast origin, and their path efficiency are dependent in fluid flow [297]. In addition to fluid shear effects on bone restructuring, proliferation, differentiation, and guidance of bone forming activity [120], [179], [288], [294], [298], shear stress has been reported to affect the migration behaviour of osteoblasts in speed and direction [119]. Recruitment of bone forming osteoblasts to the bone remodeling site contributes to the bone tissue homeostasis.

Our functional evaluation of AIS osteoblasts showed that fluid flow application does not accelerate their migration rate, compared to static culture condition (NoF). Surprisingly, AIS osteoblasts healing process was faster in stationary condition as demonstrated in the scratch test, while control osteoblast responded positively to fluid flow stimulation, closing the gap more efficiently under flow. Note that the direction of flow in

our experiment was designed to be perpendicular to the scratched lines, so that fluid flow guides the cells into the created wounds as suggested previously for mesenchymal stem cells [119]. Cilia not only sense the mechanical strain but also have been shown to play a crucial role in the cellular migration process. The primary cilium points to the direction of migration and guide the cell through extra cellular matrix by complex and closely regulated molecular signaling pathways that are not truly understood yet. Ciliary interactions with ECM, Wnt pathway and polarity signalling have been all suggested to play a role in this process [284].

Overall cellular shape is known to be coordinated to the shape of nucleus in an actin dependent manner, mostly due to physical connections between actin filaments and nucleus membrane [299]. For instance, in the process of new blood capillaries formation, endothelial cells (ECs) need to polarize and migrate which is accompanied by a large cellular elongation [300]. This shape change in ECs are usually associated with nuclear shape remodeling as well [301]. Interestingly, shape remodeling information is emerged as a potential gene expression regulator [302], through mechanical forces transmitted by the cytoskeleton [303]. Cellular responses to directional flow are determined by cell shape, strongly suggesting that cytoskeleton and adhesive structures play as an internal compass against which flow is measured [304]. We measured the angle between the longest axis of nucleus and axis of flow (α) to evaluate AIS osteoblast orientation and elongation in response to fluid flow stimulation in comparison to controls. Control osteoblasts were observed to start shifting their orientation towards perpendicular to the direction of strain. After 20h of flow application, the α angle of 41% of Ctrl-F group was measured between 60 to 90° compare to only 33% in control NoF group. While mechanical stimulation also disturbed the normal angle distribution in AIS-F cells, no particular pattern was observed in their orientation in response to flow (Table 3-1). Changes in flow direction in endothelial cells affected the expression levels of multiple growth factors and inflammatory genes. Previous studies have shown that the angle between flow direction and the cell axis, which is defined by cell shape and F-actin, dictates these flow responses, suggesting a central role for cell alignment in the response to shear stress [304].

Human vascular endothelial growth factor (VEGF) is involved in many aspects of the bone tissue such as bone growth, remodeling, healing, vascularisation, etc. It also acts

in a cellular level as an essential mediator of osteoblast, osteoclast and chondrocyte proliferation, differentiation and/or survival (reviewed in [305]). VEGF plays a role in mechanically induced bone gain and its signaling has been shown to induce actin polymerization/depolymerization and to activate focal adhesion kinases in both endothelial and osteoblast cells [302]. It has been shown that the actin cytoskeleton adaptation during osteoblast mechanotransduction is regulated by shear stress induced VEGF signaling. VEGF involved mechanisms also play an essential role in actin reorganisation in cellular migration process [306]. Following the observed abnormalities in actin remodeling responses, flow induced migration and positioning of AIS osteoblasts under flow, we decided to test the possibility of a disturbed VEGF signaling. We performed ELISA analysis on the flow conditioned media of both AIS and controls. To our expectation, the quantity of secreted VEGF in the media of Ctrl-F group almost doubled up after 20h flow induction, while fluid flow application on AIS cells did not affect the amount of VEGF in their media.

In the present pilot study, we acknowledge some limitations. The relatively small sample size of AIS cases tested, and the selection of only severe scoliosis cases should be mentioned. Secondly, it remains to be investigated if other musculoskeletal cell types harboring cilia will exhibit the same dysfunction as evidenced in AIS osteoblasts. Finally, the molecular mechanism regulating VEGF signaling and/or its secretion in AIS remains to be characterized and represents an unexplored frontier in the field of scoliosis.

In summary, our data suggests a disturbed mechanotransduction in AIS osteoblasts that goes beyond morphological changes in cilia. Changes or lack of change in response to flow can grossly affect structure, strength, shape and function of bone. Polymerization, depolymerization and arrangement of cytoskeleton filaments are playing a role in sensing and tissue adaptation to mechanical stimulation. A compromised actin dynamics in the context of AIS, can also affect ciliogenesis, resulting in a wide variation in ciliary lengths and a systemic mechanotransduction impairment [283]. At the clinical level, it is conceivable that deregulation of the mechanosensory machinery could reduce or prevent brace response in severely affected AIS patients.

3.6 Acknowledgments

We thank the patients and families who participated in this study and the orthopedic surgeons and nursing teams at Sainte-Justine University Hospital, The Montreal's Children Hospital, and The Shriners Hospital for Children in Montreal. We also thank Ms. Anita Franco, Dr. Claudia Raggi, and Dr. Erika Wee (Advanced Bio-Imaging Facility (ABIF) at McGill University) for their technical assistance and helpful suggestions. This work was supported by grants to AM from La Fondation Yves Cotrel de l'Institut de France, Paris, France.

Author contributions. NO conceived the study, designed and performed the experimental works, analyzed the data and wrote the manuscript as the lead author. KFG provided insightful discussion and revised the manuscript. AM is the principal investigator who has secured the funding of this research project, supervised and supported the study and participated in writing of the manuscript.

Competing interests. This work led to a patent application (pending) own by Sainte-Justine University Hospital (CHU Sainte-Justine). The authors declare no other potential conflicts of interest.

3.7 Figure legends

Figure 3-1. Flow induced primary cilia length adjustment is impaired in IS osteoblast independent of time. A) Immunofluorescence micrographs of cilia using acetylated α-Tubulin (green) and Hoescht (blue), in IS and control osteoblasts under static or mechanically stimulated conditions. White scale bar, 5 µm. **B)** The dynamic of cilia length adjustment in response to flow application (F) in comparison with their static counterparts (NoF) in IS and controls. n = 4 per group, 25 fields of view, red bars represent the mean. Statistical significance was determined by student t-test using JMP-14. **C)** Values of the mean and standard deviation are summarized in this table.

Figure 3-2. Flow induces actin rearrangement in control osteoblasts but not IS. A) Immunofluorescence micrographs of IS and control primary osteoblast cells after 20h of fluid flow application in comparison to their static counterparts. F-Actin is stained with Phalloidin (red) and nucleus with Hoescht (blue). White scale bar, 25 µm. **B)** Data represents the mean ± SEM of corrected total cell fluorescence (CTFC) which have been measured using Image-J software and normalized to the background of each sample. n = 4 per group, Statistical significance was determined by student t-test using JMP-14.

Figure 3-3. Fluid flow does not increase the rate of Wound healing/cell migration in IS cells. A) Grayscale Immunofluorescence micrographs (Objective 10x) of wounded monolayers of IS and control primary osteoblast at T20h with (F) or without (NoF) flow application. Cells are stained for their nucleus and actin filaments. White scale bar, 500 µm. The double headed arrow indicates the direction of flow. **B)** An example of a T0 image that shows live cells right after applying the scratch (Objective 20x), the dotted white line marks the scratched line, Scale bar, 500 µm. **C)** The schematic view of the one well chamber slide, dotted black lines show the three scratches and their positioning. We studied three fields of view of three wounds in one chamber slide per sample per condition. **D)** Data represents the mean ± SEM of wound healing percentages for IS and control cells. Each no flow (NoF) condition sample have been compared to their own flow condition (F) using student t-test using JMP-14. * p value < 0.05, ** p value < 0.005.

Figure 3-4. Cellular orientation adjustment relative to direction of flow varies between control and IS primary osteoblasts. A) Grayscale Immunofluorescence micrographs (Objective 63 oil) of stained nucleus and actin F filaments, to show how the cells orient themselves relative to the axis of flow (20 h), in almost 4 fields of view for each sample. White scale bar, 25 μm. Tow headed white arrows show the direction of oscillatory fluid flow application. **B)** For each sample 500-750 angles between the longest axis of the nucleus and axis of flow (α) were measured in 5×4 tile images (20 fields of view) as shown in this schematic figure (adapted from Yao and Wong (2015) Cells. J. Biomech. Eng. 137, 020907). **C)** Data represents the frequency of cellular alignment distribution in percentage after 20h of 1Hz flow application. Trendline of moving average is shown in dotted lines.

Figure 3-5. Fluid flow does not induce VEGF secretion in IS osteoblast cells. The quantity of secreted VEGF was measured in the medium of both IS and Control cultured cells, following 20h fluid flow application in comparison to their stationary counterparts. n = 4 per group, each standard error bar is constructed using 1 standard error from the mean in JMP-14 software. Student t-test p value = 0.035.

Figure 3-6. Annual distribution of publications on Idiopathic Scoliosis as were indexed in PubMed. NCBI PubMed database was used to extract the data. The publications in English language from 1990/01/01 till present were searched with following criteria: For total publication we searched for the keywords of "AIS" or "Idiopathic scoliosis" in the title (search details: AIS [Title] OR Idiopathic Scoliosis [Title]); For reviews we added keywords "Review" or "Systematic Review" as publication type (search details: AIS [Title] OR Idiopathic Scoliosis [Title] AND ((Review [ptype] OR systematic[sb]), For cellular work "total publication" search was performed and we searched for the keyword "Cell" in title or abstract of the paper (search details: Cellular, AIS [Title] OR Idiopathic Scoliosis [Title] AND Cell [Title/Abstract]). Then abstracts of all the listed results were manually scanned for cellular methodology and the number of

studies whit cellular work per year are listed on top of the bars. Blood cell studies were excluded.

A

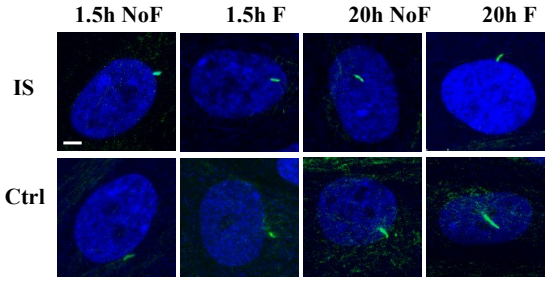

B

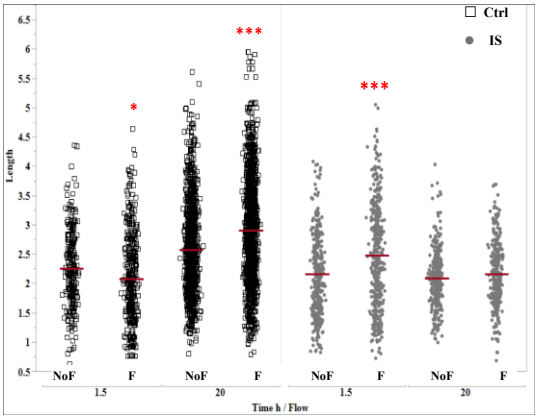

* $p < 0.005$
*** $p < 0.0001$

C

	1.5 h		20 h	
	No Flow	Flow	No Flow	Flow
Ctrl	2.26 ± 0.66	2.08 ± 0.74	2.57 ± 0.75	2.90 ± 0.87
IS	2.15 ± 0.70	2.48 ± 0.87	2.08 ± 0.50	2.15 ± 0.55

Figure 3-1. Flow induced primary cilia length adjustment is impaired in IS osteoblast independent of time.

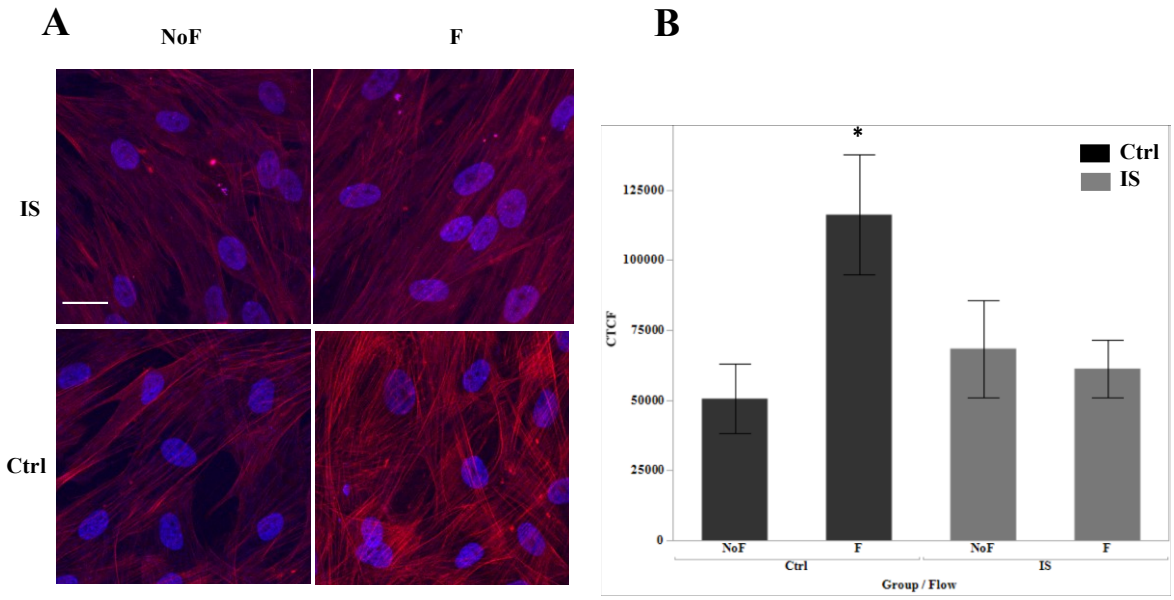

Figure 3-2. Flow induces actin rearrangement in control osteoblasts but not IS.

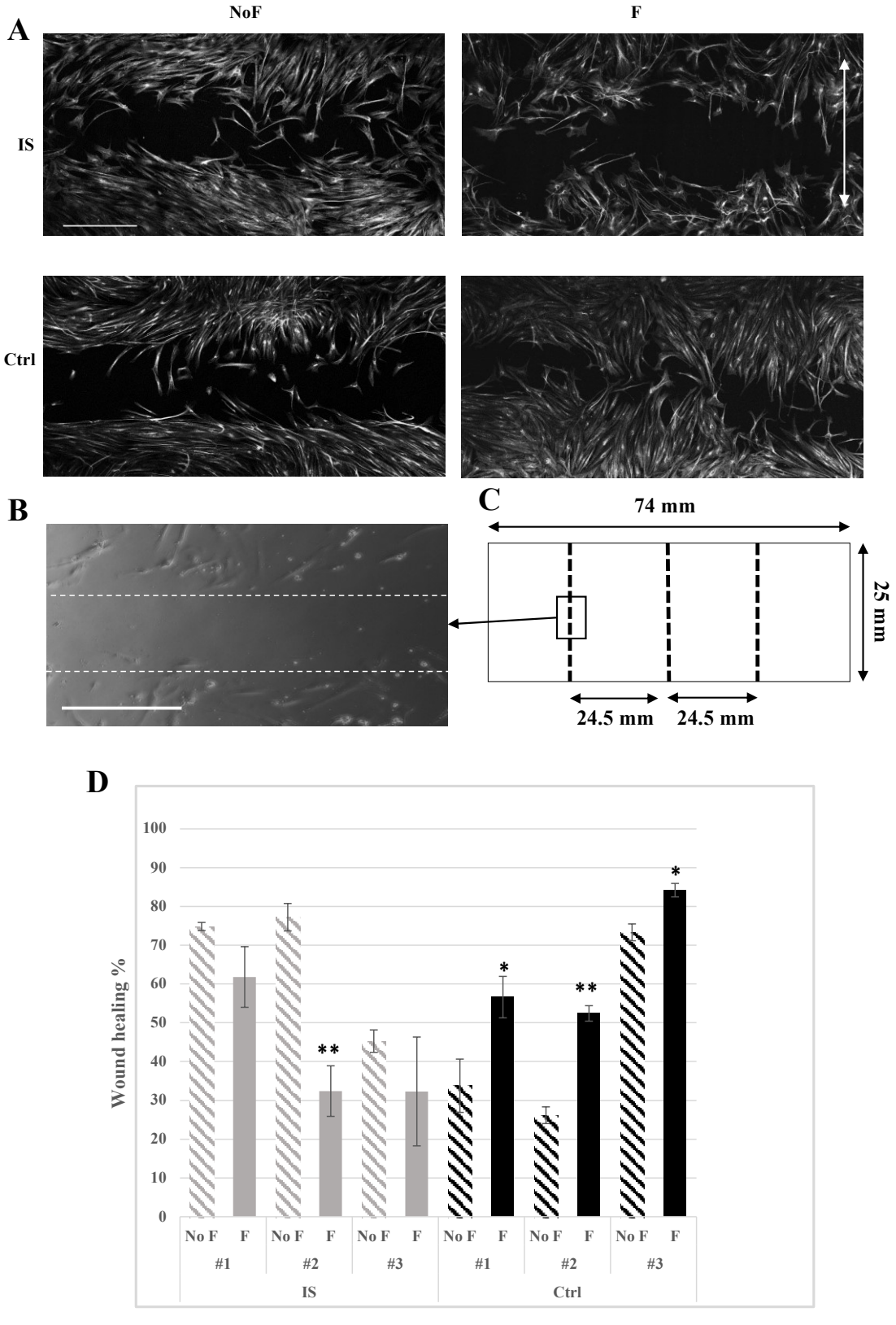

Figure 3-3. Fluid flow does not increase the rate of Wound healing/cell migration in IS cells.

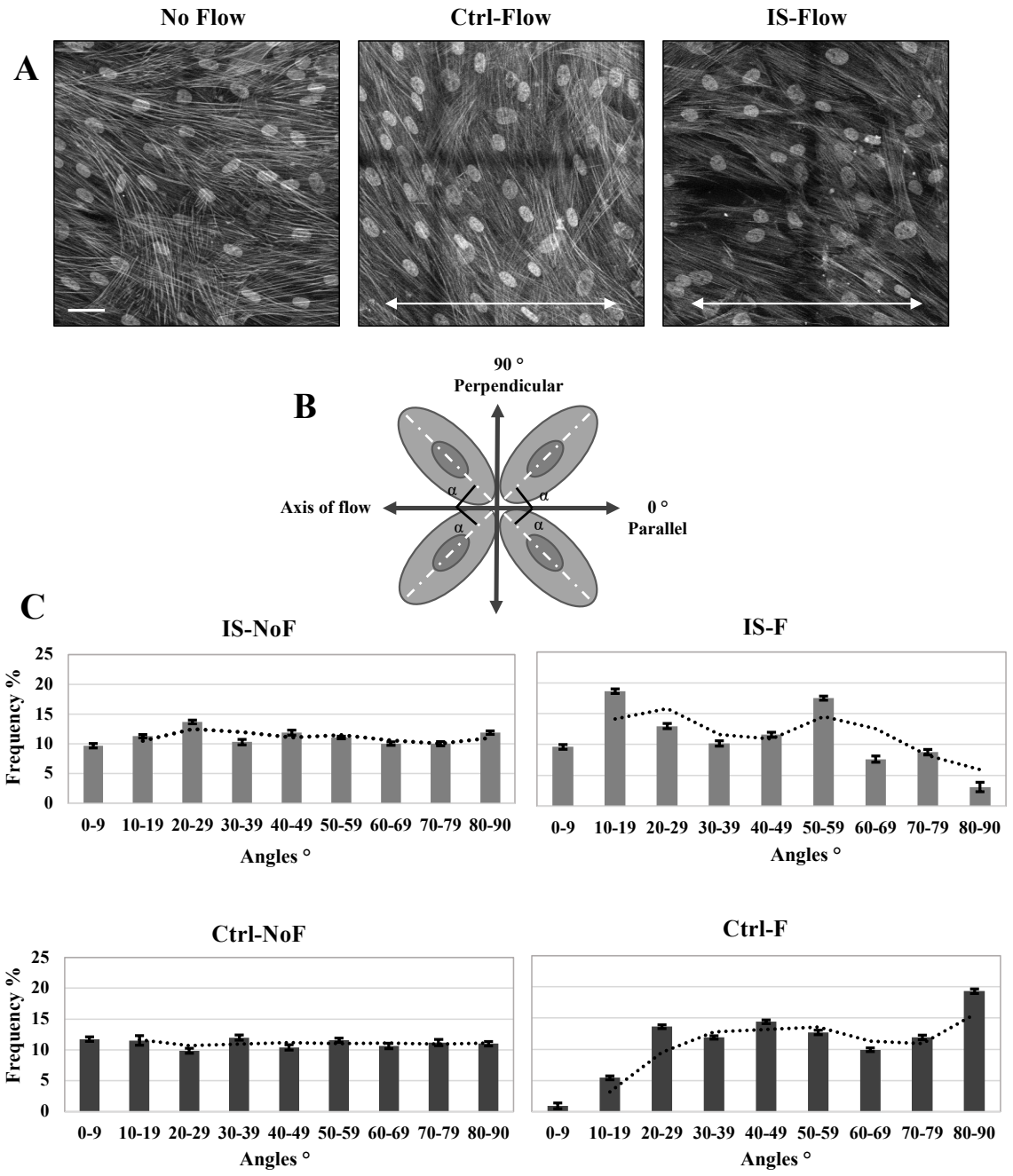

Figure 3-4. Cellular orientation adjustment relative to direction of flow varies between control and IS primary osteoblasts.

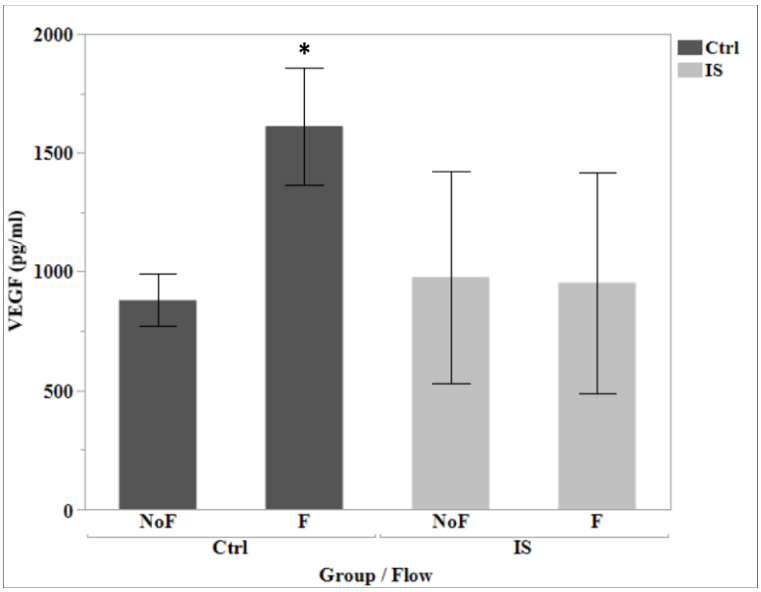

Figure 3-5. Fluid flow does not induce VEGF secretion in IS osteoblast cells.

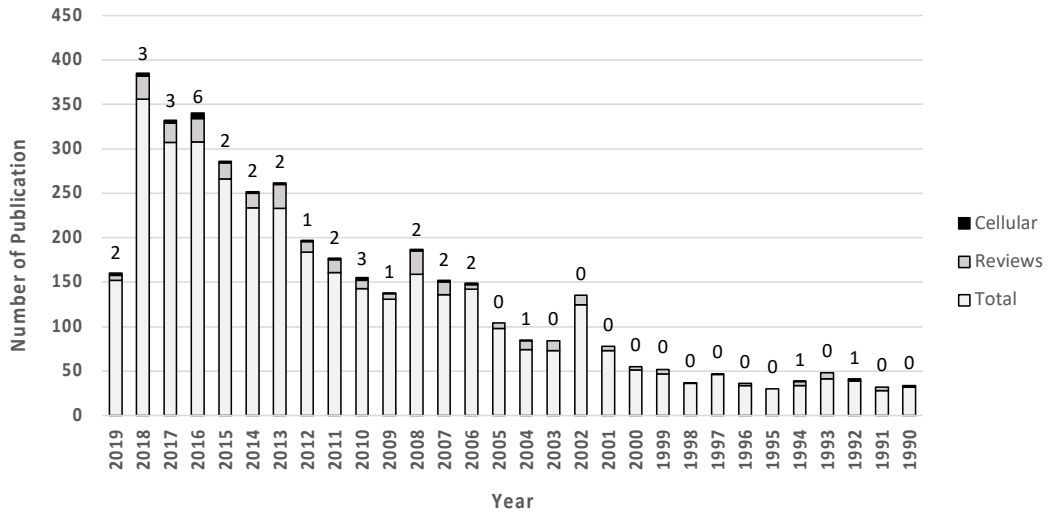

Figure 3-6. Annual distribution of publications on Idiopathic Scoliosis as were indexed in PubMed.

3.8 **Tables**

Table 3-I. The distribution of α angle in control and AIS osteoblast with or without flow application.

	AIS-No Flow	AIS-Flow	Ctrl-No Flow	Ctrl-Flow
0-30°	34.7 %	41.24 %	33.17 %	19.95 %
30-60°	33.29 %	39.27 %	33.99 %	38.97 %
60-90°	32.01 %	19.49 %	32.84 %	41.08 %

Chapter IV

Discussion

The main goal of the present dissertation was to investigate the existence of biomechanical impairments in adolescent idiopathic scoliosis and understand its basic biological aspects. The role of biomechanics in AIS have long been known. Differential growth pattern in AIS patients, effect of unique nature of forces that apply to an upright stature in AIS etiology, and the inevitable role of biomechanics in all therapeutic aspects of the disease [307] are among the clinical evidence supporting the importance of mechanotransduction. Spinal deformities are a common manifestation of animal models and human disorders with disturbed biomechanics [22], [123], [184].

Our available knowledge of basic science underlying AIS also points towards a mechanosensory impairment [43]. At the genetic level, many genes involved in AIS and several AIS animal models exhibiting similar skeletal curve phenotype are linked to the mechanosensory organelle, cilia (Table 2-1). Recent genetic studies also reported a significant contribution of rare variants accumulation in elements of cellular mechanotransduction machinery such as ECM in AIS patients [276], [277].

At the molecular level, the reduced expression of osteogenic factors [43], altered cAMP [47], [48], and reported abnormalities in both canonical Wnt and planar cell polarity pathways [43], [149] seem to be associated with a disturbed mechanosensory signaling in AIS. Data [141], [143], [146] at the cellular level also present direct association with ciliary protein disruption in the mechano-performance of bone cells, in addition to recent reports that link cilia morphology to AIS [43], [277].

Despite aforementioned evidence, our knowledge of biomechanical sensation at the cellular-molecular level in AIS is extremely limited. In this dissertation the possible involvement of an altered mechanosensation in AIS was investigated from different angles. We reported cilia abnormalities in AIS osteoblast cells as a novel cellular phenotype related to disease. We also investigated the source of these abnormalities at genetic level by performing a whole exome sequencing and a selected transcriptomic approach to identify changes in downstream biomechanical induced mRNA expression using RT-PCR method. We further performed a functional pilot study to further characterize AIS differential cellular behavior in response to mechanical induction.

4.1 Ciliary abnormalities in AIS osteoblasts

Cilium movement in response to a mechanical stimulation is a strong function of its length, stiffness and general morphology [133]. Such movements are responsible for cellular awareness about the type, duration and magnitude of applied forces. On the other hand, the sensory organelle itself is capable of adjusting its morphology using an adaptive regulatory system that helps the cell to fine tune its mechanosensory structure proportional to the applied force.

Our result showed for the very first time, that AIS osteoblasts have difficulties regulating their cilia length whether during ciliogenesis in a steady condition or post-ciliogenesis in response to different mechanical stimulation. We observed similar reduced osteogenic sensitivity and disturbed patterns in mechanotransduction molecules, specifically Wnt pathway, by inducing longer cilia in LiCl treated controls. This observation suggests the importance of the length regulation in mechanical induced cellular responses.

We induced ciliogenesis through two different conditions, starvation and cell confluency by transferring the confluent osteoblast monolayer to a serum deprived media. Both conditions force the cell to adopt a non-mitotic state. The number of ciliated AIS cells was not affected in our study and we observed similar growth rate among AIS and control cells. Therefore, cilia length abnormalities in AIS appear to be independent of the cell cycle events. Generally, the length of cilium and the percentage of ciliated cell are increased in quiescent (G0) rather than cycling cells [308]. Involvement of intracellular pathways affecting IFT proteins, however, seem plausible. The relative rate of building block transportation to and from the tip of cilia by IFT proteins govern its length both during cilia formation and during length maintenance or adjustment [289]. Cyclic AMP has been shown to play a role in a self-regulation of cilium length in response to mechanical induction through increased trafficking of anterograde IFT proteins [241], [291]. Previously reported melatonin signalling dysfunction and the following disturbance of intracellular cAMP in AIS patients by our group might explain ciliary length abnormalities observed in AIS osteoblasts [47]–[49].

4.2 Cytoskeleton abnormalities in AIS osteoblasts

Cilia interact with extra cellular matrix elements during mechanotransduction as well as events involved in cilium length regulation [133], [282], [289]. Our whole exome sequencing data confirmed the involvement of enriched rare variants in ECM elements of mechanotransduction machinery as reported by several previous studies on the ECM, cytoskeleton, genetic variations and AIS [309], [310]. Miller *et al.* [276] have more recently reported a study of five multigenerational AIS families that identified enriched categories of genes involved in cilia and other actin-based cellular projections and the ECM.

In our functional study, we observed that mechanical stimulation induced actin filaments rearrangement to thicker structures, resembling stress fibers, only in control cells. However, no significant change was observed in the actin of AIS osteoblast in response to flow. We further observed that AIS osteoblast cells do not align, elongate, or show increased migratory rate in response to applied directional strain which is consistent with the dynamics of an impaired cytoskeleton and abnormal cilia in mechanotransduction.

4.3 Molecular abnormalities in AIS osteoblasts

Physical movements induce bone gain and stimulate angiogenesis in skeletal tissue. Conversely, inactivity could result in the loss of both bone and muscle capillaries [311]. Lower bone mass density and osteopenia/osteoporosis among AIS patients are well documented. There are also some reports about capillary count and differential blood supply in scoliotic muscle and lung tissues, but they have been suggested to have a secondary adaptive origin [312], [313].

We showed a reduction in the expression of osteogenic factors in response to applied mechanical forces in AIS osteoblasts providing a direct evidence for an impaired mechanotransduction in AIS. Fluid flow induction of all three measured osteogenic mRNAs (BMP2, PTGS2 and RUNX2) were time dependent in our tested osteoblast cells. In control cells, application of 4 hours of flow resulted in 50 folds increase in BMP2 expression. BMP2 expression raised to over 100 folds at 8-hour time point and then reduced to almost basic quantity at 16 hours. A similar periodic pattern was detected for

the BMP2 expression in AIS cells but with significantly reduced values. Expression of PTGS2 showed the highest increase to over 40 folds at 4 hours post flow, decreased to over 20 folds at 8 hours and to almost normal amount at 16 hours in control cells. Again, AIS cells expression pattern followed similar temporal changes with significant reduction in response to applied force.

Mechanical induced RUNX2 expression showed much more subtle changes with the maximum increase of about 2.5 folds at 16 hours. RUNX2 changes were neither significant in controls nor in AIS cells. Nevertheless, a temporal increase in controls were visible, while in AIS cells, 4 and 8 hours of flow did not induce any changes. It took 16 hours of flow application to raise the expression of RUNX2 in AIS cells. Among all three tested osteogenic factors, the 4- and 8-hour responses were reduced in AIS, while 16-hour responses did not show significant difference between controls and AIS. It appears that AIS osteoblasts osteogenic factors exhibit a delayed and/or attenuated response profile following a mechanical induction. It is of note that baseline mRNA expression ratio of RUNX2 was significantly lower in AIS cells, while PTGS2 baseline was higher but the difference did not meet the significance threshold. We were able to induce same respective changes in control cells by elongating their cilia using LiCl.

We observed reduced baseline ratio of AXIN2, a known negative regulator of Wnt pathway, in AIS (0.508 to 1 in control) and significantly higher levels of beta-catenin (5.762 to 1 in control). These changes could explain the RUNX2 level differences, as Wnt has a regulatory role in RUNX2 expression. Non-canonical Wnt pathway have also been associated to both cilia and idiopathic scoliosis [22], [129], [149]. In an adult skeleton, both Wnt pathways, canonical and non-canonical act in parallel to transduce biomechanical cues to skeletal adaptive responses by influencing both the rate and orientation of osteoblast division [314].

Mechanical induced production of angiogenic factors such as VEGF in bone formation has also been reported [315], [316]. Osteoblasts are important sources of mechanosensitive expression of VEGF in bone [316], [317]. Mechanical induced actin polymerization is necessary for VEGF cellular mobilization [315]. On the other hand, VEGF mediated signaling is tightly related to exercise induced bone gain [318]. Observing

the disturbed responses of both bone formation factors and actin prompted us to explore the contribution of VEGF signaling in AIS pathogenesis. Indeed, we found twice the quantity of secreted VEGF-A in the ELISA of flow conditioned media of control osteoblasts compared to that of the no flow condition while no changes were observed in AIS osteoblasts.

Together our results suggest that AIS osteoblasts are unable to adjust their mechanosensitivity, which contributes to a disturbed or delayed response pattern in downstream mechanotransduction. Therefore, strain induced signaling of the Wnt pathway and osteogenic players along with cytoskeleton elements are adversely affected which in turn result in altered cellular migration, elongation and orientation in AIS osteoblasts, as we showed in the second paper.

4.4 **Study Limitations**

Our investigation introduced new findings on mechanotransduction relevant to idiopathic scoliosis. However, we acknowledge several limitations and pitfalls that perhaps need to be addressed in future works. Cilia are not the only cellular mechanosensors. To name a few, integrins and ECM proteins, cellular tethering elements, gap-junctions and ion channels are also among mechanosensors in bone [95], [282]. Our tested cohorts, both in case of cellular experiments and population whole exome sequencing, are relatively small. Validation of the reported findings and their replication using larger sample size is needed. We used bidirectional, oscillatory fluid flow in our study. However, considering the sensitivity of downstream mechanotransductory signals to the type, frequency and duration of the applied force, it would be interesting to map the profile response of AIS cells under other physiologically relevant forces such as tension and compression. Also, the molecular signaling related to VEGF, canonical Wnt pathways as well as events affecting other cell types in the skeletal tissue remain to be investigated. Finally, it should be noted that we used primary human osteoblasts in our study which means that we studied only the severe case of disease that progressed to surgery.

4.5 Potential clinical impacts

There are extensive research data available on clinical and genetic aspects of idiopathic scoliosis. However, our knowledge on molecular and particularly cellular levels is fairly limited. Designing efficient therapeutic approaches could greatly benefit from the better understanding of basic cellular behavior.

This research project was intended to explore new angles that reflect abnormalities in AIS cellular and their interaction with mechanical environment. Any effort regarding the correction of a curved skeleton involves applying some kind of force. We showed that an AIS bone does not necessarily sense nor respond to the applied pressure in the same way as a healthy bone. Considering the different behavioral patterns between a normal and a scoliotic cells in computational models could make a difference in chosen therapeutic option. The findings of the present project are hoped to pave the path for the development of new multiscale, mathematical models for numerical simulations and design optimization of therapeutic approaches such as bracing. This may be achieved by developing multiscale mathematical models for simulation of curve progression. Such multiscale models would connect the forces and stresses at macroscopic scales to cellular response at mesoscopic scales. Using such models, different corrective surgery scenarios can be considered and simulated to predict the curve progression post-surgery.

The evidence of small genetic error accumulation in the mechanotransductory network of AIS patients, provided in this and other studies, could potentially be used in prognosis. Among the questions that hopefully could be answered is whether an AIS patient is genetically predisposed to better respond to bracing. The heterogeneity observed in the bracing outcome perhaps could be explained by differential severities of mechanotransduction impairments among patients. Theoretically, if we can use the mechanotransduction profile of the patients to predict the possibility of curve progression and a corrective surgery, we could reduce or avoid the discomfort and pains associated with bracing in addition to economic and social burdens.

Chapter V

Future works & Conclusion

5.1 Future works

Adolescent idiopathic scoliosis is a common complex disorder which is yet poorly understood. Among the unknowns are when the disease exactly starts, and which tissues are involved, who is more susceptible to develop AIS, and what are the predisposing factors to curve progression. To understand the answers to these questions, we need to increase our knowledge on the basic biological aspects of what happens in the cellular level and how AIS cells differ from normal cells.

We introduced an association between cellular mechanotransduction impairment and AIS using primary bone cells. Future works include the validation of reported anomalies in a larger cohort of patients, and investigation of possible biomechanosensory abnormalities relevant to AIS in other tissues such as muscle and cartilage.

Using trauma patients tissue samples, it would be interesting to induce an elongated or shortened cilium using controlled molecular interventions rather than general cellular treatment in healthy cells to investigate the effects and try the possibilities of rescuing those effects *in vitro*.

Using animal models such as “curveback” guppy, we can investigate several tissues in the early stages of the disease to rule out which tissue is the first to reflect the biomechanical impairment.

Knowing that cilium is not the only cellular mechanosenosr, it is important to study other involved mechanosensory elements such as integrins, gap-junctions and cellular tethering elements in AIS cells. It would be interesting to find out if an AIS cell suffers from abnormalities in several of its biomechanosensory elements or not and to investigate a possibility of compensatory responses to adjust the error.

Further molecular experiments are also needed to draw a complete map of molecular changes in the AIS mechanotransduction involved pathways. Canonical Wnt and PCP pathways are both involved in AIS and are connected with a large network of upstream and downstream molecules. VEGF molecular signaling also needs to be investigated thoroughly in the context of AIS and mechanotransduction.

Considering that osteoblasts secrete a number of proteins with important autocrine and paracrine functions, studying the profile of AIS osteoblasts secreted proteins (secretome) in comparison with normal cells in stationary phase and following a mechanical induction could also shed some light into the molecular changes related to AIS. Investigating the role of noncoding RNAs such as microRNA in the observed cellular abnormalities can also be an interesting and fruitful approach in this regard. Drawing a clear image of molecular signaling changes in AIS can not only help with understanding the molecular mechanism of the disease development but also be beneficial in designing more efficient therapies perhaps at the cellular-molecular level.

More ambitiously, we could compare the cellular biomechanical characteristics of patients who respond well to bracing to those that do not. This could not only help classifying patients based on most efficient therapy approaches but also help find molecular modifiers that may address the mechanotransduction abnormalities observed in AIS.

5.2 **Conclusions**

In the current dissertation we hypothesized, investigated and validated a role for cellular mechanotransduction impairments in AIS etiology. We showed that AIS osteoblasts do not sense the forces of biomechanics normally, are not able to adjust their mechanical sensitivity and therefore, cannot respond correctly to the surrounding mechanical stimulations. We narrowed down the affected cellular apparatus to cilia as a mechanosensory organelle and actin fibers in cytoskeleton. We showed decreased mechanical induced osteogenic response and the involvement of Wnt pathway in the altered mechanosensory nature of AIS osteoblasts. We then characterized the consequences of these molecular impairments in the cellular behavior of AIS cells.

In conclusion our results suggest a strong role for an impaired cellular bio-mechano-transduction in the etiology of AIS, adding significant novel information to the field. Idiopathic scoliosis onset occurs in the period of rapid growth when the bone cellular machinery works fast to build and shape an adult skeleton and it needs to be at the peak of its performance to be able to create a healthy stature. Osteoblasts with disturbed mechanosensory could potentially cause more errors during this growth spurt period, which

could accumulate and manifest in the curvature that suddenly appears as AIS. Looking into this intertwined complex network it is challenging to understand what the cause is and what comes as a consequence but finding the areas that AIS bone cells lack in their functionality helps to tackle the problem from a closer angle.

Reference list

[1] H. A. Keim, “Scoliosis,” in *The Adolescent Spine*, New York, NY: Springer US, 1976, pp. 107–136.

[2] J. C. Cheng *et al.*, “Adolescent idiopathic scoliosis,” *Nat. Rev. Dis. Prim.*, vol. 1, p. 15030, Sep. 2015.

[3] M. R. Konieczny, H. Senyurt, and R. Krauspe, “Epidemiology of adolescent idiopathic scoliosis,” *J. Child. Orthop.*, vol. 7, no. 1, p. 3, Feb. 2013.

[4] “Scoliosis Research Society. Morbidity & Mortality Committee annual report.,” 1997.

[5] K. D. K. Luk *et al.*, “Clinical Effectiveness of School Screening for Adolescent Idiopathic Scoliosis,” *Spine (Phila. Pa. 1976).*, vol. 35, no. 17, pp. 1607–1614, Aug. 2010.

[6] M. A. Asher and D. C. Burton, “Adolescent idiopathic scoliosis: natural history and long term treatment effects.,” *Scoliosis*, vol. 1, no. 1, p. 2, Jan. 2006.

[7] M. Romano *et al.*, “Exercises for Adolescent Idiopathic Scoliosis,” *Spine (Phila. Pa. 1976).*, vol. 38, no. 14, pp. E883–E893, Jun. 2013.

[8] M. Plaszewski, “Letter to the Editor concerning ‘Efficacy of exercise therapy for the treatment of adolescent idiopathic scoliosis: a review of the literature’ by Mordecai SC and Dabke HV (2012) Eur Spine J 21:382–389,” *Eur. Spine J.*, vol. 22, no. 6, pp. 1438–1439, Jun. 2013.

[9] J. Bettany-Saltikov, E. Parent, M. Romano, M. Villagrasa, and S. Negrini, “Physiotherapeutic scoliosis-specific exercises for adolescents with idiopathic scoliosis.,” *Eur. J. Phys. Rehabil. Med.*, vol. 50, no. 1, pp. 111–21, Feb. 2014.

[10] S. L. Weinstein, L. A. Dolan, J. C. Cheng, A. Danielsson, and J. A. Morcuende, “Adolescent idiopathic scoliosis,” *Lancet*, vol. 371, no. 9623, pp. 1527–1537, 2008.

[11] L. Xu *et al.*, “Brace treatment in adolescent idiopathic scoliosis patients with curve more than 40 degrees: effectiveness and related factors,” *World Neurosurg.*, Mar. 2019.

[12] J. O. Sanders, P. O. Newton, R. H. Browne, D. E. Katz, J. G. Birch, and J. A. Herring, “Bracing for Idiopathic Scoliosis: How Many Patients Require Treatment to Prevent One Surgery?,” *J. Bone Jt. Surgery-American Vol.*, vol. 96, no. 8, pp. 649–653, Apr. 2014.

[13] M. van den Bogaart, B. J. van Royen, T. M. Haanstra, M. de Kleuver, and S. S. A. Faraj, “Predictive factors for brace treatment outcome in adolescent idiopathic scoliosis: a best-evidence synthesis,” *Eur. Spine J.*, vol. 28, no. 3, pp. 511–525, Mar. 2019.

[14] D. Schlenzka and T. Yrjönen, “Bracing in adolescent idiopathic scoliosis,” *J. Child. Orthop.*, vol. 7, no. 1, p. 51, 2013.

[15] K. F. Gorman, C. Julien, and A. Moreau, “The genetic epidemiology of idiopathic scoliosis.,” *Eur. Spine J.*, vol. 21, no. 10, pp. 1905–19, Oct. 2012.

[16] W. J. Wang *et al.*, “Top Theories for the Etiopathogenesis of Adolescent Idiopathic Scoliosis,” *J. Pediatr. Orthop.*, vol. 31, no. 1 Suppl, pp. S14–S27, 2011.

[17] R. G. Burwell, “Aetiology of idiopathic scoliosis: current concepts,” *Pediatr. Rehabil.*, vol. 6, no. 3–4, pp. 137–170, Jul. 2003.

[18] T. G. Lowe *et al.*, “Etiology of idiopathic scoliosis: current trends in research.,” *J. Bone Joint Surg. Am.*, vol. 82-A, no. 8, pp. 1157–68, Aug. 2000.

[19] K. F. Gorman, C. Julien, N. Oliazadeh, Q. Tang, and A. Moreau, “Genetics of idiopathic scoliosis,” *eLS.*, 2014.

[20] S. Sharma *et al.*, “Genome-wide association studies of adolescent idiopathic scoliosis suggest candidate susceptibility genes.,” *Hum. Mol. Genet.*, vol. 20, no. 7, pp. 1456–66, Apr. 2011.

[21] C. M. Justice, N. H. Miller, B. Marosy, J. Zhang, and A. F. Wilson, “Familial idiopathic scoliosis: evidence of an X-linked susceptibility locus.,” *Spine (Phila. Pa. 1976).*, vol. 28, no. 6, pp. 589–594, 2003.

[22] M. Hayes *et al.*, “ptk7 mutant zebrafish models of congenital and idiopathic scoliosis implicate dysregulated Wnt signalling in disease,” *Nat. Commun.*, vol. 5, pp. 1–11, 2014.

[23] S. R. Wiener-Vacher and K. Mazda, “Asymmetric otolith vestibulo-ocular responses in children with idiopathic scoliosis.,” *J. Pediatr.*, vol. 132, no. 6, pp. 1028–32, Jun. 1998.

[24] D. ROUSIE, J. C. HACHE, P. PELLERIN, J. P. DEROUBAIX, P. TICHELEN, and A. BERTHOZ, “Oculomotor, Postural, and Perceptual Asymmetries Associated with a Common Cause: Craniofacial Asymmetries and Asymmetries in Vestibular Organ Anatomy,” *Ann. N. Y. Acad. Sci.*, vol. 871, no. 1 OTOLITH FUNCT, pp. 439–446, May 1999.

[25] S. Mallau, G. Bollini, J.-L. Jouve, and C. Assaiante, “Locomotor skills and balance strategies in adolescents idiopathic scoliosis.,” *Spine (Phila. Pa. 1976).*, vol. 32, no. 1, pp. E14-22, Jan. 2007.

[26] X. Guo, W. W. Chau, C. W. Y. Hui-Chan, C. S. K. Cheung, W. W. N. Tsang, and J. C. Y. Cheng, “Balance control in adolescents with idiopathic scoliosis and disturbed somatosensory function.,” *Spine (Phila. Pa. 1976).*, vol. 31, no. 14, pp. E437-40, Jun. 2006.

[27] D. LONSTEIN, “Adolescent idiopathic scoliosis,” *Lancet*, vol. 344, no. 8934, pp. 1407–1412, Nov. 1994.

[28] M. Latalski, A. Danielewicz-Bromberek, M. Fatyga, M. Latalska, M. Kröber, and P. Zwolak, “Current insights into the aetiology of adolescent idiopathic scoliosis,” *Arch. Orthop. Trauma Surg.*, vol. 137, no. 10, pp. 1327–1333, Oct. 2017.

[29] T. Fukuda *et al.*, “Sema3A regulates bone-mass accrual through sensory innervations,” *Nature*, vol. 497, no. 7450, pp. 490–493, May 2013.

[30] S. Roberts, J. Menage, and S. M. Eisenstein, “The cartilage end-plate and intervertebral disc in scoliosis: Calcification and other sequelae,” *J. Orthop. Res.*, vol. 11, no. 5, pp. 747–757, Sep. 1993.

[31] C. M. Karner, F. Long, L. Solnica-Krezel, K. R. Monk, and R. S. Gray, "*Gpr126/Adgrg6* deletion in cartilage models idiopathic scoliosis and pectus excavatum in mice," *Hum. Mol. Genet.*, vol. 24, no. 15, pp. 4365–4373, Aug. 2015.

[32] K. T. Suh, S.-S. Lee, S. H. Hwang, S.-J. Kim, and J. S. Lee, "Elevated soluble receptor activator of nuclear factor-κB ligand and reduced bone mineral density in patients with adolescent idiopathic scoliosis," *Eur. Spine J.*, vol. 16, no. 10, pp. 1563–1569, Oct. 2007.

[33] M. Chiru, "Adolescent idiopathic scoliosis and osteopenia).," *Maedica (Buchar).*, vol. 6, no. 1, pp. 17–22, Jan. 2011.

[34] A. Kulis *et al.*, "Participation of sex hormones in multifactorial pathogenesis of adolescent idiopathic scoliosis," *Int. Orthop.*, vol. 39, no. 6, pp. 1227–1236, Jun. 2015.

[35] S. Zhou *et al.*, "Increased expression of receptor activator of nuclear factor-κB ligand in osteoblasts from adolescent idiopathic scoliosis patients with low bone mineral density," *J. Huazhong Univ. Sci. Technol. [Medical Sci.*, vol. 32, no. 5, pp. 686–690, Oct. 2012.

[36] L. Lu, Z. Dai, G. Lv, Y. Kang, and Y. Jiang, "A novel therapeutic strategy for adolescent idiopathic scoliosis based on osteoporotic concept," *Med. Hypotheses*, vol. 80, no. 6, pp. 773–775, Jun. 2013.

[37] H. Zhang *et al.*, "The association of rs1149048 polymorphism in Matrilin-1(MATN1) gene with adolescent idiopathic scoliosis susceptibility: a meta-analysis," *Mol. Biol. Rep.*, vol. 41, no. 4, pp. 2543–2549, Apr. 2014.

[38] B. Wang, Z.-J. Chen, Y. Qiu, and W.-J. Liu, "[Decreased circulating matrilin-1 levels in adolescent idiopathic scoliosis].," *Zhonghua Wai Ke Za Zhi*, vol. 47, no. 21, pp. 1638–41, Nov. 2009.

[39] M. D. Briggs *et al.*, "Pseudoachondroplasia and multiple epiphyseal dysplasia due to mutations in the cartilage oligomeric matrix protein gene," *Nat. Genet.*, vol. 10, no. 3, pp. 330–336, Jul. 1995.

[40] P. Gerdhem, C. Topalis, A. Grauers, J. Stubendorff, A. Ohlin, and K. M. Karlsson, "Serum level of cartilage oligomeric matrix protein is lower in children with idiopathic scoliosis than in non-scoliotic controls," *Eur. Spine J.*, vol. 24, no. 2, pp. 256–261, Feb. 2015.

[41] K. Fendri *et al.*, "Recent advances in the study of candidate genes for adolescent idiopathic scoliosis.," *Stud. Health Technol. Inform.*, vol. 158, pp. 3–7, 2010.

[42] G. Haller *et al.*, "A polygenic burden of rare variants across extracellular matrix genes among individuals with adolescent idiopathic scoliosis.," *Hum. Mol. Genet.*, vol. 25, no. 1, pp. 202–9, Jan. 2016.

[43] N. Oliazadeh, K. F. Gorman, R. Eveleigh, G. Bourque, and A. Moreau, "Identification of Elongated Primary Cilia with Impaired Mechanotransduction in Idiopathic Scoliosis Patients," *Sci. Rep.*, vol. 7, 2017.

[44] D. Nada and A. Moreau, "Biochemistry of Idiopathic Scoliosis: From Discovery to Diagnostic Biomarkers," in *Pathogenesis of Idiopathic Scoliosis*, M. Machida, S. L. Weinstein, and J. Dubousset, Eds. Springer Tokyo, 2018, pp. 99–124.

[45] K. Kindsfater, T. Lowe, D. Lawellin, D. Weinstein, and J. Akmakjian, “Levels of platelet calmodulin for the prediction of progression and severity of adolescent idiopathic scoliosis.,” *J. Bone Joint Surg. Am.*, vol. 76, no. 8, pp. 1186–92, Aug. 1994.

[46] T. Lowe *et al.*, “Platelet calmodulin levels in adolescent idiopathic scoliosis: do the levels correlate with curve progression and severity?,” *Spine (Phila. Pa. 1976).*, vol. 27, no. 7, pp. 768–75, Apr. 2002.

[47] A. Moreau *et al.*, “Melatonin signaling dysfunction in adolescent idiopathic scoliosis.,” *Spine (Phila. Pa. 1976).*, vol. 29, no. 16, pp. 1772–81, Aug. 2004.

[48] B. Azeddine, K. Letellier, D. S. Wang, F. Moldovan, and A. Moreau, “Molecular determinants of melatonin signaling dysfunction in adolescent idiopathic scoliosis.,” *Clin. Orthop. Relat. Res.*, vol. 462, no. 462, pp. 45–52, Sep. 2007.

[49] M.-Y. Akoume *et al.*, “Cell-based screening test for idiopathic scoliosis using cellular dielectric spectroscopy.,” *Spine (Phila. Pa. 1976).*, vol. 35, no. 13, pp. E601-8, Jun. 2010.

[50] M.-Y. Akoume, A. Franco, and A. Moreau, “Cell-based Assay Protocol for the Prognostic Prediction of Idiopathic Scoliosis Using Cellular Dielectric Spectroscopy,” *J. Vis. Exp.*, no. 80, p. e50768, Oct. 2013.

[51] A. Moreau *et al.*, “High Circulating Levels of Osteopontin Are Associated with Idiopathic Scoliosis Onset and Spinal Deformity Progression,” in *Spine Journal Meeting Abstracts*, 2009, p. 109.

[52] N. Xie, M. Li, T. Wu, J. Liu, B. Wang, and F. Tang, “Does elevated osteopontin level play an important role in the development of scoliosis in bipedal mice?,” *Spine J.*, vol. 15, no. 7, pp. 1660–1664, Jul. 2015.

[53] M. C. Yadav *et al.*, “Ablation of osteopontin improves the skeletal phenotype of phospho1(-/-) mice.,” *J. Bone Miner. Res.*, vol. 29, no. 11, pp. 2369–81, Nov. 2014.

[54] J. Oyama, I. Murai, K. Kanazawa, and M. Machida, “Bipedal ambulation induces experimental scoliosis in C57BL/6J mice with reduced plasma and pineal melatonin levels,” *J. Pineal Res.*, vol. 40, no. 3, pp. 219–224, Apr. 2006.

[55] E. D. Wang, D. S. Drummond, J. P. Dormans, T. Moshang, R. S. Davidson, and D. Gruccio, “Scoliosis in patients treated with growth hormone.,” *J. Pediatr. Orthop.*, vol. 17, no. 6, pp. 708–11.

[56] S. Willner and O. Johnell, “Study of biochemical and hormonal data in idiopathic scoliosis in girls.,” *Arch. Orthop. Trauma. Surg.*, vol. 98, no. 4, pp. 251–5, 1981.

[57] T. Ahl, K. Albertsson-Wikland, and R. Kalén, “Twenty-four-hour growth hormone profiles in pubertal girls with idiopathic scoliosis.,” *Spine (Phila. Pa. 1976).*, vol. 13, no. 2, pp. 139–42, Feb. 1988.

[58] A. Juul *et al.*, “Serum levels of insulin-like growth factor (IGF)-binding protein-3 (IGFBP-3) in healthy infants, children, and adolescents: the relation to IGF-I, IGF-II, IGFBP-1, IGFBP-2, age, sex, body mass index, and pubertal maturation.,” *J. Clin. Endocrinol. Metab.*, vol. 80, no. 8, pp. 2534–2542, Aug. 1995.

[59] V. Hesse *et al.*, “Insulin-like growth factor I correlations to changes of the hormonal status

in puberty and age," *Exp. Clin. Endocrinol. Diabetes*, vol. 102, no. 04, pp. 289–298, Jul. 2009.

[60] S. Nikolova *et al.*, "Positive Association between TGFB1 Gene and Susceptibility to Idiopathic Scoliosis in Bulgarian Population.," *Anal. Cell. Pathol. (Amst).*, vol. 2018, p. 6836092, 2018.

[61] Y. Takahashi *et al.*, "Lack of association between adolescent idiopathic scoliosis and previously reported single nucleotide polymorphisms in MATN1, MTNR1B, TPH1, and IGF1 in a Japanese population," *J. Orthop. Res.*, vol. 29, no. 7, pp. 1055–1058, Jul. 2011.

[62] Y. Yang *et al.*, "Adolescent Idiopathic Scoliosis and the Single-Nucleotide Polymorphism of the Growth Hormone Receptor and IGF-1 Genes," *Orthopedics*, vol. 32, no. 6, pp. 411–416, Jun. 2009.

[63] E. S. Moon *et al.*, "Analysis of Single Nucleotide Polymorphism in Adolescent Idiopathic Scoliosis in Korea: For Personalized Treatment," *Yonsei Med. J.*, vol. 54, no. 2, p. 500, 2013.

[64] H. Y. Yeung *et al.*, "Genetic association study of insulin-like growth factor-I (IGF-I) gene with curve severity and osteopenia in adolescent idiopathic scoliosis.," *Stud. Health Technol. Inform.*, vol. 123, pp. 18–24, 2006.

[65] T. B. Grivas, E. Vasiliadis, V. Mouzakis, C. Mihas, and G. Koufopoulos, "Association between adolescent idiopathic scoliosis prevalence and age at menarche in different geographic latitudes," *Scoliosis*, vol. 1, no. 1, p. 9, Dec. 2006.

[66] M. P. Warren, J. B. Gunn, L. H. Hamilton, L. F. Warren, and W. G. Hamilton, "Scoliosis and Fractures in Young Ballet Dancers," *N. Engl. J. Med.*, vol. 314, no. 21, pp. 1348–1353, May 1986.

[67] T. Esposito *et al.*, "Estrogen receptor polymorphism, estrogen content and idiopathic scoliosis in human: A possible genetic linkage," *J. Steroid Biochem. Mol. Biol.*, vol. 116, no. 1–2, pp. 56–60, Aug. 2009.

[68] A. Kulis, D. Zarzycki, and J. Jaśkiewicz, "Concentration of estradiol in girls with idiophatic scoliosis.," *Ortop. Traumatol. Rehabil.*, vol. 8, no. 4, pp. 455–9, Aug. 2006.

[69] D. Leboeuf, K. Letellier, N. Alos, P. Edery, and F. Moldovan, "Do estrogens impact adolescent idiopathic scoliosis?," *Trends Endocrinol. Metab.*, vol. 20, no. 4, pp. 147–52, May 2009.

[70] K. Letellier *et al.*, "Estrogen cross-talk with the melatonin signaling pathway in human osteoblasts derived from adolescent idiopathic scoliosis patients.," *J. Pineal Res.*, vol. 45, no. 4, pp. 383–93, Nov. 2008.

[71] S. Zheng *et al.*, "Estrogen promotes the onset and development of idiopathic scoliosis via disproportionate endochondral ossification of the anterior and posterior column in a bipedal rat model," *Exp. Mol. Med.*, vol. 50, no. 11, p. 144, Nov. 2018.

[72] Y. Qiu *et al.*, "Decreased Circulating Leptin Level and Its Association With Body and Bone Mass in Girls With Adolescent Idiopathic Scoliosis," *Spine (Phila. Pa. 1976).*, vol. 32, no. 24, pp. 2703–2710, Nov. 2007.

[73] E. M. S. Tam *et al.*, “Are Volumetric Bone Mineral Density and Bone Micro-Architecture Associated with Leptin and Soluble Leptin Receptor Levels in Adolescent Idiopathic Scoliosis? – A Case-Control Study,” *PLoS One*, vol. 9, no. 2, p. e87939, Feb. 2014.

[74] Z. Liu *et al.*, “Abnormal Leptin Bioavailability in Adolescent Idiopathic Scoliosis,” *Spine (Phila. Pa. 1976).*, vol. 37, no. 7, pp. 599–604, Apr. 2012.

[75] E. M. lam *et al.*, “Morphological and bone strength indices in girls with adolescent idiopathic scoliosis and their correlations with leptin and soluble leptin receptor,” *Scoliosis*, vol. 10, no. S1, p. O13, Dec. 2015.

[76] R. G. Burwell *et al.*, “Pathogenesis of adolescent idiopathic scoliosis in girls - a double neuro-osseous theory involving disharmony between two nervous systems, somatic and autonomic expressed in the spine and trunk: possible dependency on sympathetic nervous system and hormon,” *Scoliosis*, vol. 4, no. 1, p. 24, Dec. 2009.

[77] B. L. Riggs, S. Khosla, L. J. Melton, and III, “The assembly of the adult skeleton during growth and maturation: implications for senile osteoporosis.,” *J. Clin. Invest.*, vol. 104, no. 6, pp. 671–2, Sep. 1999.

[78] J. E. Lonstein and J. M. Carlson, “The prediction of curve progression in untreated idiopathic scoliosis during growth.,” *J. Bone Joint Surg. Am.*, vol. 66, no. 7, pp. 1061–71, Sep. 1984.

[79] C. Siu King Cheung *et al.*, “Abnormal Peri-pubertal Anthropometric Measurements and Growth Pattern in Adolescent Idiopathic Scoliosis: A Study of 598 Patients,” *Spine (Phila. Pa. 1976).*, vol. 28, no. 18, pp. 2152–2157, Sep. 2003.

[80] M. Shohat, T. Shohat, M. Nitzan, M. Mimouni, R. Kedem, and Y. L. Danon, “Growth and ethnicity in scoliosis.,” *Acta Orthop. Scand.*, vol. 59, no. 3, pp. 310–3, Jun. 1988.

[81] C. S. K. Cheung *et al.*, “Generalized osteopenia in adolescent idiopathic scoliosis--association with abnormal pubertal growth, bone turnover, and calcium intake?,” *Spine (Phila. Pa. 1976).*, vol. 31, no. 3, pp. 330–8, Feb. 2006.

[82] C. J. Goldberg, F. E. Dowling, and E. E. Fogarty, “Adolescent idiopathic scoliosis--early menarche, normal growth.,” *Spine (Phila. Pa. 1976).*, vol. 18, no. 5, pp. 529–35, Apr. 1993.

[83] W. L. Burner, V. M. Badger, and F. C. Sherman, “Osteoporosis and acquired back deformities.,” *J. Pediatr. Orthop.*, vol. 2, no. 4, pp. 383–5, Oct. 1982.

[84] B. Pourabbas Tahvildari, M.-A. Erfani, H. Nouraei, and M. Sadeghian, “Evaluation of bone mineral status in adolescent idiopathic scoliosis.,” *Clin. Orthop. Surg.*, vol. 6, no. 2, pp. 180–4, Jun. 2014.

[85] M. Sadat-Ali, A. Al-Othman, D. Bubshait, and D. Al-Dakheel, “Does scoliosis causes low bone mass? A comparative study between siblings,” *Eur. Spine J.*, vol. 17, no. 7, pp. 944–947, Jul. 2008.

[86] X.-F. Li, H. Li, Z.-D. Liu, and L.-Y. Dai, “Low bone mineral status in adolescent idiopathic scoliosis,” *Eur. Spine J.*, vol. 17, no. 11, pp. 1431–1440, Nov. 2008.

[87] W. T. K. Lee *et al.*, “Association of osteopenia with curve severity in adolescent

idiopathic scoliosis: a study of 919 girls," *Osteoporos. Int.*, vol. 16, no. 12, pp. 1924–1932, Dec. 2005.

[88] V. W. Y. Hung *et al.*, "Osteopenia: A new prognostic factor of curve progression in adolescent idiopathic scoliosis," *J. Bone Jt. Surg. - Ser. A*, vol. 87, no. 12 I, pp. 2709–2716, Dec. 2005.

[89] E. Sornay-Rendu, S. Boutroy, F. Munoz, and P. D. Delmas, "Alterations of Cortical and Trabecular Architecture Are Associated With Fractures in Postmenopausal Women, Partially Independent of Decreased BMD Measured by DXA: The OFELY Study," *J. Bone Miner. Res.*, vol. 22, no. 3, pp. 425–433, Mar. 2007.

[90] W. Pistoia, B. van Rietbergen, E.-M. Lochmüller, C. A. Lill, F. Eckstein, and P. Rüegsegger, "Estimation of distal radius failure load with micro-finite element analysis models based on three-dimensional peripheral quantitative computed tomography images.," *Bone*, vol. 30, no. 6, pp. 842–8, Jun. 2002.

[91] L. Pothuaud *et al.*, "Combination of topological parameters and bone volume fraction better predicts the mechanical properties of trabecular bone," *J. Biomech.*, vol. 35, no. 8, pp. 1091–1099, Aug. 2002.

[92] W. S. Yu *et al.*, "Bone structural and mechanical indices in Adolescent Idiopathic Scoliosis evaluated by high-resolution peripheral quantitative computed tomography (HR-pQCT)," *Bone*, vol. 61, pp. 109–115, Apr. 2014.

[93] and therapy. J. Osteoporosis prevention, diagnosis, "NIH Consensus Prevention, diagnosis and therapy of osteoporosis," *JAMA*, vol. 17, no. 1, pp. 1–45, 2000.

[94] Z. Wang *et al.*, "Unique local bone tissue characteristics in iliac crest bone biopsy from adolescent idiopathic scoliosis with severe spinal deformity," *Sci. Rep.*, vol. 7, no. 1, p. 40265, Dec. 2017.

[95] M. P. Yavropoulou and J. G. Yovos, "The molecular basis of bone mechanotransduction," *J. Musculoskelet. Neuronal Interact.*, vol. 16, no. 3, pp. 221–236, 2016.

[96] H. M. Frost, "Bone 'mass' and the 'mechanostat': A proposal," *Anat. Rec.*, vol. 219, no. 1, pp. 1–9, Sep. 1987.

[97] J. A. Buckwalter, M. J. Glimcher, R. R. Cooper, and R. Recker, "Bone Biology," 1995.

[98] U. Kini and B. N. Nandeesh, "Physiology of Bone Formation, Remodeling, and Metabolism," in *Radionuclide and Hybrid Bone Imaging*, Berlin, Heidelberg: Springer Berlin Heidelberg, 2012, pp. 29–57.

[99] R. Florencio-Silva, G. Rodrigues Da, S. Sasso, E. Sasso-Cerri, M. J. Simões, and P. S. Cerri, "Biology of Bone Tissue: Structure, Function, and Factors That Influence Bone Cells," 2015.

[100] A. Cappariello, A. Maurizi, V. Veeriah, and A. Teti, "The Great Beauty of the osteoclast," *Arch. Biochem. Biophys.*, vol. 558, pp. 70–78, Sep. 2014.

[101] J. Caetano-Lopes, H. Canhão, and J. E. Fonseca, "Osteoblasts and bone formation.," *Acta Reum. Port.*, vol. 32, no. 2, pp. 103–10.

[102] T. Bellido, L. I. Plotkin, and A. Bruzzaniti, *Chapter 2. Bone Cells*. 2013.

[103] M. G. Mullender, D. D. van der Meer, R. Huiskes, and P. Lips, "Osteocyte density changes in aging and osteoporosis," *Bone*, vol. 18, no. 2, pp. 109–113, Feb. 1996.

[104] M. Capulli, R. Paone, and N. Rucci, "Osteoblast and osteocyte: Games without frontiers," *Arch. Biochem. Biophys.*, vol. 561, pp. 3–12, Nov. 2014.

[105] C. Galli, G. Passeri, and G. M. Macaluso, "Osteocytes and WNT: the Mechanical Control of Bone Formation," *J Dent Res*, vol. 89, no. 4, pp. 331–343, 2010.

[106] L. F. Bonewald, "Mechanosensation and transduction in osteocytes," *BoneKEy-Osteovision*, vol. 3, no. 10, pp. 7–15, Oct. 2006.

[107] M. Prideaux, D. M. Findlay, and G. J. Atkins, "Osteocytes: The master cells in bone remodelling," *Curr. Opin. Pharmacol.*, vol. 28, pp. 24–30, Jun. 2016.

[108] M. Sato *et al.*, "Osteocytes Regulate Primary Lymphoid Organs and Fat Metabolism," *Cell Metab.*, vol. 18, no. 5, pp. 749–758, Nov. 2013.

[109] L. I. Plotkin, I. Mathov, J. I. Aguirre, A. M. Parfitt, S. C. Manolagas, and T. Bellido, "Mechanical stimulation prevents osteocyte apoptosis: requirement of integrins, Src kinases, and ERKs," *Am. J. Physiol. Physiol.*, vol. 289, no. 3, pp. C633–C643, Sep. 2005.

[110] B. S. Noble *et al.*, "Mechanical loading: biphasic osteocyte survival and targeting of osteoclasts for bone destruction in rat cortical bone," *Am. J. Physiol. Physiol.*, vol. 284, no. 4, pp. C934–C943, Apr. 2003.

[111] W. D. Clark, E. L. Smith, K. A. Linn, J. R. Paul-Murphy, P. Muir, and M. E. Cook, "Osteocyte Apoptosis and Osteoclast Presence in Chicken Radii 0–4 Days Following Osteotomy," *Calcif. Tissue Int.*, vol. 77, no. 5, pp. 327–336, Nov. 2005.

[112] L. Cardoso, B. C. Herman, O. Verborgt, D. Laudier, R. J. Majeska, and M. B. Schaffler, "Osteocyte Apoptosis Controls Activation of Intracortical Resorption in Response to Bone Fatigue," *J. Bone Miner. Res.*, vol. 24, no. 4, pp. 597–605, Apr. 2009.

[113] O. Verborgt, G. J. Gibson, and M. B. Schaffler, "Loss of Osteocyte Integrity in Association with Microdamage and Bone Remodeling After Fatigue In Vivo," *J. Bone Miner. Res.*, vol. 15, no. 1, pp. 60–67, Jan. 2000.

[114] S. Tatsumi *et al.*, "Targeted Ablation of Osteocytes Induces Osteoporosis with Defective Mechanotransduction," *Cell Metab.*, vol. 5, no. 6, pp. 464–475, Jun. 2007.

[115] X. Shen *et al.*, "Magnitude-dependent response of osteoblasts regulated by compressive stress," *Sci. Rep.*, vol. 7, no. 1, p. 44925, Dec. 2017.

[116] Y. Yan *et al.*, "Mechanical Strain Regulates Osteoblast Proliferation through Integrin-Mediated ERK Activation," *PLoS One*, vol. 7, no. 4, p. 35709, 2012.

[117] C. R. Jacobs *et al.*, "The role of actin cytoskeleton in oscillatory fluid flow-induced signaling in MC3T3-E1 osteoblasts," *Am. J. Physiol. Physiol.*, vol. 292, no. 5, pp. C1830–C1836, 2007.

[118] S. M. Norvell, M. Alvarez, J. P. Bidwell, and F. M. Pavalko, "Fluid shear stress induces

beta-catenin signaling in osteoblasts.," *Calcif. Tissue Int.*, vol. 75, no. 5, pp. 396–404, 2004.

[119] B. D. Riehl, J. S. Lee, L. Ha, I. K. Kwon, and J. Y. Lim, "Flowtaxis (SUP) of osteoblast migration under fluid shear and the effect of RhoA kinase silencing.," *PLoS One*, vol. 12, no. 2, p. e0171857, Feb. 2017.

[120] F. M. Pavalko *et al.*, "Fluid shear-induced mechanical signaling in MC3T3-E1 osteoblasts requires cytoskeleton-integrin interactions.," *Am. J. Physiol.*, vol. 275, no. 6 Pt 1, pp. C1591-601, Dec. 1998.

[121] G. N. Bancroft *et al.*, "Fluid flow increases mineralized matrix deposition in 3D perfusion culture of marrow stromal osteoblasts in a dose-dependent manner."

[122] S. C. Cowin, "Mechanosensation and fluid transport in living bone," 2002.

[123] A. M. Nguyen and C. R. Jacobs, "Emerging role of primary cilia as mechanosensors in osteocytes.," *Bone*, vol. 54, no. 2, pp. 196–204, Jun. 2013.

[124] X. Yuan and S. Yang, "Primary Cilia and Intraflagellar Transport Proteins in Bone and Cartilage," *J. Dent. Res.*, vol. 95, no. 12, pp. 1341–1349, Nov. 2016.

[125] G. Novarino, N. Akizu, and J. G. Gleeson, "Modeling Human Disease in Humans: The Ciliopathies," *Cell*, vol. 147, no. 1, pp. 70–79, Sep. 2011.

[126] S. Temiyasathit and C. R. Jacobs, "The osteocyte primary cilium and its role in bone mechanotransduction."

[127] D. A. Hoey, S. Tormey, S. Ramcharan, F. J. O'Brien, and C. R. Jacobs, "Primary Cilia-Mediated Mechanotransduction in Human Mesenchymal Stem Cells," *Stem Cells*, vol. 30, no. 11, pp. 2561–2570, 2012.

[128] E. Stavenschi and D. A. Hoey, "Pressure-induced mesenchymal stem cell osteogenesis is dependent on intermediate filament remodeling," *FASEB J.*, p. fj.201801474RR, Dec. 2018.

[129] H. L. May-Simera and M. W. Kelley, "Cilia, Wnt signaling, and the cytoskeleton.," *Cilia*, vol. 1, no. 1, p. 7, Jan. 2012.

[130] J. H. W. Jansen *et al.*, "Stretch-induced inhibition of Wnt/β-catenin signaling in mineralizing osteoblasts," *J. Orthop. Res.*, vol. 28, no. 3, p. n/a-n/a, 2009.

[131] D. A. Glass *et al.*, "Canonical Wnt Signaling in Differentiated Osteoblasts Controls Osteoclast Differentiation," *Dev. Cell*, vol. 8, no. 5, pp. 751–764, May 2005.

[132] M. Gosset, F. Berenbaum, S. Thirion, and C. Jacques, "Primary culture and phenotyping of murine chondrocytes," 2008.

[133] H. Khayyeri, S. Barreto, and D. Lacroix, "Primary cilia mechanics affects cell mechanosensation: A computational study.," *J. Theor. Biol.*, May 2015.

[134] A. M. D. Malone *et al.*, "Primary cilia mediate mechanosensing in bone cells by a calcium-independent mechanism.," *Proc. Natl. Acad. Sci. U. S. A.*, vol. 104, no. 33, pp. 13325–30, Aug. 2007.

[135] J. C. Chen, D. A. Hoey, M. Chua, R. Bellon, and C. R. Jacobs, “Mechanical signals promote osteogenic fate through a primary cilia-mediated mechanism,” *FASEB J.*, vol. 30, no. 4, pp. 1504–1511, Apr. 2016.

[136] L. C. Espinha, D. A. Hoey, P. R. Fernandes, H. C. Rodrigues, and C. R. Jacobs, “Oscillatory fluid flow influences primary cilia and microtubule mechanics,” *Cytoskeleton*, vol. 71, no. 7, pp. 435–445, Jul. 2014.

[137] A. M. Nguyen, Y.-N. Young, and C. R. Jacobs, “The primary cilium is a self-adaptable, integrating nexus for mechanical stimuli and cellular signaling,” *Biol. Open*, vol. 4, no. 12, pp. 1733–1738, Dec. 2015.

[138] C. J. Haycraft *et al.*, “Intraflagellar transport is essential for endochondral bone formation,” *Development*, vol. 134, no. 2, pp. 307–316, Jan. 2007.

[139] E. Kolpakova-Hart, M. Jinnin, B. Hou, N. Fukai, and B. R. Olsen, “Kinesin-2 controls development and patterning of the vertebrate skeleton by Hedgehog- and Gli3-dependent mechanisms.,” *Dev. Biol.*, vol. 309, no. 2, pp. 273–84, Sep. 2007.

[140] B. Liu, S. Chen, D. Cheng, W. Jing, and J. A. Helms, “Primary Cilia Integrate Hedgehog and Wnt Signaling during Tooth Development,” *J. Dent. Res.*, vol. 93, no. 5, pp. 475–482, May 2014.

[141] S. Temiyasathit *et al.*, “Mechanosensing by the Primary Cilium: Deletion of Kif3A Reduces Bone Formation Due to Loading,” *PLoS One*, vol. 7, no. 3, p. e33368, Mar. 2012.

[142] N. Qiu *et al.*, “Disruption of Kif3a in osteoblasts results in defective bone formation and osteopenia,” *J. Cell Sci.*, vol. 125, no. 8, pp. 1945–1957, Apr. 2012.

[143] X. Yuan *et al.*, “Ciliary IFT80 balances canonical versus non-canonical hedgehog signalling for osteoblast differentiation,” *Nat. Commun.*, vol. 7, no. 1, p. 11024, Dec. 2016.

[144] G. Sánchez-Duffhues *et al.*, “SLUG Is Expressed in Endothelial Cells Lacking Primary Cilia to Promote Cellular Calcification,” *Arterioscler. Thromb. Vasc. Biol.*, vol. 35, no. 3, pp. 616–627, Mar. 2015.

[145] N. Qiu, L. Cao, V. David, L. D. Quarles, and Z. Xiao, “Kif3a Deficiency Reverses the Skeletal Abnormalities in Pkd1 Deficient Mice by Restoring the Balance Between Osteogenesis and Adipogenesis,” *PLoS One*, vol. 5, no. 12, p. e15240, Dec. 2010.

[146] Z. Xiao, S. Zhang, L. Cao, N. Qiu, V. David, and L. D. Quarles, “Conditional Disruption of *Pkd1* in Osteoblasts Results in Osteopenia Due to Direct Impairment of Bone Formation,” *J. Biol. Chem.*, vol. 285, no. 2, pp. 1177–1187, Jan. 2010.

[147] Z. Xiao *et al.*, “Conditional deletion of Pkd1 in osteocytes disrupts skeletal mechanosensing in mice,” *FASEB J.*, vol. 25, no. 7, pp. 2418–2432, Jul. 2011.

[148] K. Noda, M. Kitami, K. Kitami, M. Kaku, and Y. Komatsu, “Canonical and noncanonical intraflagellar transport regulates craniofacial skeletal development.,” *Proc. Natl. Acad. Sci. U. S. A.*, vol. 113, no. 19, pp. E2589-97, May 2016.

[149] M. Hayes, M. Naito, A. Daulat, S. Angers, and B. Ciruna, “Ptk7 promotes non-canonical Wnt/PCP-mediated morphogenesis and inhibits Wnt/ -catenin-dependent cell fate

decisions during vertebrate development," *Development*, vol. 140, no. 8, pp. 1807–1818, Apr. 2013.

[150] K. S. Kang and A. G. Robling, "New Insights into Wnt-Lrp5/6-beta-Catenin Signaling in Mechanotransduction," *Front. Endocrinol. (Lausanne).*, vol. 5, Jan. 2015.

[151] R. Baron and G. Rawadi, "Targeting the Wnt/β-Catenin Pathway to Regulate Bone Formation in the Adult Skeleton," *Endocrinology*, vol. 148, no. 6, pp. 2635–2643, Jun. 2007.

[152] D. G. McEwen and M. Peifer, "Wnt signaling: Moving in a new direction," *Curr. Biol.*, vol. 10, no. 15, pp. R562–R564, Aug. 2000.

[153] V. Krishnan, H. U. Bryant, and O. A. Macdougald, "Regulation of bone mass by Wnt signaling.," *J. Clin. Invest.*, vol. 116, no. 5, pp. 1202–9, May 2006.

[154] R. Baron and M. Kneissel, "WNT signaling in bone homeostasis and disease: from human mutations to treatments," *Nat. Med.*, vol. 19, no. 2, pp. 179–192, Feb. 2013.

[155] J. H. Kim *et al.*, "Wnt signaling in bone formation and its therapeutic potential for bone diseases.," *Ther. Adv. Musculoskelet. Dis.*, vol. 5, no. 1, pp. 13–31, Feb. 2013.

[156] T. P. Hill, D. Später, M. M. Taketo, W. Birchmeier, and C. Hartmann, "Canonical Wnt/β-Catenin Signaling Prevents Osteoblasts from Differentiating into Chondrocytes," *Dev. Cell*, vol. 8, no. 5, pp. 727–738, May 2005.

[157] T. F. Day, X. Guo, L. Garrett-Beal, and Y. Yang, "Wnt/β-Catenin Signaling in Mesenchymal Progenitors Controls Osteoblast and Chondrocyte Differentiation during Vertebrate Skeletogenesis," *Dev. Cell*, vol. 8, no. 5, pp. 739–750, May 2005.

[158] T. P. Hill, "Multiple roles of mesenchymal beta-catenin during murine limb patterning," *Development*, vol. 133, no. 7, pp. 1219–1229, Apr. 2006.

[159] L. M. Boyden *et al.*, "High Bone Density Due to a Mutation in LDL-Receptor–Related Protein 5," *N. Engl. J. Med.*, vol. 346, no. 20, pp. 1513–1521, May 2002.

[160] Y. Gong *et al.*, "LDL Receptor-Related Protein 5 (LRP5) Affects Bone Accrual and Eye Development," *Cell*, vol. 107, no. 4, pp. 513–523, Nov. 2001.

[161] I. Takada *et al.*, "A histone lysine methyltransferase activated by non-canonical Wnt signalling suppresses PPAR-γ transactivation," *Nat. Cell Biol.*, vol. 9, no. 11, pp. 1273–1285, Nov. 2007.

[162] J. B. Regard, Z. Zhong, B. O. Williams, and Y. Yang, "Wnt Signaling in Bone Development and Disease: Making Stronger Bone with Wnts," *Cold Spring Harb. Perspect. Biol.*, vol. 4, no. 12, Dec. 2012.

[163] B. Javaheri *et al.*, "Deletion of a Single β-Catenin Allele in Osteocytes Abolishes the Bone Anabolic Response to Loading," *J. Bone Miner. Res.*, vol. 29, no. 3, pp. 705–715, Mar. 2014.

[164] L. K. Saxon, B. F. Jackson, T. Sugiyama, L. E. Lanyon, and J. S. Price, "Analysis of multiple bone responses to graded strains above functional levels, and to disuse, in mice in vivo show that the human Lrp5 G171V High Bone Mass mutation increases the

osteogenic response to loading but that lack of Lrp5 activity reduces it," *Bone*, vol. 49, no. 2, pp. 184–193, Aug. 2011.

[165] A. G. Robling *et al.*, "Mechanical stimulation of bone in vivo reduces osteocyte expression of Sost/sclerostin.," *J. Biol. Chem.*, vol. 283, no. 9, pp. 5866–75, Feb. 2008.

[166] I. Kramer *et al.*, "Osteocyte Wnt/beta-catenin signaling is required for normal bone homeostasis.," *Mol. Cell. Biol.*, vol. 30, no. 12, pp. 3071–85, Jun. 2010.

[167] D. Liu *et al.*, "Activation of extracellular-signal regulated kinase (ERK1/2) by fluid shear is Ca2+- and ATP-dependent in MC3T3-E1 osteoblasts," *Bone*, vol. 42, no. 4, pp. 644–652, Apr. 2008.

[168] B. Wang, T. Du, Y. Wang, C. Yang, S. Zhang, and X. Cao, "Focal adhesion kinase signaling pathway is involved in mechanotransduction in MG-63 Cells," *Biochem. Biophys. Res. Commun.*, vol. 410, no. 3, pp. 671–676, Jul. 2011.

[169] N. A. Chatzizacharias, G. P. Kouraklis, and S. E. Theocharis, "Disruption of FAK signaling: A side mechanism in cytotoxicity," *Toxicology*, vol. 245, no. 1–2, pp. 1–10, Mar. 2008.

[170] C. T. Hung, S. R. Pollack, T. M. Reilly, and C. T. Brighton, "Real-time calcium response of cultured bone cells to fluid flow.," *Clin. Orthop. Relat. Res.*, no. 313, pp. 256–69, Apr. 1995.

[171] T. N. McAllister and J. A. Frangos, "Steady and Transient Fluid Shear Stress Stimulate NO Release in Osteoblasts Through Distinct Biochemical Pathways," *J. Bone Miner. Res.*, vol. 14, no. 6, pp. 930–936, Jun. 1999.

[172] S. W. Donahue, H. J. Donahue, and C. R. Jacobs, "Osteoblastic cells have refractory periods for fluid-flow-induced intracellular calcium oscillations for short bouts of flow and display multiple low-magnitude oscillations during long-term flow.," *J. Biomech.*, vol. 36, no. 1, pp. 35–43, Jan. 2003.

[173] R. Y. Kwon, S. Temiyasathit, P. Tummala, C. C. Quah, and C. R. Jacobs, "Primary cilium-dependent mechanosensing is mediated by adenylyl cyclase 6 and cyclic AMP in bone cells," *FASEB J.*, vol. 24, no. 8, pp. 2859–2868, Aug. 2010.

[174] B. Lisowska, D. Kosson, and K. Domaracka, "Lights and shadows of NSAIDs in bone healing: the role of prostaglandins in bone metabolism.," *Drug Des. Devel. Ther.*, vol. 12, pp. 1753–1758, 2018.

[175] N. D. Searby, C. R. Steele, and R. K. Globus, "Influence of increased mechanical loading by hypergravity on the microtubule cytoskeleton and prostaglandin E_2 release in primary osteoblasts," *Am. J. Physiol. Physiol.*, vol. 289, no. 1, pp. C148–C158, Jul. 2005.

[176] N. N. Batra *et al.*, "Effects of short-term recovery periods on fluid-induced signaling in osteoblastic cells," *J. Biomech.*, vol. 38, no. 9, pp. 1909–1917, Sep. 2005.

[177] K. Thorsen, A. O. Kristoffersson, U. H. Lerner, and R. P. Lorentzon, "In situ microdialysis in bone tissue. Stimulation of prostaglandin E2 release by weight-bearing mechanical loading.," *J. Clin. Invest.*, vol. 98, no. 11, pp. 2446–2449, Dec. 1996.

[178] E. Stavenschi, M. A. Corrigan, G. P. Johnson, M. Riffault, and D. A. Hoey, "Physiological

cyclic hydrostatic pressure induces osteogenic lineage commitment of human bone marrow stem cells: A systematic study," *Stem Cell Res. Ther.*, vol. 9, no. 1, 2018.

[179] N. Oliazadeh, K. F. Gorman, R. Eveleigh, G. Bourque, and A. Moreau, "Identification of Elongated Primary Cilia with Impaired Mechanotransduction in Idiopathic Scoliosis Patients," *Sci. Rep.*, vol. 7, no. 1, p. 44260, Dec. 2017.

[180] G. L. Galea, J. S. Price, and L. E. Lanyon, "Estrogen receptors' roles in the control of mechanically adaptive bone (re)modeling," *Bonekey Rep.*, vol. 2, 2013.

[181] J. Klein-Nulend, R. F. M. van Oers, A. D. Bakker, and R. G. Bacabac, "Bone cell mechanosensitivity, estrogen deficiency, and osteoporosis," *J. Biomech.*, 2015.

[182] K. F. Gorman and F. Breden, "Teleosts as models for human vertebral stability and deformity," *Comparative Biochemistry and Physiology - C Toxicology and Pharmacology*, vol. 145, no. 1. pp. 28–38, Feb-2007.

[183] M. M. A. Janssen, R. F. de Wilde, J.-W. M. Kouwenhoven, and R. M. Castelein, "Experimental animal models in scoliosis research: a review of the literature," *Spine J.*, vol. 11, no. 4, pp. 347–358, Apr. 2011.

[184] K. F. Gorman, S. J. Tredwell, and F. Breden, "The mutant guppy syndrome curveback as a model for human heritable spinal curvature.," *Spine (Phila. Pa. 1976).*, vol. 32, no. 7, pp. 735–41, Apr. 2007.

[185] R. Keller, "Shaping the Vertebrate Body Plan by Polarized Embryonic Cell Movements," *Science (80-.).*, vol. 298, no. 5600, pp. 1950–1954, Dec. 2002.

[186] X. He, "Cilia put a brake on Wnt signalling," *Nat. Cell Biol.*, vol. 10, no. 1, pp. 11–13, Jan. 2008.

[187] F. Hefti, "Pathogenesis and biomechanics of adolescent idiopathic scoliosis (AIS).," *J. Child. Orthop.*, vol. 7, no. 1, pp. 17–24, Feb. 2013.

[188] R. W. Porter, "Idiopathic scoliosis: the relation between the vertebral canal and the vertebral bodies.," *Spine (Phila. Pa. 1976).*, vol. 25, no. 11, pp. 1360–6, Jun. 2000.

[189] I. A. F. Stokes and L. Windisch, "Vertebral Height Growth Predominates Over Intervertebral Disc Height Growth in Adolescents With Scoliosis," *Spine (Phila. Pa. 1976).*, vol. 31, no. 14, pp. 1600–1604, Jun. 2006.

[190] W. Wang *et al.*, "The association of disproportionate skeletal growth and abnormal radius dimension ratio with curve severity in adolescent idiopathic scoliosis," *Eur. Spine J.*, vol. 19, no. 5, pp. 726–731, May 2010.

[191] W. C. W. Chu *et al.*, "Relative shortening and functional tethering of spinal cord in adolescent idiopathic scoliosis?: study with multiplanar reformat magnetic resonance imaging and somatosensory evoked potential.," *Spine (Phila. Pa. 1976).*, vol. 31, no. 1, pp. E19-25, Jan. 2006.

[192] R. M. Castelein, J. H. van Dieën, T. H. Smit, J. H. van Dieën, and T. H. Smit, "The role of dorsal shear forces in the pathogenesis of adolescent idiopathic scoliosis--a hypothesis.," *Med. Hypotheses*, vol. 65, no. 3, pp. 501–8, Jan. 2005.

[193] T. Do, C. Fras, S. Burke, R. F. Widmann, B. Rawlins, and O. Boachie-Adjei, “Clinical value of routine preoperative magnetic resonance imaging in adolescent idiopathic scoliosis. A prospective study of three hundred and twenty-seven patients.,” *J. Bone Joint Surg. Am.*, vol. 83-A, no. 4, pp. 577–9, Apr. 2001.

[194] P. Deacon, I. A. Archer, and R. A. Dickson, “The anatomy of spinal deformity: a biomechanical analysis.,” *Orthopedics*, vol. 10, no. 6, pp. 897–903, Jun. 1987.

[195] A. G. Veldhuizen, D. J. Wever, and P. J. Webb, “The aetiology of idiopathic scoliosis: biomechanical and neuromuscular factors.,” *Eur. Spine J.*, vol. 9, no. 3, pp. 178–84, Jun. 2000.

[196] D. J. Wever *et al.*, “A biomechanical analysis of the vertebral and rib deformities in structural scoliosis.,” *Eur. Spine J.*, vol. 8, no. 4, pp. 252–60, 1999.

[197] L. Samuelsson, D. Lindell, and H. Kogler, “Spinal cord and brain stem anomalies in scoliosis. MR screening of 26 cases.,” *Acta Orthop. Scand.*, vol. 62, no. 5, pp. 403–6, Oct. 1991.

[198] W. A. Phillips, R. N. Hensinger, and T. F. Kling, “Management of scoliosis due to syringomyelia in childhood and adolescence.,” *J. Pediatr. Orthop.*, vol. 10, no. 3, pp. 351–4.

[199] M. Machida *et al.*, “Pathogenesis of idiopathic scoliosis: SEPs in chicken with experimentally induced scoliosis and in patients with idiopathic scoliosis.,” *J. Pediatr. Orthop.*, vol. 14, no. 3, pp. 329–35.

[200] N. H. Miller, “Adolescent Idiopathic Scoliosis: Etiology,” *Pediatr. Spine*, p. 354, 2001.

[201] S. A. Patten *et al.*, “Functional variants of POC5 identified in patients with idiopathic scoliosis.,” *J. Clin. Invest.*, vol. 125, no. 3, pp. 1124–8, Mar. 2015.

[202] E. E. Baschal *et al.*, “Exome sequencing identifies a rare HSPG2 variant associated with familial idiopathic scoliosis.,” *G3 (Bethesda).*, vol. 5, no. 2, pp. 167–74, Feb. 2015.

[203] S. Atzal, M. Ramzan, M. Farooq, and G. Rasul, “Biomechanics of spinal deformity,” *JK Pract.*, vol. 11, no. 1, pp. 1–10, 2004.

[204] M. M. A. Janssen *et al.*, “Sagittal spinal profile and spinopelvic balance in parents of scoliotic children,” *Spine J.*, vol. 13, no. 12, pp. 1789–1800, 2013.

[205] A. B. Schultz, “Biomechanical factors in the progression of idiopathic scoliosis.,” *Ann. Biomed. Eng.*, vol. 12, no. 6, pp. 621–30, 1984.

[206] A. Resnick, “Mechanical properties of a primary cilium as measured by resonant oscillation.,” *Biophys. J.*, vol. 109, no. 1, pp. 18–25, Jul. 2015.

[207] K. L. Lee, M. D. Guevarra, A. M. Nguyen, M. C. Chua, Y. Wang, and C. R. Jacobs, “The primary cilium functions as a mechanical and calcium signaling nexus.,” *Cilia*, vol. 4, p. 7, 2015.

[208] M. Delling *et al.*, “Primary cilia are not calcium-responsive mechanosensors,” *Nature*, vol. 531, no. 7596, pp. 656–660, Mar. 2016.

[209] P. Leucht *et al.*, “Primary cilia act as mechanosensors during bone healing around an implant.,” *Med. Eng. Phys.*, vol. 35, no. 3, pp. 392–402, Mar. 2013.

[210] R. M. Delaine-Smith, A. Sittichokechaiwut, and G. C. Reilly, “Primary cilia respond to fluid shear stress and mediate flow-induced calcium deposition in osteoblasts,” *FASEB J.*, vol. 28, no. 1, pp. 430–439, Jan. 2014.

[211] M.-G. Ascenzi *et al.*, “Effect of localization, length and orientation of chondrocytic primary cilium on murine growth plate organization.,” *J. Theor. Biol.*, vol. 285, no. 1, pp. 147–55, Sep. 2011.

[212] C. Huber and V. Cormier-Daire, “Ciliary disorder of the skeleton,” *Am. J. Med. Genet. Part C Semin. Med. Genet.*, vol. 160 C, no. 3, pp. 165–174, 2012.

[213] D. Kobayashi, N. Iijima, H. Hagiwara, K. Kamura, H. Takeda, and T. Yokoyama, “Characterization of the medaka (Oryzias latipes) primary ciliary dyskinesia mutant, jaodori: Redundant and distinct roles of dynein axonemal intermediate chain 2 (dnai2) in motile cilia,” *Dev. Biol.*, vol. 347, no. 1, pp. 62–70, 2010.

[214] J. G. Buchan *et al.*, “Kinesin family member 6 (kif6) is necessary for spine development in zebrafish.,” *Dev. Dyn.*, vol. 243, no. 12, pp. 1646–57, Dec. 2014.

[215] S. Lee *et al.*, “Optimal unified approach for rare-variant association testing with application to small-sample case-control whole-exome sequencing studies.,” *Am. J. Hum. Genet.*, vol. 91, no. 2, pp. 224–37, Aug. 2012.

[216] E. S. Seeley and M. V. Nachury, “The perennial organelle: assembly and disassembly of the primary cilium,” *J. Cell Sci.*, vol. 123, no. 4, pp. 511–518, 2010.

[217] C. L. Thompson, A. Wiles, C. A. Poole, and M. M. Knight, “Lithium chloride modulates chondrocyte primary cilia and inhibits Hedgehog signaling.”

[218] R. G. Bacabac, T. H. Smit, M. G. Mullender, S. J. Dijcks, J. J. W. A. Van Loon, and J. Klein-Nulend, “Nitric oxide production by bone cells is fluid shear stress rate dependent.,” *Biochem. Biophys. Res. Commun.*, vol. 315, no. 4, pp. 823–9, Mar. 2004.

[219] F. Loth, M. A. Yardimci, and N. Alperin, “Hydrodynamic Modeling of Cerebrospinal Fluid Motion Within the Spinal Cavity,” *J. Biomech. Eng.*, vol. 123, no. 1, p. 71, Sep. 2001.

[220] X. Yuan, R. a Serra, and S. Yang, “Function and regulation of primary cilia and intraflagellar transport proteins in the skeleton.,” *Ann. N. Y. Acad. Sci.*, vol. 1335, pp. 78–99, 2014.

[221] T. J. Vaughan, C. a. Mullen, S. W. Verbruggen, and L. M. McNamara, “Bone cell mechanosensation of fluid flow stimulation: a fluid–structure interaction model characterising the role integrin attachments and primary cilia,” *Biomech. Model. Mechanobiol.*, vol. 2, 2014.

[222] N. Kumamoto *et al.*, “A role for primary cilia in glutamatergic synaptic integration of adult-born neurons.,” *Nat. Neurosci.*, vol. 15, no. 3, pp. 399–405, S1, 2012.

[223] K. C. Corbit *et al.*, “Kif3a constrains beta-catenin-dependent Wnt signalling through dual ciliary and non-ciliary mechanisms.,” *Nat. Cell Biol.*, vol. 10, no. 1, pp. 70–6, Jan. 2008.

[224] Y.-H. Fan *et al.*, "SNP rs11190870 near LBX1 is associated with adolescent idiopathic scoliosis in southern Chinese.," *J. Hum. Genet.*, vol. 57, no. 4, pp. 244–6, Apr. 2012.

[225] H. Jiang *et al.*, "Association of rs11190870 near LBX1 with adolescent idiopathic scoliosis susceptibility in a Han Chinese population.," *Eur. Spine J.*, vol. 22, no. 2, pp. 282–6, Mar. 2013.

[226] A. McKenna *et al.*, "The Genome Analysis Toolkit: a MapReduce framework for analyzing next-generation DNA sequencing data.," *Genome Res.*, vol. 20, no. 9, pp. 1297–303, Sep. 2010.

[227] M. C. Wu, S. Lee, T. Cai, Y. Li, M. Boehnke, and X. Lin, "Rare-variant association testing for sequencing data with the sequence kernel association test.," *Am. J. Hum. Genet.*, vol. 89, no. 1, pp. 82–93, Jul. 2011.

[228] T. J. van Dam, G. Wheway, G. G. Slaats, M. a Huynen, and R. H. Giles, "The SYSCILIA gold standard (SCGSv1) of known ciliary components and its applications within a systems biology consortium.," *Cilia*, vol. 2, no. 1, p. 7, 2013.

[229] J. Kim *et al.*, "Functional genomic screen for modulators of ciliogenesis and cilium length.," *Nature*, vol. 464, no. 7291, pp. 1048–1051, 2010.

[230] R. J. McMurray, A. K. T. Wann, C. L. Thompson, J. T. Connelly, and M. M. Knight, "Surface topography regulates wnt signaling through control of primary cilia structure in mesenchymal stem cells.," *Sci. Rep.*, vol. 3, p. 3545, Jan. 2013.

[231] P. Satir, L. B. Pedersen, and S. T. Christensen, "The primary cilium at a glance.," *J. Cell Sci.*, vol. 123, no. Pt 4, pp. 499–503, Feb. 2010.

[232] H. A. Praetorius and K. R. Spring, "Removal of the MDCK cell primary cilium abolishes flow sensing.," *J. Membr. Biol.*, vol. 191, no. 1, pp. 69–76, Jan. 2003.

[233] A. K. T. Wann *et al.*, "Primary cilia mediate mechanotransduction through control of ATP-induced Ca2+ signaling in compressed chondrocytes.," *FASEB J.*, vol. 26, no. 4, pp. 1663–71, Apr. 2012.

[234] M. A. Lancaster, J. Schroth, and J. G. Gleeson, "Subcellular spatial regulation of canonical Wnt signalling at the primary cilium.," *Nat. Cell Biol.*, vol. 13, no. 6, pp. 700–8, Jun. 2011.

[235] F. Kugimiya *et al.*, "GSK-3beta controls osteogenesis through regulating Runx2 activity.," *PLoS One*, vol. 2, no. 9, p. e837, Sep. 2007.

[236] M. Simons *et al.*, "Inversin, the gene product mutated in nephronophthisis type II, functions as a molecular switch between Wnt signaling pathways," *Nat. Genet.*, vol. 37, no. 5, pp. 537–543, May 2005.

[237] J. You *et al.*, "Osteopontin Gene Regulation by Oscillatory Fluid Flow via Intracellular Calcium Mobilization and Activation of Mitogen-activated Protein Kinase in MC3T3-E1 Osteoblasts," *J. Biol. Chem.*, vol. 276, no. 16, pp. 13365–71, Apr. 2001.

[238] X. Zhang, E. M. Schwarz, D. A. Young, J. E. Puzas, R. N. Rosier, and R. J. O'Keefe, "Cyclooxygenase-2 regulates mesenchymal cell differentiation into the osteoblast lineage and is critically involved in bone repair.," *J. Clin. Invest.*, vol. 109, no. 11, pp. 1405–15,

Jun. 2002.

[239] K. Ishida *et al.*, “Relationship between bone density and bone metabolism in adolescent idiopathic scoliosis.,” *Scoliosis*, vol. 10, no. 1, p. 9, Jan. 2015.

[240] S. D. Cook *et al.*, “Trabecular bone mineral density in idiopathic scoliosis.,” *J. Pediatr. Orthop.*, vol. 7, no. 2, pp. 168–74, Jan. .

[241] D. Jin *et al.*, “Prostaglandin signalling regulates ciliogenesis by modulating intraflagellar transport.,” *Nat. Cell Biol.*, vol. 16, no. 9, pp. 841–51, Sep. 2014.

[242] J. B. Litzenberger, J.-B. Kim, P. Tummala, and C. R. Jacobs, “Beta1 integrins mediate mechanosensitive signaling pathways in osteocytes.,” *Calcif. Tissue Int.*, vol. 86, no. 4, pp. 325–32, Apr. 2010.

[243] S. R. McGlashan, C. G. Jensen, and C. A. Poole, “Localization of extracellular matrix receptors on the chondrocyte primary cilium.,” *J. Histochem. Cytochem.*, vol. 54, no. 9, pp. 1005–14, Sep. 2006.

[244] J.-C. Kuo, “Mechanotransduction at focal adhesions: integrating cytoskeletal mechanics in migrating cells.,” *J. Cell. Mol. Med.*, vol. 17, no. 6, pp. 704–12, Jun. 2013.

[245] P. Clément-Lacroix *et al.*, “Lrp5-independent activation of Wnt signaling by lithium chloride increases bone formation and bone mass in mice.,” *Proc. Natl. Acad. Sci. U. S. A.*, vol. 102, no. 48, pp. 17406–11, Nov. 2005.

[246] B. M. Harvey *et al.*, “Effect of daily lithium chloride administration on bone mass and strength in growing broiler chickens, [1],” *Poult. Sci.*, vol. 94, no. 2, pp. 296–301, Feb. 2015.

[247] J. de Boer, R. Siddappa, C. Gaspar, A. van Apeldoorn, R. Fodde, and C. van Blitterswijk, “Wnt signaling inhibits osteogenic differentiation of human mesenchymal stem cells,” *Bone*, vol. 34, no. 5, pp. 818–826, 2004.

[248] G. M. Boland, G. Perkins, D. J. Hall, and R. S. Tuan, “Wnt 3a promotes proliferation and suppresses osteogenic differentiation of adult human mesenchymal stem cells,” *J. Cell. Biochem.*, vol. 93, no. 6, pp. 1210–1230, 2004.

[249] T. Y. Besschetnova, E. Kolpakova-Hart, Y. Guan, J. Zhou, B. R. Olsen, and J. V. Shah, “Identification of signaling pathways regulating primary cilium length and flow-mediated adaptation.,” *Curr. Biol.*, vol. 20, no. 2, pp. 182–7, Jan. 2010.

[250] S. Yuan, J. Li, D. R. Diener, M. A. Choma, J. L. Rosenbaum, and Z. Sun, “Target-of-rapamycin complex 1 (Torc1) signaling modulates cilia size and function through protein synthesis regulation.,” *Proc. Natl. Acad. Sci. U. S. A.*, vol. 109, no. 6, pp. 2021–6, Feb. 2012.

[251] S. R. McGlashan *et al.*, “Mechanical loading modulates chondrocyte primary cilia incidence and length.,” *Cell Biol. Int.*, vol. 34, no. 5, pp. 441–6, May 2010.

[252] B. Marosy *et al.*, “Identification of susceptibility loci for scoliosis in FIS families with triple curves.,” *Am. J. Med. Genet. A*, vol. 152A, no. 4, pp. 846–55, Apr. 2010.

[253] Z. Zhu *et al.*, “Genome-wide association study identifies new susceptibility loci for

adolescent idiopathic scoliosis in Chinese girls.," *Nat. Commun.*, vol. 6, p. 8355, Jan. 2015.

[254] J. Azimzadeh *et al.*, "hPOC5 is a centrin-binding protein required for assembly of full-length centrioles," *J. Cell Biol.*, vol. 185, no. 1, pp. 101–114, 2009.

[255] A. Das, D. J. Dickinson, C. C. Wood, B. Goldstein, and K. C. Slep, "Crescerin uses a TOG domain array to regulate microtubules in the primary cilium.," *Mol. Biol. Cell*, vol. 26, no. 23, pp. 4248–64, Nov. 2015.

[256] C. P. Samora, B. Mogessie, L. Conway, J. L. Ross, A. Straube, and A. D. McAinsh, "MAP4 and CLASP1 operate as a safety mechanism to maintain a stable spindle position in mitosis.," *Nat. Cell Biol.*, vol. 13, no. 9, pp. 1040–50, Sep. 2011.

[257] A. S. Tsvetkov, A. Samsonov, A. Akhmanova, N. Galjart, and S. V Popov, "Microtubule-binding proteins CLASP1 and CLASP2 interact with actin filaments.," *Cell Motil. Cytoskeleton*, vol. 64, no. 7, pp. 519–30, Jul. 2007.

[258] R. M. Gallo *et al.*, "Regulation of the actin cytoskeleton by Rho kinase controls antigen presentation by CD1d.," *J. Immunol.*, vol. 189, no. 4, pp. 1689–98, Aug. 2012.

[259] T. Suzuki *et al.*, "Essential roles of Lyn in fibronectin-mediated filamentous actin assembly and cell motility in mast cells.," *J. Immunol.*, vol. 161, no. 7, pp. 3694–701, Oct. 1998.

[260] T. Martins, A. F. Maia, S. Steffensen, and C. E. Sunkel, "Sgt1, a co-chaperone of Hsp90 stabilizes Polo and is required for centrosome organization.," *EMBO J.*, vol. 28, no. 3, pp. 234–47, Feb. 2009.

[261] L.-Y. Chen and J. Lingner, "AUF1/HnRNP D RNA binding protein functions in telomere maintenance.," *Mol. Cell*, vol. 47, no. 1, pp. 1–2, Jul. 2012.

[262] A. Liedert, L. Wagner, L. Seefried, R. Ebert, F. Jakob, and A. Ignatius, "Estrogen receptor and Wnt signaling interact to regulate early gene expression in response to mechanical strain in osteoblastic cells," 2010.

[263] J. Fairbank, "Historical perspective: William Adams, the forward bending test, and the spine of Gideon Algernon Mantell.," *Spine (Phila. Pa. 1976).*, vol. 29, no. 17, pp. 1953–5, Sep. 2004.

[264] W. F. M., *Fluid Mechanics*, 7th ed. McGraw-Hill, 2010.

[265] Y. C. Fung, *Motion*. New York, NY: Springer New York, 1990.

[266] X. Zhou, D. Liu, L. You, and L. Wang, "Quantifying fluid shear stress in a rocking culture dish," *J. Biomech.*, vol. 43, no. 8, pp. 1598–1602, 2010.

[267] N. Homer, B. Merriman, and S. F. Nelson, "BFAST: an alignment tool for large scale genome resequencing.," *PLoS One*, vol. 4, no. 11, p. e7767, Jan. 2009.

[268] U. Paila, B. A. Chapman, R. Kirchner, and A. R. Quinlan, "GEMINI: integrative exploration of genetic variation and genome annotations.," *PLoS Comput. Biol.*, vol. 9, no. 7, p. e1003153, Jan. 2013.

[269] M. Kircher, D. M. Witten, P. Jain, B. J. O'Roak, G. M. Cooper, and J. Shendure, "A general framework for estimating the relative pathogenicity of human genetic variants.," *Nat. Genet.*, vol. 46, no. 3, pp. 310–5, Mar. 2014.

[270] S. Lee, C. Fuchsberger, S. Kim, and L. Scott, "An efficient resampling method for calibrating single and gene-based rare variant association analysis in case-control studies.," *Biostatistics*, vol. 17, no. 1, pp. 1–15, Jan. 2016.

[271] P. C. Sham and S. M. Purcell, "Statistical power and significance testing in large-scale genetic studies," *Nat. Rev. Genet.*, vol. 15, no. 5, pp. 335–346, Apr. 2014.

[272] D. Y. T. Fong *et al.*, "A Meta-Analysis of the Clinical Effectiveness of School Scoliosis Screening," *Spine (Phila. Pa. 1976).*, vol. 35, no. 10, pp. 1061–1071, May 2010.

[273] N. Miller, O. Surgery, and N. C. Street, "Adolescent Idiopathic Scoliosis : A Brief Summary On Genetics," pp. 1–4.

[274] M. Machida, S. L. Weinstein, and J. Dubousset, *Pathogenesis of idiopathic scoliosis revisited*, vol. 74, no. 1. Springer Nature, 2003.

[275] I. A. Stokes, H. Spence, D. D. Aronsson, and N. Kilmer, "Mechanical modulation of vertebral body growth. Implications for scoliosis progression.," *Spine (Phila. Pa. 1976).*, vol. 21, no. 10, pp. 1162–7, May 1996.

[276] E. E. Baschal *et al.*, "Idiopathic Scoliosis Families Highlight Actin-Based and Microtubule-Based Cellular Projections and Extracellular Matrix in Disease Etiology.," *G3 (Bethesda).*, vol. 8, no. 8, pp. 2663–2672, 2018.

[277] A. Hassan *et al.*, "Adolescent idiopathic scoliosis associated POC5 mutation impairs cell cycle, cilia length and centrosome protein interactions," *PLoS One*, vol. 14, no. 3, p. e0213269, Mar. 2019.

[278] B. Huang *et al.*, "Osteoblasts secrete Cxcl9 to regulate angiogenesis in bone," *Nat. Commun.*, vol. 7, no. 1, p. 13885, Dec. 2016.

[279] J. Schindelin *et al.*, "Fiji: an open-source platform for biological-image analysis," *Nat. Methods*, vol. 9, no. 7, pp. 676–682, Jul. 2012.

[280] D. Sakai *et al.*, "Remodeling of actin cytoskeleton in mouse periosteal cells under mechanical loading induces periosteal cell proliferation during bone formation," *PLoS One*, vol. 6, no. 9, 2011.

[281] S. M. Ponik, J. W. Triplett, and F. M. Pavalko, "Osteoblasts and osteocytes respond differently to oscillatory and unidirectional fluid flow profiles.," *J. Cell. Biochem.*, vol. 100, no. 3, pp. 794–807, Feb. 2007.

[282] W. R. Thompson, C. T. Rubin, and J. Rubin, *Mechanical regulation of signaling pathways in bone*, vol. 503, no. 2. 2012, pp. 179–193.

[283] M. J. Ford, P. L. Yeyati, G. R. Mali, I. J. Jackson, P. Mill, and R. L. M. Correspondence, "A Cell/Cilia Cycle Biosensor for Single-Cell Kinetics Reveals Persistence of Cilia after G1/S Transition Is a General Property in Cells and Mice," *Dev. Cell*, vol. 47, pp. 509–523, 2018.

[284] I. Rønn Veland, L. Lindbaek, and S. T. Christensen, “Linking the Primary Cilium to Cell Migration in Tissue Repair and Brain Development,” *Bioscience*, vol. 64, no. 12, p. 1115, 2014.

[285] M. Maninová, M. P. Iwanicki, and T. Vomastek, “Emerging role for nuclear rotation and orientation in cell migration,” *Cell Adhes. Migr.*, vol. 8, no. 1, pp. 42–48, 2014.

[286] R. Yao and J. Y. Wong, “The Effects of Mechanical Stimulation on Controlling and Maintaining Marrow Stromal Cell Differentiation Into Vascular Smooth Muscle Cells,” *J. Biomech. Eng.*, vol. 137, no. 2, p. 020907, 2014.

[287] A. E. Rutkovskiy, K.-O. E. Stensløkken, I. Jarle Vaage Corresponding Author, and A. Rutkovskiy, “Osteoblast Differentiation at a Glance,” 2016.

[288] C. R. Jacobs, C. E. Yellowley, B. R. Davis, Z. Zhou, J. M. Cimbala, and H. J. Donahue, “Differential effect of steady versus oscillating flow on bone cells.,” *J. Biomech.*, vol. 31, no. 11, pp. 969–76, Nov. 1998.

[289] J. Keeling, L. Tsiokas, and D. Maskey, “cells Cellular Mechanisms of Ciliary Length Control.”

[290] K. J. Palmer, L. MacCarthy-Morrogh, N. Smyllie, and D. J. Stephens, “A role for Tctex-1 (DYNLT1) in controlling primary cilium length,” *Eur. J. Cell Biol.*, vol. 90, no. 10, pp. 865–871, Oct. 2011.

[291] Y. Ou, Y. Ruan, M. Cheng, J. J. Moser, J. B. Rattner, and F. a van der Hoorn, “Adenylate cyclase regulates elongation of mammalian primary cilia.,” *Exp. Cell Res.*, vol. 315, no. 16, pp. 2802–17, Oct. 2009.

[292] F. M. Pavalko *et al.*, “Fluid shear-induced mechanical signaling in MC3T3-E1 osteoblasts requires cytoskeleton-integrin interactions.”

[293] E. J. Arnsdorf, P. Tummala, R. Y. Kwon, and C. R. Jacobs, “Mechanically induced osteogenic differentiation - the role of RhoA, ROCKII and cytoskeletal dynamics,” *J. Cell Sci.*, vol. 122, no. 4, pp. 546–553, Feb. 2009.

[294] W. M. Jackson, M. J. Jaasma, R. Y. Tang, and T. M. Keaveny, “Mechanical loading by fluid shear is sufficient to alter the cytoskeletal composition of osteoblastic cells,” *Am J Physiol Cell Physiol*, vol. 295, pp. 1007–1015, 2008.

[295] S. J. Jones and A. Boyde, “The migration of osteoblasts.,” *Cell Tissue Res.*, vol. 184, no. 2, pp. 179–93, Oct. 1977.

[296] A. Thiel, M. K. Reumann, A. Boskey, J. Wischmann, R. von Eisenhart-Rothe, and P. Mayer-Kuckuk, “Osteoblast migration in vertebrate bone.,” *Biol. Rev. Camb. Philos. Soc.*, vol. 93, no. 1, pp. 350–363, 2018.

[297] B. D. Riehl, J. S. Lee, L. Ha, and J. Y. Lim, “Fluid-flow-induced mesenchymal stem cell migration: role of focal adhesion kinase and RhoA kinase sensors.,” *J. R. Soc. Interface*, vol. 12, p. 20141351, 2015.

[298] J. D. Gardinier, S. Majumdar, R. L. Duncan, and L. Wang, “Cyclic Hydraulic Pressure and Fluid Flow Differentially Modulate Cytoskeleton Re-Organization in MC3T3 Osteoblasts,” *Cell. Mol. Bioeng.*, vol. 2, no. 1, pp. 133–143, Mar. 2009.

[299] M. Versaevel, T. Grevesse, and S. Gabriele, “Spatial coordination between cell and nuclear shape within micropatterned endothelial cells,” *Nat. Commun.*, vol. 3, no. 1, p. 671, Jan. 2012.

[300] R. M. H. Merks, S. V. Brodsky, M. S. Goligorksy, S. A. Newman, and J. A. Glazier, “Cell elongation is key to in silico replication of in vitro vasculogenesis and subsequent remodeling,” *Dev. Biol.*, vol. 289, no. 1, pp. 44–54, Jan. 2006.

[301] J. R. Sims, S. Karp, and D. E. Ingber, “Altering the cellular mechanical force balance results in integrated changes in cell, cytoskeletal and nuclear shape.,” *J. Cell Sci.*, vol. 103 (Pt 4), pp. 1215–22, Dec. 1992.

[302] C. H. Thomas, J. H. Collier, C. S. Sfeir, and K. E. Healy, “Engineering gene expression and protein synthesis by modulation of nuclear shape,” *Proc. Natl. Acad. Sci.*, vol. 99, no. 4, pp. 1972–1977, Feb. 2002.

[303] A. J. Maniotis, C. S. Chen, and D. E. Ingber, “Demonstration of mechanical connections between integrins, cytoskeletal filaments, and nucleoplasm that stabilize nuclear structure.,” *Proc. Natl. Acad. Sci. U. S. A.*, vol. 94, no. 3, pp. 849–54, Feb. 1997.

[304] C. Wang, B. M. Baker, C. S. Chen, and M. A. Schwartz, “Endothelial cell sensing of flow direction,” *Arterioscler. Thromb. Vasc. Biol.*, vol. 33, no. 9, pp. 2130–2136, 2013.

[305] K. Hu and B. R. Olsen, “The roles of vascular endothelial growth factor in bone repair and regeneration.,” *Bone*, vol. 91, pp. 30–8, 2016.

[306] M. M. Thi, S. O. Suadicani, and D. C. Spray, “Fluid flow-induced soluble vascular endothelial growth factor isoforms regulate actin adaptation in osteoblasts,” *J. Biol. Chem.*, vol. 285, no. 40, pp. 30931–30941, Oct. 2010.

[307] S. Jf, C. Rm, A. Maqsood, and A. C-e, “The Biomechanics of Induction in Adolescent Idiopathic Scoliosis: Theoretical Factors John,” *J. BONE Jt. Surg.*, vol. 22, pp. 18–23, 2019.

[308] O. V Plotnikova, E. N. Pugacheva, and E. A. Golemis, “Primary cilia and the cell cycle.,” *Methods Cell Biol.*, vol. 94, pp. 137–60, 2009.

[309] R. Nowak, M. Kwiecien, M. Tkacz, and U. Mazurek, “Transforming Growth Factor-Beta (TGF-β) Signaling in Paravertebral Muscles in Juvenile and Adolescent Idiopathic Scoliosis,” *Biomed Res. Int.*, vol. 2014, Sep. 2014.

[310] G. Haller *et al.*, “A polygenic burden of rare variants across extracellular matrix genes among individuals with adolescent idiopathic scoliosis,” *Hum. Mol. Genet.*, vol. 25, no. 1, pp. 202–209, Jan. 2016.

[311] J. Street and B. Lenehan, “Vascular endothelial growth factor regulates osteoblast survival - evidence for an autocrine feedback mechanism.,” *J. Orthop. Surg. Res.*, vol. 4, p. 19, Jun. 2009.

[312] C. Zetterberg, A. Aniansson, and G. Grimby, “Morphology of the paravertebral muscles in adolescent idiopathic scoliosis.,” *Spine (Phila. Pa. 1976).*, vol. 8, no. 5, pp. 457–62.

[313] W. A. Littler, S. R. Reuben, and D. J. Lane, “Lung blood flow studies in patients with scoliosis and neuromuscular weakness,” *Thorax*, p. 209, 1973.

[314] G. L. Galea *et al.*, “Planar Cell Polarity Aligns Osteoblast Division in Response to Substrate Strain.”

[315] C. Faure *et al.*, “Mechanical signals modulated vascular endothelial growth factor-A (VEGF-A) alternative splicing in osteoblastic cells through actin polymerisation,” *Bone*, vol. 42, no. 6, pp. 1092–1101, Jun. 2008.

[316] Y. Wang *et al.*, “The hypoxia-inducible factor α pathway couples angiogenesis to osteogenesis during skeletal development,” *J. Clin. Invest.*, vol. 117, no. 6, pp. 1616–1626, Jun. 2007.

[317] M. M. THI, D. A. IACOBAS, S. IACOBAS, and D. C. SPRAY, “Fluid Shear Stress Upregulates Vascular Endothelial Growth Factor Gene Expression in Osteoblasts,” *Ann. N. Y. Acad. Sci.*, vol. 1117, no. 1, pp. 73–81, Nov. 2007.

[318] Z. Yao, M.-H. Lafage-Proust, J. Plouët, S. Bloomfield, C. Alexandre, and L. Vico, “Increase of Both Angiogenesis and Bone Mass in Response to Exercise Depends on VEGF,” *J. Bone Miner. Res.*, vol. 19, no. 9, pp. 1471–1480, Jun. 2004.

Annex

7.1 **Review Article: Genetics of Idiopathic Scoliosis**

Published: Journal eLS. John Wiley & Sons, Ltd. Jan. 2014, DOI: 10.1002/9780470015902.a0025313

Kristen F. Gorman[1], Cedric Julien1, Niaz Oliazadeh[1,2], Qilin Tang[1,2] and Alain Moreau[1,2,3]

[1]Viscogliosi Laboratory in Molecular Genetics of Musculoskeletal Diseases, Saint Justine Children's Hospital Research Center. Montreal, QC, Canada.

[2]Department of Biochemistry, Faculty of Medicine, University of Montreal, QC, Canada.

[3]Department of Stomatology, Faculty of Dentistry, Université de Montréal, Montreal, QC, Canada.

Author contributions:

Kristen F. Gorman: Designed the manuscript and wrote the paper as the lead author.

Cedric Julien: Participated in writing of the manuscript.

Niaz Oliazadeh: Wrote one of three major sections (Mendelian hypothesis), contributed in literature review and the design of the whole paper.

Qilin Tang: Wrote one of the three major sections (Hypothesis 3)

Alain Moreau: The principal investigator who supervised the study and participated in writing of the manuscript.

7.1.1 Abstract

Genetic approaches to complex diseases are subject to the currently available technological innovations, and successes or failures using these approaches influence our hypotheses for the genetic contributions to complex dis- eases. Common complex diseases with a genetic con- tribution result in the bulk of healthcare expenses through chronic care. It is thought that an understanding of the genetic contributions to common complex diseases will allow for advances in disease prevention, mitigation of disease pathogenesis and curative treatments. The authors discuss genetic approaches to complex diseases from the perspective of idiopathic scoliosis, a prevalent vertebral deformity syndrome that involves the integra- tion of clinical, psychological, mechanical, and basic science disciplines. The authors focus specifically on the different hypotheses and approaches for genetic study, drawing on past studies and discussing possible future studies, with consideration of technological innovations.

Key words: Complex, idiopathic, scoliosis, genetic, disease, association, Mendelian, pedigree, GWAS

Key Concepts:

- *The genetic basis of idiopathic scoliosis is not well understood.*
- *Idiopathic Scoliosis is a complex deformity syndrome with a complex genetic component.*

7.1.2 Introduction:

Idiopathic scoliosis (IS) is a complex developmental syndrome that manifest primarily as an abnormal structural curvature of the spine that involves changes in the frontal, sagittal, and transverse planes. Eighty percent of all spinal curvatures are idiopathic (MIM 181800), making IS the most common form of spinal deformity. The global incidence among children is 0.15%-10.0%, depending on curve severity (Asher & Burton, 2006; Lonstein, 1994; Reamy & Slakey, 2001). Since its first documentation by Hippocrates (Hippocrates. Articulations, par. 47), the diagnosis, cause, and treatment of IS have been the focus of a great deal of research and yet the etiology remains enigmatic. The two main research questions that endure are, what factors predispose a child to develop a curvature? And, what explains why one curve will progress while others do not? Barriers to answer these questions are rooted in the phenotypic and presumed genetic complexities for IS. Phenotypic complexity is manifested as variation in curve morphology, curve magnitude, the age for curve onset, and the propensity for a curve to increase in magnitude or to stabilize or to resolve with growth. Genetic complexity is inferred from inconsistent inheritance (Cowell et al., 1972; Riseborough & Wynne-Davies, 1973; Horton 2002), discordance among monozygotic twins (Andersen et al., 2007; Hermus et al., 2007; Weiss, 2007), and highly variable results from human genetic studies.

As a consequence of its persistently idiopathic nature, the standard care for IS has not significantly changed in decades. Current patients are treated in a similar manner to those twenty or thirty years ago: observation, bracing, and spinal fusion surgery as a last resort (Fazal & Edgar, 2006). One important outcome from identifying genes for IS would be earlier detection. Idiopathic scoliosis imposes a substantial healthcare cost through bracing, hospitalizations, surgery, and chronic back pain. An understanding of the genetic basis could help to identify at-risk individuals, and potentially lead to the establishment of preventive and/or therapeutic procedures.

7.1.3 Hypothesis 1: Idiopathic scoliosis is a Mendelian disease

7.1.3.1 Support

A genetic contribution to idiopathic scoliosis has been observed as far back as 1896, when Tubby considered a hereditary factor to be common and important, as demonstrated

by two families from his practice, each of which had several members with scoliosis (Tubby 1896). Furthermore, nearly 80 years ago, Garland considered the importance of the role played by genetics to be underestimated (Garland 1934). Despite this distinct observation of heredity however, the mode of inheritance for IS appears to be inconsistent. A recent study of the mode of inheritance among 70 patients, reports IS inheritance to be autosomal dominant (AD), autosomal recessive (AR), and multifactorial (Aulisa et al. 2012). It appears that historically the most common mode of inheritance reported is autosomal dominant, starting in 1934 when Garland described it as "simple Mendelian dominant" in a five-generation family without any other associated disease or disabilities (Garland 1934). A recent review shows that almost 65% of all inheritance studies found patterns of AD for a locus, either within a family or between small family collections. Reported loci with AD inheritance are: 17p11, 9q31.2-q34.2, 18q12.1-q12.2, 3q12.1, 5q13.3, 19p13.3, 17q25.3-qtel, 6p, 6q and17p (reviewed by Gorman et al., 2012).

Other modes of inheritance reported for IS are X-linked dominant (Cowell et al., 1972; Justice et al., 2003) and autosomal recessive (Raggio et al. 2009). Due to lack of clear support for male-to-male transfer from one generation to the other, a X-linked model has been proposed (Cowell et al. 1972). Justice and others recognized X-linked dominant inheritance in a subset of a large collection of families and identified a region of interest at Xq22.3- q27.2 (Justice et al. 2003). In their genome-wide linkage study using seven multigenerational families with multiple affected members, Raggio and others identified a predisposing locus at 12p that fits both the autosomal dominant and autosomal recessive models of inheritance (Raggio et al. 2009). None of the families demonstrate a clearly recessive mode of inheritance however, leading the authors to surmise an additive genetic model where both dominant and recessive genes contribute to the phenotype. Thus, although early studies of IS inheritance consider the possibility of complex transmission (De George & Fisher 1967; Wynne-Davies 1968) in order to make progress in gene discovery, studies were conducted on families demonstrating discernable Mendelian inheritance. However, even those studies with AD inheritance do not always demonstrate the same curve phenotype among affected members. This may be due to behavioural differences impacting the biomechanical influences on curve pathogenesis, or it may be due to environmental factors, or genetic differences. Indeed, even studies of IS among

monozygotic twins show inconsistency among curve phenotypes (Inoue et al. 1998; Weiss 2007).

7.1.3.2 Approach

Early genetic studies for IS needed to understand the mode of inheritance in order to enable the identification of at-risk individuals and facilitate gene discovery. The first IS genetic study used 4 families with AD inheritance to test whether three collagen genes were correlated to curvature (Carr et al. 1992). They used genetic markers to observe whether certain alleles of the genes were segregating with curvature but could not demonstrate any linkage. Since then there have been 5 additional candidate gene studies (Miller et al. 1996; Zorkol'tseva et al. 2002; Morcuende et al. 2003; Marosy et al. 2006; Montanaro et al. 2006) and almost 15 genomic studies for IS that have employed the use of pedigrees and linkage analysis (LA) (reviewed in Gorman et al., 2012). The method of linkage analysis surveys differential segregation of alleles among affected and non-affected family members. See also: DOI: 10.1038/npg.els.0005397. Genetic markers are used to define an allele, and recombination (or lack thereof) between markers will denote loci that are physically close to specific regions implicated in the disease. Linkage analysis is the traditional approach for genetic study in Mendelian disorders, and success expanded its application from Mendelian simple to complex diseases, or at least subtypes of complex diseases that demonstrate a distinct mode of inheritance (Baron 2001). Unfortunately, however, inconsistency among results gradually raised some serious discussions about the limitation of applying these types of studies to complex diseases.

Linkage analysis applied to IS needs large multiplex families, and those demonstrating a distinct mode of inheritance are relatively rare (Edery et al. 2011). In addition, extensive family information should be available for all individuals, which can be costly and time consuming and is sometimes inaccessible. Even if all the information is obtained, inconsistency for the phenotype's definition raises fundamental questions. Considerations for IS such as the minimum Cobb angle that defines case vs control, and whether to subdivide patients based on the type of curvature or other phenotypic subdivisions (such as age of onset, and rate of progression) might be necessary.

Furthermore, some studies assess the phenotype clinically while others by questionnaire, which might confound consistency between studies. For complex disorders, the existence of subgroups having Mendelian inheritance has been demonstrated and there are several successful examples of gene identification using linkage analysis within these groups (e.g. BRCA1 and BRCA2 for breast cancer, APC for colon cancer, the LDL receptor gene for heart disease (McPherson et al. 2007; Baron 2001). Thus, genetic correlations in even a small subgroup of patients can shed light on our understanding of a disease and help to improve therapeutic approaches for at least that subgroup of patients (Baron 2001).

7.1.3.3 Current perspectives

Many IS candidate genes tested using pedigrees have not been confirmed (reviewed in Gorman et al., 2012), and from the two loci (19p13.3 and 10q23-25.3) that have been replicated (Chan et al. 2002; Alden et al. 2006; Marosy et al. 2010; Takahashi et al. 2011), one (10q23-25.3) is the result of a recent genome-wide population-based study rather than being inheritance based. Linkage analysis studies typically have low resolution in that the locus identified is comprised of million bases of genetic information, including many genes and regulatory regions (Smith 2012). To refine such a locus prior to affordable sequencing options would require a large family cohort, and that has proven to be prohibitive considering the multiplicative inheritance for IS. However, the current availability of sequencing technologies such as exome sequencing or targeted sequencing could facilitate gene identification in smaller pedigree cohorts.

Although linkage studies have been successful with the discovery of Mendelian (i.e. simple) disease genes that confer a high relative risk, the majority have failed to successfully identify genes for complex diseases (Tabor et al. 2002). The initial pedigree-based genetic studies for IS have fostered the perspective that it is a genetically heterogeneous, multifactorial disease with possibly the existence of a subgroup of patients harbouring autosomal dominant monogenic inheritance (Wise et al. 2008). As with other common complex diseases, IS might be a consequence of multiple genes of modest effect, differentially segregating among families. Linkage analysis studies are generally most suitable for detecting genes with a large effect and considering that complex diseases might

be caused by the accumulation of several DNA variants with small effects, to achieve the required statistical power for detecting a modest effect gene would require an unrealistic sample size (Risch & Merikangas 1996).

7.1.4 Hypothesis 2: Idiopathic scoliosis is caused by multiple genes of minor effect

7.1.4.1 Support

Despite the strong evidence for a genetic contribution to idiopathic scoliosis, without a distinctive pattern of inheritance, linkage studies have achieved limited success in identifying genetic determinants. Thus, it is possible that IS is a consequence of a moderate to large number of common genetic variants, each of which contributes to several per cent of the risk for curvature and/or progression. For complex common diseases with an apparent polygenic inheritance, the common disease-common variant hypothesis (CDCV hypothesis) has motivated the pursuit of genome wide association studies (GWAS) (Lander 1996). The goal of GWAS is to identify the causative variants that are underlying genomic markers associated with a disease, and then to characterize their functional effects (Stranger et al. 2011). If the major source of genetic variance for IS susceptibility is due to a differential accumulation of common variants in cases versus controls, then it is possible that hundreds or thousands of loci contribute in each case and the loci identified in a GWAS represent the largest effect sizes drawn from a Poisson distribution (Gibson 2011).

7.1.4.2 Approach

In the pre-genomic era, the genetic dissection of complex traits was done using classical linkage studies and candidate gene-based association studies. The classical linkage study is a powerful approach to identify rare and highly penetrant disease variants. The candidate gene approach in the pre-genomic era has been limited to a few genetic markers for genes that are suspected to be involved in the pathogenesis of the disease. The GWAS approach was first proposed by Risch and Merikangas in 1996 as a statistically more powerful approach to detect common variants with a modest genetic effect, compared to a linkage study design (Stranger et al. 2011). See also DOI: 10.1002/9780470015902.a0021458.

The aim of a GWAS is to detect significant associations in a population (P value <5E-8) between common diseases and common genetic variants. In particular, a GWAS is designed to examine millions of single nucleotide polymorphisms (or 'SNPs') in the genome, using commercially available chips to survey the genotypes of thousands of individuals. Variant SNP alleles that are differentially associated with a disease cohort compared to controls are thought to denote susceptibility regions that contain genetic correlates to the disease (i.e. genes or genetic deletions/duplications). Any positive association should be confirmed in a different population using a larger sample size.

The first genome-wide association study of IS was conducted in 2011. First, Sharma et al. generated a list of the top 100 significantly IS-associated SNPs from a genomic survey in 419 trio-families (affected children and their parents) in Utah (Sharma *et al.* 2011). Combined with three independent replication studies having a total of 3431 individuals, rs10510181 was observed the most significant (odds ratio: OR=1.37; 95% confidence interval: CI = 1.20-1.58, *P* = 8.22E-7). The results suggested that CHL1, a member of the L1 gene family of neural cell adhesion molecules and a neural recognition molecule that may be involved in signal transduction pathways, might be associated with the susceptibility of IS. The authors then surveyed variants significantly associated with other genes involved in the axon guidance pathway: DSCAM (*P* = 2.26E-5 for rs2222973) and CNTNAP2 (*P* = 6.20E-5 for rs11770843). However, further studies in larger cohorts are necessary to verify their findings and to identify additional susceptibility loci for IS.

Next, Takahashi *et al.* demonstrated an association in an East Asian population between IS and common variants near LBX1, a transcription factor required for the development of inhibitory interneurons in the dorsal horn of the spinal cord as well as migration and further development of hypaxial muscle precursor cells for limb muscles. They suggested the relevance of somatosensory pathways in the disease etiology (Takahashi *et al.* 2011). For the three associated SNPs, authors of a replication study using a Chinese Han population observed the same direction of effect (increased risk in IS population). Two other Chinese replication studies that confirm the loci are shown in Table I.

To identify additional IS susceptibility loci, Takahashi et al. recently extended their previous GWAS by comparing the genomes of 1,819 Japanese individuals with IS to 25,939 Japanese individuals without IS (Kou et al., 2013). The most significant SNP identified was rs6570507 (P = 2.25E-10, OR=1.28, 95% CI=1.18-1.38), located in an intron of the GPR126 gene. GPR126 is involved in the process of myelination and in the growth and development of the spine during childhood. Functional analysis by the group showed that the knockdown of gpr126 in zebrafish embryos caused delayed ossification of the developing spine. Further, Takahashi et al. replicated the association and the same effect size in Han Chinese and European-ancestry populations (combined P=1.27E-14, OR=1.27, 95% CI=1.20-1.35) (Kou *et al.* 2013).

7.1.4.3 Current perspectives:

There are some important limitations to consider with GWAS. First, to avoid false significant associations by testing ~500,000 SNPs in several thousand individuals, a threshold of p value less than 10-7 or 10-8 must be used. At the same time however, this decreases the power to detect SNPs of minor effect independently, which may have strong associations when considering the interplay of genes and environmental factors. We are still lacking models and methods that consider gene-by-environment interactions between multiple genetic variants. Second, the effectiveness of a study is subject to multiple factors. When evaluating the results of a GWA study, it is important to consider the sample sizes, the odds ratios, the allele frequencies, the threshold of significance, and the performance of the commercial microarrays in a population (Mägi et al. 2007; Jorgenson & Witte 2006).

Even with such limitations, GWAS has become more and more prevalent in human disease research. There was a total of 494 GWA studies in 2011, 528 studies in 2012, and 333 studies until the end of July 2013 (http://hugenavigator.net). This is likely due to the decreasing cost for the technologies. The recent generation of commercially available chips also has improved the genomic coverage and the representation of alleles that occur at a minor frequency in the population. For example, in December 2012, Illumina launched their Omni5 BeadChip, covering MAF (minor allele frequency) as low as 0.01. There are expected to be more GWA and follow-up studies for IS in the near future, based on

published abstracts from recent meetings (Dormans et al., 2011, Nelson et al., 2011). For example, the IL17RC gene has been reported as a susceptibility locus through a GWAS with ~550,000 SNPs in 137 IS cases of European ancestry and 2,126 controls (P=1.18E-9, OR=2.28 for rs708567) (Dormans et al., 2011). To verify this association and other findings from the previous studies by Sharma (Sharma et al., 2011), Zhou et al. genotyped significant SNPs in associated genes (IL-17RC, CHL1, DSCAM and CNTNAP2) among Chinese population, and observed SNP rs708567 in IL-17RC gene significantly associated with IS both in susceptibility and curve severity (P value=0.023 and 0.007, in a case-control study (529:512) and a case-only study (241 AIS patients), respectively) (Zhou et al. 2012). As this association was not reported in previous GWA studies for Utah and Japanese populations (Sharma et al. 2011; Takahashi et al. 2011), it's necessary to perform an additional study to confirm the result in a larger sample size and in different populations.

Taken as a whole, there has been very little success in identifying genetic risk factors for complex multifactorial diseases prior to the advent of GWAS, an approach that is based on the common disease-common variant model. Most of the risk alleles that have been identified by GWAS have a population frequency of >5%, and confer a small effect size (odds ratio, OR<1.5). Since 2007, GWA studies have identified >600 variants associated with various complex diseases, although even when combining all available GWAS identified loci for a particular disorder, these associated polymorphisms usually explain less than 5%–10% of the risk of disease (Riancho 2012). See also: DOI: 10.1002/9780470015902.a0021995. Since GWAS failed to explain the vast majority of complex human diseases, this has led to another hypothesis that the variation for most complex diseases is due to rare alleles of large effect (RALE).

7.1.5 Hypothesis 3: Idiopathic scoliosis is caused by rare genetic variants of major effect

7.1.5.1 Support

GWAS depends on pervasive SNP markers that enable genome-wide surveys test the influence of common genetic variation on disease susceptibility. Despite the notable success of GWAS in revealing numerous new disease-associated genes and loci, all the identified SNPs collectively account for a small proportion of the heritability for complex

diseases. Indeed, taken together, the recent GWAS evidence for the association of three genes (CHL1, LBX1 and GPR126) with IS (Sharma et al. 2011; Takahashi et al. 2011; Kou et al. 2013), barely accounts for 1% the observed phenotypic variance. The failure of GWAS-SNPs to account for most heritability of complex diseases has invoked some considerable discussion on the reasons for 'missing heritability' (e.g. Manolio et al. 2009; Eichler et al. 2010; Chaufan & Joseph 2013; Brookfield 2013). Factors thought to contribute to this missing heritability are genetic interactions (Zuk et al. 2012), and rare variants (Asimit & Zeggini 2009), both of which have yet to be well examined in GWAS.

Rare disease variants are thought to exist as recently derived highly penetrant alleles that have a low population frequency (typically <1%) but account for high disease susceptibility (Gibson 2011). Disease could occur from an accumulation of these rare variants in a pathway of functional significance. Rare variants can occur as point mutations, or as gene deletions/duplications. The contribution of rare variants to complex diseases has been the topic of much consideration and early investigations have suggested promising results (O'Roak et al. 2012; Chesi et al. 2013; Walters et al. 2013; Zahnleiter et al. 2013; reviewed in de Ligt et al. 2013). Considering the heterogeneous inheritance for IS, it is possible that there are rare variants differentially segregating among families. Currently, tools such as whole exome sequencing and targeted sequencing are readily available for the investigation of rare variants and IS. See also: DOI: 10.1002/9780470015902.a0022658.

7.1.5.2 Approach

Alignment of patient sequences against the reference human genome and an annotation step helps to discriminate known from unknown/rare variants. Generally, sequences of diseased individuals are compared with a healthy-control cohort and/or with existing databases like 1,000 Genomes Project (www.1000genomes.org), to allow for the identification of genes in which there is an elevated aggregation of rare variants (Li & Leal 2008; Morris & Zeggini 2010). When applied to a large pedigree, exome sequencing has the potential to identify rare family specific genetic correlates to IS that might explain some of the cases in the population at large (Peng et al. 2013). When applied to a population,

exome sequencing can suggest important genes and pathways that are enriched with rare variants in case versus control (Myers et al. 2011; Moens et al. 2011). Of course the limitation with exome sequencing is that these rare variants are surveyed in the coding region of the genome only.

7.1.5.3 Current perspectives

Efforts to examine whether rare coding variants contribute to aspects of IS are underway and we expect that in the next few years there will be the publication of multiple studies and a variety of insights. Another important consideration for explaining the "missing heritability" in common complex diseases is gene-gene and gene-environment interactions. This aspect of complex disease has proven to be challenging to approach (DeYoung & Clark 2012; Jiao et al. 2012; Ackert-Bicknell & Karasik 2013; Okser et al. 2013).

7.1.6 Untested hypotheses for idiopathic scoliosis

a) Micro ribonucleic acids (miRNAs) are a class of small noncoding RNAs that are involved in a range of physiological processes, with each miRNA regulating on average 200 target genes. Many genes contain target sites for one or more miRNA. See also: DOI: 10.1002/9780470015902.a0021754. Different forms of miRNAs, which target specific mRNAs, can regulate gene expression in a tissue-specific way (Ameres & Zamore 2013). A mis-regulation of key genes by miRNAs can somehow explain an aspect of the etiopathology of complex diseases. Expression arrays allow researchers to investigate the expression level of miRNAs along with other mRNAs in specific tissues. Identification of targeted genes can point out new pathways or pathways already incriminated in complex disease (Martins et al. 2011; Junn et al. 2009). In November 2012, Affymetrix introduced the only commercially available high-density miRNA Target Site Genotyping Arrays, which interrogates 238,000 SNPs and indels in genes for all parts of the miRNA cascade including miRNAs, their mRNA target sites, and silencing machinery. Since miRNA has been announced by the Encyclopedia of DNA Elements (ENCODE) Consortium to contain

important regulatory elements with functional importance, the studies using miRNA arrays are promising to show valuable results.

b) Gene expression can be influenced by genome modifications other than variations in the sequence itself but by alteration of DNA methylation, histones modification (i.e. epigenetics). It is thought that epigenetic modifications influence observed phenotypic variability for complex diseases without modification of the gene sequence (reviewed by Schumacher & Petronis 2006). Importantly, genetic variation can influence epigenome dynamics (Zhi et al. 2013), which can create an added dimension of phenotypic complexity by altering gene expression and cellular function (Figueroa et al. 2010). The classical example of Prader-Willi and Angelman syndromes demonstrate the importance of epigenetics in disease symptom manifestation (Mann & Bartolomei 1999). Considering the variation for the IS phenotype among monozygotic twins, it is feasible to presume that epigenetic modification may be modulating the phenotype (Inoue et al. 1998; Weiss 2007). The most established methods to investigate epigenetic signatures have been gene specific, although methods to survey genomic epigenetic signatures are being improved (reviewed by Tollefsbol 2011).

7.1.7 Other genetic approaches applied to idiopathic scoliosis

a) Gene expression studies could generate hypotheses for which genes and/or pathways are being affected in a complex disease. However, for those diseases where multiple tissues are affected, the choice of which tissue to explore is of concern. Moreover, in a developmental syndrome such as IS, the time of sample collection could have an impact on the outcome of gene expression inquiries. Regarding to IS, beyond the tissue type and time of collection, another issue to consider whether the patients or a subset of the patients have been treated by bracing. Genes can be differentially regulated in response to the mechanical stresses induced by bracing and this could cause false correlations when looking for differentially expressed genes related to the IS etiopathogenesis (Chan et al. 2010; Chiquet 1999; Luna et al. 2009).

The choice of controls is another important concern for IS expression studies. If the patient spinal samples are from spinal obtained from intraoperative specimens (bone,

intervertebral disc, muscle), the choice of control is extremely limited. Pediatric spinal surgery is seldom performed and so tissues for non-affected would have to be obtained from age matched trauma patients. Because the gene expression for some genes is known to differ depending on the anatomical location, differential gene expression between case and control could simply be due to the different anatomical positions and not the etiology of the disease. Gene expression is an important tool for generating hypotheses, provided that the limitations are well considered and the research questions expected to be answered are not exceeding these.

b) Endophenotypes are conceptualized as "microscopic and internal" (John & Lewis 1966) components of a disease, in contrast to those that are observable on a clinical scale. They can be considered as being on the putative path from the causative genes, via molecular mechanisms, to the clinical phenotype (Gottesman & Gould 2003; Chan & Gottesman 2008).

Endophenotypes are heritable and also state independent, in the regard that they are present before the onset of symptoms. Furthermore, endophenotypes can occur in some unaffected relatives of affected patients. However, it is expected that asymptomatic individuals who inherit the endophenotype or vulnerability associated with the disease is expected to be at a higher prevalence than in the general population (Chan & Gottesman 2008). Endophenotypes applied to complex diseases can allow for the partitioning of variation on a molecular level in order to describe subclinical correlates to subtypes of the disease. This is an important approach to a disease such as IS because environmental, behavioural, and mechanical influences may confound molecular variation to create the observed clinical variability. Recent work into the biological basis of IS by Moreau and colleagues has demonstrated the existence of endophenotypes among patients (Akoume et al. 2010).

c) Model genetic organisms can contribute to the understanding of a complex human genetic disease several ways. Gene mapping experiments in animals with a similar phenotype as the human disease, or components of the disease, can provide important candidate genes for study in the human population. Also, transgenic techniques can provide a means by which candidate genes discovered from human genetic studies can be validated

on a functional level. Currently only fish models have demonstrated an idiopathic-type of curvature that is similar to the human phenotype (Gorman et al. 2007). Identification of the major gene defect causing spinal curvature in the curveback guppy model will provide (Gorman et al. 2011) important candidate molecules and pathways to examine in human IS genetic studies, and genes identified in human genetic studies can be tested in model species such as the medaka (Takeda & Shimada 2010).

7.1.8 Conclusions

To date, the candidate gene approach has been the prevalent type of genetic inquiry for IS. The choice of a candidate gene for IS has been largely based on hypotheses regarding the biological systems driving the deformity, and these have been based on clinical observations (reviewed by Gorman et al. 2012). In addition, partially hypothesis-driven choices for candidate genes include those genes that are contained within loci identified by linkage analysis studies. In such cases, the loci are investigated using an increased marker density and/or sequencing technologies, and candidates are prioritized based on statistical analyses and researcher hypotheses (i.e. Qiu et al. 2008; Miller et al. 2012).

Before direct sequencing of candidates became an affordable option, candidate gene studies relied on genetic markers to denote different alleles. Linkage studies would test for differential segregation of alleles between diseased and non-affected family members, association studies would test whether alleles are differentially associated with cases (IS) vs control cohorts in a population. The major criticism of candidate gene studies is that significant associations are rarely replicated in subsequent association studies. Indeed, none of the positive associations from IS candidate genes tested have been confirmed (reviewed by Gorman et al. 2012). This could be due to false positive results reported in the initial study, or because of the population specificity of reported association. Conversely, negative candidate gene studies that use small cohorts do not rule-out the potential contribution of that candidate as a minor effect gene, such as a modifier of curve pathogenesis. Candidate genes for IS can now be derived from non-hypothesis-based approaches such as GWAS or exome sequencing.

Although the molecular and genetic etiopathogenesis of IS has been enigmatic for hundreds, if not thousands of years, biological sciences are currently poised for breakthrough. Technological innovations are rapidly progressing, and such progress allows researchers to be able to afford and access the means of investigating the genomes of more individuals more thoroughly.

Further Reading:

- Lindsey Allen Ho (2010): Novel Statistical Methods for the Study Design and Analysis of Genome-Wide Association Studies. Chapel Hill, N.C. University of North Carolina at Chapel Hill
- Ammar Al-Chalabi (2009): Genetics of Complex Human Diseases: A Laboratory Manual. Laura Almasy (editor); Cold Spring Harbor Lab Press; Oxford University Press, Incorporated
- StrachanT., Read A, (2010), Human Molecular Genetics, 4th edn. New york: Garland Science.
- Zeggini E., Morris A., (2011), Analysis of Complex Disease Association Studies, A Practical Guide,1st edn. USA, Academic press-Elsevier,
- Collins A.R., (2007), Linkage Disequilibrium and Association Mapping: Analysis and Applications, 1st edn. New Jersey, Humana press inc.

Glossary

Cobb angle: The primary measurement for the magnitude of coronal deviation of the spine in scoliosis. From a radiograph, a line is drawn along the superior endplate of the uppermost vertebra demonstrating the greatest tilt but the least rotation and/or displacement. A second line is drawn along the inferior end plate of the lowest vertebra with the most tilt and lease displacement. The angle between these lines (or lines drawn perpendicular to these lines) is the Cobb angle. A greater Cobb angle denotes a more severe curve.

Genetic association studies: a useful tool to test for a correlation between disease status and genetic variation to identify candidate genes or genome regions that contribute to a specific disease. A higher frequency of a single-nucleotide polymorphism (SNP) allele or genotype in a series of individuals affected with a disease can be interpreted as meaning that the tested variant increases the risk of a specific disease.

Endophenotype: An intermediate phenotype that is heritable and associated with a disease but is not itself a symptom of the disease. Endophenotypes are believed to have a polygenic background with multifactorial origins and would be a more tractable target for genetic analysis than the relevant disease state itself.

Exome: the collection of known exons in our genome. Exome is the protein-coding portion of the genome. As exons comprise only 1% of the genome and contain the most easily understood, functionally relevant information, sequencing of only the exome is a cost-effective method of identifying most of the variants that are most likely to affect a trait.

Minor Allele Frequency (MAF): the frequency at which the less common allele of the SNP occurs in a given population. Although the definition of a rare variant is one present with a MAF of less than 1%, the frequency boundaries used in the literature vary. Recently, variants with MAFs between 0.1% and 1% are defined as rare variants and MAFs of less than 0.1% as novel, MAFs of greater than 5% as common.

Quantitative Trait Locus (QTL): a region of DNA that is associated with a particular phenotypic trait, identified by QTL mapping. Knowing the number of QTLs tells us about the genetic architecture of a trait and identifies candidate genes underlying a trait by sequencing.

1000 Genomes Project: An international research consortium that will sequence the genomes of 1,200 individuals of various ethnicities. Most individuals will be sequenced to low coverage, or in exons only. The goals are to catalogue human variation with minor allele frequencies of ~1% or greater and to refine and optimize strategies for sequencing large numbers of genomes.

Micro-RNA (miRNA): short (22 nucleotides), single-stranded, non-coding RNAs that bind messenger RNA (mRNA) in a sequence-specific manner to regulate gene expression . usually resulting in gene silencing via translational repression or target degradation. The human genome may encode over 1000 miRNAs, which may target about 60% of mammalian genes and are abundant in many human cell types. miRNAs play an essential role in fundamental biological processes such as differentiation, proliferation, apoptosis and homeostasis and are promising class of molecular biomarkers.

Table I. Genome wide association studies and subsequent case-control studies in Japanese and Chinese population for associations between genetic variants near LBX1 and Idiopathic Scoliosis.

Reference	# Case vs. Control	rs11190870		rs625039		rs11598564	
		P value	Odds ratio (95% CI)	P value	Odds ratio (95% CI)	P value	Odds ratio (95% CI)
Takahashi Y. et al. (2011)	1359:11296	1.24E-19	1.56 (1.41-1.71)	8.13E-15	1.49 (1.34-1.64)	5.98E-14	1.42 (1.30-1.56)
Fan Y.H. et al. (2012)	300:788	9.10E-10	1.85 (1.52-2.25)	NA	NA	NA	NA
Gao. W, et al. (2013)	513:440	1.17E-08	1.70 (1.42-2.04)	5.09E-05	1.49 (1.23-1.80)	5.54E-06	1.52 (1.27-1.83)
Jiang. H, et al. (2013)	949:976	1.80E-09	1.51 (1.33-1.71)	NA	NA	NA	NA

References

Ackert-Bicknell, C.L. & Karasik, D., 2013. Impact of the Environment on the Skeleton: Is it Modulated by Genetic Factors? Current osteoporosis reports.

Akoume, M.-Y. et al., 2010. Cell-based screening test for idiopathic scoliosis using cellular dielectric spectroscopy. Spine, 35(13), pp.E601–8.

Alden, K.J. et al., 2006. Idiopathic scoliosis: identification of candidate regions on chromosome 19p13. Spine, 31(16), pp.1815–1819.

Ali Fazal, M. & Edgar, M., 2006. Detection of adolescent idiopathic scoliosis. Acta orthopaedica Belgica, 72(2), pp.184–6.

Ameres, S.L. & Zamore, P.D., 2013. Diversifying microRNA sequence and function. Nature Reviews Molecular Cell Biology, 14(8), pp.475–88.

Andersen, M.O., Thomsen, K. & Kyvik, K.O., 2007. Adolescent idiopathic scoliosis in twins: a population-based survey. Spine, 32(8), pp.927–30.

Asher, M.A. & Burton, D.C., 2006. Adolescent idiopathic scoliosis: natural history and long term treatment effects. Scoliosis, 1(1), p.2.

Asimit, J. & Zeggini, E., 2009. Testing for rare variant associations in complex diseases. Genome medicine, 1(11), p.24.

Aulisa, A. et al., 2012. The familiarity of idiopathic scoliosis: statistical analysis and clinical considerations. Scoliosis, 7(Suppl 1), p.O73.

Baron, M., 2001. The search for complex disease genes: fault by linkage or fault by association? Molecular Psychiatry, 6(2), pp.143–149.

Brookfield, J.F.Y., 2013. Quantitative genetics: heritability is not always missing. Current biology : CB, 23(7), pp.R276–8.

Carr, A.J. et al., 1992. Segregation of structural collagen genes in adolescent idiopathic scoliosis. Clinical orthopaedics and related research, (274), pp.305–10.

Chan, M.W.C., Hinz, B. & McCulloch, C.A., 2010. Mechanical induction of gene expression in connective tissue cells. Methods in cell biology, 98, pp.178–205.

Chan, R.C.K. & Gottesman, I.I., 2008. Neurological soft signs as candidate endophenotypes for schizophrenia: a shooting star or a Northern star? Neuroscience and biobehavioral reviews, 32(5), pp.957–71.

Chan, V. et al., 2002. A genetic locus for adolescent idiopathic scoliosis linked to chromosome 19p13.3. American journal of human genetics, 71(2), pp.401–6.

Chaufan, C. & Joseph, J., 2013. The "missing heritability" of common disorders: should health researchers care? International journal of health services : planning, administration, evaluation, 43(2), pp.281–303.

Chesi, A. et al., 2013. Exome sequencing to identify de novo mutations in sporadic ALS trios. Nature neuroscience, 16(7), pp.851–5.

Chiquet, M., 1999. Regulation of extracellular matrix gene expression by mechanical stress. Matrix biology : journal of the International Society for Matrix Biology, 18(5), pp.417–26.

Cowell, H.R., Hall, J.N. & MacEven, G.D., 1972. Genetic Aspects of Idiopathic Scoliosis. Clinical Orthopaedics and Related Research, 86, pp.121–131.

DeYoung, C.G. & Clark, R., 2012. The gene in its natural habitat: the importance of gene-trait interactions. Development and psychopathology, 24(4), pp.1307–18.

Dormans JP, Grant SF, Sampson NR,Chiavacci R,Hakonarson H.(2011) A Genome Wide Association Study Identifies IL17RC as an Adolescent Idiopathic Scoliosis Locus. Spine: Affiliated Society Meeting Abstracts: 96

Edery, P. et al., 2011. New disease gene location and high genetic heterogeneity in idiopathic scoliosis. European journal of human genetics : EJHG, 19(8), pp.865–9.

Eichler, E.E. et al., 2010. Missing heritability and strategies for finding the underlying causes of complex disease. Nature reviews. Genetics, 11(6), pp.446–50.

Figueroa, M.E. et al., 2010. Leukemic IDH1 and IDH2 mutations result in a hypermethylation phenotype, disrupt TET2 function, and impair hematopoietic differentiation. Cancer cell, 18(6), pp.553–67.

Garland, H., 1934. Hereditary scoliosis. British medical journal, p.1934.

De George, F. V & Fisher, R.L., 1967. Idiopathic scoliosis: genetic and environmental aspects. Journal of medical genetics, 4(4), pp.251–7.

Gibson, G., 2011. Rare and common variants: twenty arguments. Nature reviews. Genetics, 13(2), pp.135–45.

Gorman, K.F. et al., 2011. A major QTL controls susceptibility to spinal curvature in the curveback guppy. BMC genetics, 12(1), p.16.

Gorman, K.F., Julien, C. & Moreau, A., 2012. The genetic epidemiology of idiopathic scoliosis. European spine journal : official publication of the European Spine Society, the European Spinal Deformity Society, and the European Section of the Cervical Spine Research Society, 21(10), pp.1905–19.

Gorman, K.F., Tredwell, S.J. & Breden, F., 2007. The mutant guppy syndrome curveback as a model for human heritable spinal curvature. Spine, 32(7), pp.735–41.

Gottesman, I.I. & Gould, T.D., 2003. The endophenotype concept in psychiatry: etymology and strategic intentions. The American journal of psychiatry, 160(4), pp.636–45.

Hermus, J.P.S., van Rhijn, L.W. & van Ooij, A., 2007. Non-genetic expression of adolescent idiopathic scoliosis: a case report and review of the literature. European spine journal : official publication of the European Spine Society, the European Spinal Deformity Society, and the European Section of the Cervical Spine Research Society, 16 Suppl 3, pp.338–41.

Inoue, M. et al., 1998. Idiopathic scoliosis in twins studied by DNA fingerprinting: the incidence and type of scoliosis. The Journal of bone and joint surgery. British volume, 80(2), pp.212–7.

Jiao, S. et al., 2012. Genome-wide search for gene-gene interactions in colorectal cancer. PloS one, 7(12), p.e52535.

John, B. & Lewis, K.R., 1966. Chromosome variability and geographic distribution in insects. Science (New York, N.Y.), 152(3723), pp.711–21.

Jorgenson, E. & Witte, J.S., 2006. Coverage and power in genomewide association studies. American journal of human genetics, 78(5), pp.884–8.

Junn, E. et al., 2009. Repression of alpha-synuclein expression and toxicity by microRNA-7. Proceedings of the National Academy of Sciences of the United States of America, 106(31), pp.13052–7.

Justice, C.M. et al., 2003. Familial idiopathic scoliosis: evidence of an X-linked susceptibility locus. Spine, 28(6), pp.589–594.

Kou, I. et al., 2013. Genetic variants in GPR126 are associated with adolescent idiopathic scoliosis. Nature genetics, 45(6), pp.676–9.

Lander, E.S., 1996. The New Genomics: Global Views of Biology. Science, 274(5287), pp.536–539.

Li, B. & Leal, S.M., 2008. Methods for detecting associations with rare variants for common diseases: application to analysis of sequence data. American journal of human genetics, 83(3), pp.311–21.

De Ligt, J., Veltman, J.A. & Vissers, L.E., 2013. Point mutations as a source of de novo genetic disease. Current opinion in genetics & development, 23(3), pp.257–63.

LONSTEIN, D., 1994. Adolescent idiopathic scoliosis. The Lancet, 344(8934), pp.1407–1412.

Luna, C. et al., 2009. Alterations in gene expression induced by cyclic mechanical stress in trabecular meshwork cells. Molecular vision, 15, pp.534–44.

Mägi, R. et al., 2007. Evaluating the performance of commercial whole-genome marker sets for capturing common genetic variation. BMC genomics, 8, p.159.

Mann, M.R. & Bartolomei, M.S., 1999. Towards a molecular understanding of Prader-Willi and Angelman syndromes. Human molecular genetics, 8(10), pp.1867–73.

Manolio, T.A. et al., 2009. Finding the missing heritability of complex diseases. Nature, 461(7265), pp.747–53.

Marosy, B. et al., 2010. Identification of susceptibility loci for scoliosis in FIS families with triple curves. American journal of medical genetics. Part A, 152A(4), pp.846–55.

Marosy, B. et al., 2006. Lack of association between the aggrecan gene and familial idiopathic scoliosis. Spine, 31(13), pp.1420–5.

Martins, M. et al., 2011. Convergence of miRNA expression profiling, α-synuclein interacton and GWAS in Parkinson's disease. PloS one, 6(10), p.e25443.

McPherson, R. et al., 2007. A common allele on chromosome 9 associated with coronary heart disease. Science (New York, N.Y.), 316(5830), pp.1488–91.

Miller, N.H. et al., 1996. Genetic analysis of structural elastic fiber and collagen genes in familial adolescent idiopathic scoliosis. Journal of orthopaedic research : official publication of the Orthopaedic Research Society, 14(6), pp.994–9.

Miller, N.H. et al., 2012. Intra-familial tests of association between familial idiopathic scoliosis and linked regions on 9q31.3-q34.3 and 16p12.3-q22.2. Human heredity, 74(1), pp.36–44.

Moens, L.N. et al., 2011. Sequencing of DISC1 pathway genes reveals increased burden of rare missense variants in schizophrenia patients from a northern Swedish population. PloS one, 6(8), p.e23450.

Montanaro, L. et al., 2006. Evidence of a linkage between matrilin-1 gene (MATN1) and idiopathic scoliosis. Scoliosis, 1, p.21.

Morcuende, J.A. et al., 2003. Allelic variants of human melatonin 1A receptor in patients with familial adolescent idiopathic scoliosis. Spine, 28(17), pp.2025–8; discussion 2029.

Morris, A.P. & Zeggini, E., 2010. An evaluation of statistical approaches to rare variant analysis in genetic association studies. Genetic epidemiology, 34(2), pp.188–93.

Myers, R.A. et al., 2011. A population genetic approach to mapping neurological disorder genes using deep resequencing. PLoS genetics, 7(2), p.e1001318.

Nelson LM,Chettier R, Ogilvie JW, Ward K.(2011) Candidate Genes for Susceptibility of Adolescent Idiopathic Scoliosis Identified Through a Large Genome-Wide Association Study. Spine: Affiliated Society Meeting Abstracts: 96-97

O'Roak, B.J. et al., 2012. Multiplex targeted sequencing identifies recurrently mutated genes in autism spectrum disorders. Science (New York, N.Y.), 338(6114), pp.1619–22.

Okser, S., Pahikkala, T. & Aittokallio, T., 2013. Genetic variants and their interactions in disease risk prediction - machine learning and network perspectives. BioData mining, 6(1), p.5.

Peng, G. et al., 2013. Rare variant detection using family-based sequencing analysis. Proceedings of the National Academy of Sciences of the United States of America, 110(10), pp.3985–90.

Qiu, X.S. et al., 2008. Association study between adolescent idiopathic scoliosis and the DPP9 gene which is located in the candidate region identified by linkage analysis. Postgraduate medical journal, 84(995), pp.498–501.

Raggio, C.L. et al., 2009. A novel locus for adolescent idiopathic scoliosis on chromosome 12p. Journal of orthopaedic research : official publication of the Orthopaedic Research Society, 27(10), pp.1366–72.

Reamy, B. V & Slakey, J.B., 2001. Adolescent idiopathic scoliosis: review and current concepts. American family physician, 64(1), pp.111–6.

Riancho, J.A., 2012. Genome-wide association studies (GWAS) in complex diseases: advantages and limitations. Reumatología clinica, 8(2), pp.56–7.

Rimoin, David, Reed Pyeritz, B.K., 2002. Emery and Rimoin's Principles and Practice of Medical Genetics, Amsterdam: Churchill Livingstone Elsevier.

Risch, N. & Merikangas, K., 1996. The Future of Genetic Studies of Complex Human Diseases. , 273(September), pp.1516–1517.

Riseborough, E.J. & Wynne-Davies, R., 1973. A Genetic Survey of Idiopathic Scoliosis in Boston, Massachusetts. The Journal of Bone & Joint Surgery, 55(5), pp.974–982.

Schumacher, A. & Petronis, A., 2006. Epigenetics of complex diseases: from general theory to laboratory experiments. Current topics in microbiology and immunology, 310, pp.81–115.

Sharma, S. et al., 2011. Genome-wide association studies of adolescent idiopathic scoliosis suggest candidate susceptibility genes. Human molecular genetics, 20(7), pp.1456–66.

Smith, A.V., 2012. Genetic analysis: moving between linkage and association. Cold Spring Harbor protocols, 2012(2), pp.174–82.

Stranger, B.E., Stahl, E.A. & Raj, T., 2011. Progress and promise of genome-wide association studies for human complex trait genetics. Genetics, 187(2), pp.367–83.

Tabor, H.K., Risch, N.J. & Myers, R.M., 2002. Candidate-gene approaches for studying complex genetic traits: practical considerations. Nature reviews. Genetics, 3(5), pp.391–7.

Takahashi, Y. et al., 2011. A genome-wide association study identifies common variants near LBX1 associated with adolescent idiopathic scoliosis. Nature genetics, 43(12), pp.1237–40.

Takeda, H. & Shimada, A., 2010. The art of medaka genetics and genomics: what makes them so unique? Annual review of genetics, 44, pp.217–41.

Tollefsbol, T.O., 2011. Advances in epigenetic technology. Methods in molecular biology (Clifton, N.J.), 791, pp.1–10.

Tubby, A.H., 1896. Deformities: A Treatise on Orthopædic Surgery,

Walters, R.G. et al., 2013. Rare genomic structural variants in complex disease: lessons from the replication of associations with obesity. N. J. Timpson, ed. PloS one, 8(3), p.e58048.

Weiss, H.-R., 2007. Idiopathic scoliosis: how much of a genetic disorder? Report of five pairs of monozygotic twins. Developmental neurorehabilitation, 10(1), pp.67–73.

Wise, C. a et al., 2008. Understanding Genetic Factors in Idiopathic Scoliosis, a Complex Disease of Childhood. Current Genomics, 9(1), pp.51–59.

Wynne-Davies, R., 1968. Familial (idiopathic) scoliosis. A family survey. The Journal of bone and joint surgery. British volume, 50(1), pp.24–30.

Zahnleiter, D. et al., 2013. Rare copy number variants are a common cause of short stature. PLoS genetics, 9(3), p.e1003365.

Zhi, D. et al., 2013. SNPs located at CpG sites modulate genome-epigenome interaction. Epigenetics : official journal of the DNA Methylation Society, 8(8).

Zhou, S. et al., 2012. A single-nucleotide polymorphism rs708567 in the IL-17RC gene is associated with a susceptibility to and the curve severity of adolescent idiopathic scoliosis in a Chinese Han population: a case-control study. BMC musculoskeletal disorders, 13, p.181.

Zorkol'tseva, I. V et al., 2002. [Analysis of polymorphism of the number of tandem repeats in the aggrecan gene exon G3 in the families with idiopathic scoliosis]. Genetika, 38(2), pp.259–63.

Zuk, O. et al., 2012. The mystery of missing heritability: Genetic interactions create phantom heritability. Proceedings of the National Academy of Sciences of the United States of America, 109(4), pp.1193–8.